

Louisiana State University LSU Digital Commons

LSU Master's Theses

Graduate School

2002

Characterization of an in vivo diode dosimetry system for clinical use

Kai Huang

Louisiana State University and Agricultural and Mechanical College

Follow this and additional works at: https://digitalcommons.lsu.edu/gradschool_theses



Part of the [Physical Sciences and Mathematics Commons](#)

Recommended Citation

Huang, Kai, "Characterization of an in vivo diode dosimetry system for clinical use" (2002). *LSU Master's Theses*. 2765.
https://digitalcommons.lsu.edu/gradschool_theses/2765

This Thesis is brought to you for free and open access by the Graduate School at LSU Digital Commons. It has been accepted for inclusion in LSU Master's Theses by an authorized graduate school editor of LSU Digital Commons. For more information, please contact gradetd@lsu.edu.

CHARACTERIZATION OF AN *IN VIVO* DIODE DOSIMETRY SYSTEM
FOR CLINICAL USE

A Thesis

Submitted to Graduate Faculty of the
Louisiana State University and
Agricultural and Mechanical College
in partial fulfillment of the
Requirements for the degree of
Master of Science

in

The Department of Physics and Astronomy

by

Kai Huang

B.S., Sichuan University, China, 1990

M.S., University of Miami, FL, 2000

December 2002

Acknowledgments

To begin with, I am deeply grateful to my advisor, Dr. Oscar Hidalgo-Salvatierra, for the invaluable guidance and encouragement throughout the thesis project. I am especially grateful to Dr. William Bice without whose invaluable guidance and infinite discussions I would have been lost.

I would like to express my sincere appreciation to the members of my thesis examining committee: Dr. M. L. Williams, Dr. E. Sajo, and Dr. S. Johnson for kindly agreeing to serve on my examining committee.

I am deeply grateful to the professional and dedicated faculty of the Louisiana State University Nuclear Science Center for providing the foundation of knowledge necessary.

I am deeply grateful to the entire staff at Mary Bird Perkins Cancer Center, especially the physicists, dosimetrists, and therapists for their guidance and contribution to my preparation for entering into the medical physics profession. Special thanks go to Dr. T. Kirby and Ms. A. Stam for their valuable guidance and support.

Finally I am deeply grateful to the physicians at Mary Bird Perkins Cancer Center for the clinical knowledge they provided.

Table of Contents

ACKNOWLEDGMENTS	ii
LIST OF TABLES	iv
LIST OF FIGURES	v
ABSTRACT	viii
CHAPTER 1. INTRODUCTION	1
CHAPTER 2. LITERATURE REVIEW	8
CHAPTER 3. MATERIALS AND METHODS	15
CHAPTER 4. RESULTS AND DISCUSSIONS	27
I. PHOTONS.....	27
II. ELECTRONS.....	51
CHAPTER 5. SUMMARY AND CONCLUSION	58
REFERENCES	62
APPENDIX A. 600C (BR, S/N 039) MEASUREMENTS	65
APPENDIX B. 21EX (BR, S/N 1412) MEASUREMENTS	69
APPENDIX C. 21C (BR, S/N 090) MEASUREMENTS	82
APPENDIX D. 21EX (COV, S/N 1251) MEASUREMENTS.....	91
APPENDIX E. 2000CR (HAM, S/N 951) MEASUREMENTS	98
APPENDIX F. THE FORTRAN PROGRAM FOR CALCULATING DCF	105
APPENDIX G. LAYOUT OF THE DIODE CALCULATION WORKSHEET [33] ...	118
VITA	119

List of Tables

Table 3.1 Linacs, modalities and energies at MBPCC.	19
Table 3.2 Diode correction factors data collection table for open fields of photons, where 5 x 5 is the field size in cm ² , and 70 is the SSD in cm.	20
Table 3.3 The field sizes used for wedged fields.	20
Table 3.4 Data collection table used for electrons, where 6x6 is the cone size in cm ² and 105 is the SSD in cm.	21
Table 4.1 Parameters for field size correction for each photon diode.	40
Table 4.2(a)(b)(c) Parameters for wedge correction for each photon diode.	41
Table 4.3 Coefficients of fitting polynomials for each photon diode.	43
Table 4.4 Parameters for field size correction for compiled 6MV and 18MV.	43
Table 4.5(a)(b) Parameters for wedge correction for compiled 6MV and 18MV.	44
Table 4.6 Coefficients of fitting polynomials for compiled 6MV and 18MV.	44
Table 4.7 Diode factors for each energy of each electron diode.	56
Table 4.8 Coefficients of fitting polynomials for electrons.	57

List of Figures

Figure 1.1 Sensitivity variation with pre-irradiation dose with 20 MeV electrons for an n type (•) and a p type (°) diode detector [3].	5
Figure 2.1 Determination the exit calibration factor for the diode	9
Figure 3.1 IVD Model 1131.....	15
Figure 3.2 QED diodes and Isorad-p diodes.....	16
Figure 4.1 Diode correction factors as a function of the source to surface distance, SSD, for entrance measurements. All data in this figure are for open fields with field size 10 x 10 cm ²	27
Figure 4.2 DCF as a function of the field size, FS, for entrance measurements. All data in this figure are for open fields with SSD 100 cm.....	28
Figure 4.3 DCF of 6MV QED diode of 20CR(Ham) as a function of the field size, FS, for entrance measurements. All data in this figure are for SSD 100 cm.	30
Figure 4.4 DCF of 18MV Isorad-p diode of 21C(BR) as a function of the field size, FS, for entrance measurements. All data in this figure are for SSD 100 cm.	31
Figure 4.5 DCF as a function of the wedge angle for entrance measurements. All data in this figure are for SSD 100 cm and FS=10x10 cm ² , and only for narrow and upper wedges.....	31
Figure 4.6 Diode correction factors as a function of the SSD for entrance measurements. All data in this figure are for field size 10 x 10 cm ² . (6MV QED photon diode of 20CR(Ham)).	32
Figure 4.7 Diode correction factors as a function of the SSD for entrance measurements. All data in this figure are for field size 10 x 10 cm ² . (15MV QED photon diode of 20CR(Ham)).	32
Figure 4.8 Wedge factors for diode as a function of the SSD for entrance measurements. All data in this figure are for field size 10 x 10 cm ² (QED 6MV photon diode at 21EX(COV))......	33
Figure 4.9 SSD dependence of QED 6MV photon diode of 21EX(COV) for different FSs (all for 60 degree wedged fields).	34
Figure 4.10 FS dependence of QED 6MV photon diode of 21EX(COV) for different SSDs (all for 60 degree wedged fields).	34

Figure 4.11 The SSD dependence for upper and lower wedged beams with 10x10 cm ² field size. The diode is 4MV QED photon diode at 21EX(BR).	36
Figure 4.12 The fitted curve and polynomial of 6MV QED diode at 600C(BR).	37
Figure 4.13 The fitted curve and polynomial of 4MV QED diode at 21EX(BR).	37
Figure 4.14 The fitted curve and polynomial of 10MV QED diode at 21EX(BR).	38
Figure 4.15 The fitted curve and polynomial of 6MV Isorad-p diode at 21C(BR).	38
Figure 4.16 The fitted curve and polynomial of 18MV Isorad-p diode at 21C(BR).	38
Figure 4.17 The fitted curve and polynomial of 6MV QED diode at 21EX(COV).	39
Figure 4.18 The fitted curve and polynomial of 18MV QED diode at 21EX(COV).	39
Figure 4.19 The fitted curve and polynomial of 6MV QED diode at 21CR(Ham).	39
Figure 4.20 The fitted curve and polynomial of 15MV QED diode at 21CR(Ham).	40
Figure 4.21 (a) The fitted curve and polynomial of all 6MV diodes at MBPCC. (b) The fitted curve and polynomial of all 18MV diodes at MBPCC.	45
Figure 4.22 (a) The fitted curve and polynomial of all 6MV diodes, with diode factors included. The diode factors are 1.0, 0.732, 1.072, 1.160 for 21C(BR), 20CR(Ham), 600C(BR), 21EX(COV), respectively. (b) The fitted curve and polynomial of all 18MV diodes, with diode factors included. The diode factors are 1.0, 0.908 for 21EX(COV) and 21C(BR), respectively.	46
Figure 4.23 The SSD dependence of diodes for 6MV open field with 10x10 FS.	46
Figure 4.24 The FS dependence of diodes for 6MV open field with 100 SSD.	47
Figure 4.25 The SSD dependence of diodes for 18MV 60 degree wedged field with 10x10 FS.	47
Figure 4.26 The FS dependence of diodes for 18MV open field with 100 SSD.	47
Figure 4.27 The FS dependence of Isorad-p diode (21C) for 18MV wedged fields with 100 SSD. One for 30 degree narrow wedge, another one for 30 degree wide wedge.	48
Figure 4.28 Off-axis correction for 4MV diode with 60° wedged field at 21EX(BR), where ‘-’ corresponds skinny side of the wedge. 100 SSD, 15x15 FS.	50

Figure 4.29 Diode correction factors of 6MeV electrons as a function of the SSD, for entrance measurements. QED electron diode at 2000CR(Ham).	51
Figure 4.30 Diode correction factors of 6MeV electrons as a function of the SSD, for entrance measurements. QED electron diode at 21EX(BR).	52
Figure 4.31 Diode correction factors of 9MeV electrons as a function of the cone size, for entrance measurements. SSD = 100 cm.	52
Figure 4.32 Diode correction factors of 9MeV electrons as a function of the cone size, for entrance measurements. QED electron diode at 21EX(BR).	53
Figure 4.33 The fitted curve and polynomial of 6MeV QED diode at 20CR(Ham).	53
Figure 4.34 The fitted curve and polynomial of all 6MeV data.	54
Figure 4.35 The fitted curve and polynomial of all 9MeV data.	54
Figure 4.36 The fitted curve and polynomial of all 12MeV data	55
Figure 4.37 The fitted curve and polynomial of all 16MeV data.	55
Figure 4.38 The fitted curve and polynomial of all 20MeV data.	55

Abstract

An in vivo dosimetry system that uses p-type semiconductor diodes with buildup caps was characterized for clinical use. The dose per pulse dependence was investigated. This was done by altering the source-surface distance (SSD), field size and wedge for photons, and by altering SSD and cone size for electrons. The off-axis correction and effect of changing repetition rate were also investigated. A model was made to fit the measured diode correction factors.

Chapter 1

Introduction

After x-rays were discovered by Wilhelm Conrad Roentgen in 1895, the ionization radiation has been used for the treatment of cancer. Nowadays, surgery, radiotherapy and chemotherapy are the three main methods for treating cancer. The radiotherapy consists of teletherapy and brachytherapy. Teletherapy mainly applies high energy photons or electrons from a medical linear accelerator to treat the tumor from different directions, while brachytherapy mainly applies radioactive seeds to treat the tumor. Here only teletherapy is considered.

The medical linear accelerator (Linac) is the most widely used device for external beam radiotherapy. The Linac beam delivery system includes gun, guide, bending magnet, target, flattening filter, monitor ionization chamber and mobile collimators [1]. The aim of radiotherapy is to deliver a high dose to the target while delivering the lowest possible dose to the surrounding healthy structures. Conformal therapy and intensity modulated radiation therapy (IMRT) greatly improve the ability to reach this aim.

Experimental and clinical evidence shows that small changes in the dose of 7% to 15% can reduce local tumor control significantly [26]. So the International Commission on Radiological Units and Measurements (ICRU) recommends that the dose delivered to a tumor be within 5.0% of the prescribed dose [27].

Each of the many steps in the treatment planning and execution will contribute to the overall uncertainty in the dose delivered. Therefore, some organizations (AAPM [28], ICRU [27]) recommend that *in vivo* dosimetry (i.e. assess the dose directly in the patient)

should be made. *In vivo* treatment verification includes geometrical and dosimetrical verification.

The geometry, i.e. the patient anatomy and tumor location, can be obtained by using a simulator, CT or MRI. Usually the CT and/or MRI data (image fusion) are used to design the 3D treatment plan with a computer treatment planning system. However, due to setup errors and internal organ motion, the planned high dose volume may not agree with the target very well. The laser alignment system, immobilization system etc. can reduce the setup and motion errors effectively, and portal imaging and electronic portal imaging devices (EPIDs) can be used to check the position of a patient during the irradiation. However, internal organ motion is somewhat difficult to control and check. The typical examples are the lung and the prostate. Their movements are up to several centimeters. Some techniques are used to reduce the effect of the motion, say, the rectal balloon technique and respiratory gated therapy, however this may still not give sufficient accuracy. Generally IMRT is not suitable for lung cancer, since IMRT conforms to the target very well and the internal motion will lead to a bad results: some surrounding healthy structures may get too high dose while some parts of the tumor get too low dose. Researchers have been working on this, and a new real-time tracking system was introduced [29]. The method is to implant a x-rays opaque (golden) seed into the patient first, near or within the tumor, and then use a fluoroscopic x-ray system to track the golden seed and therefore track the motion of tumor. Similar image guidance technology is also used on the CyberKnife[®] system [30], the only Stereotactic Radiosurgery (SRS) system that tracks patient and lesion positions during treatment. Real time image-guided radiotherapy is one of the main trends for next generation systems.

The dosimetric treatment verification is also very important. Each step can contribute to the final dose uncertainty, for example, geometry errors mentioned above, errors introduced by transferring treatment data from the treatment planning system or simulator to the accelerator, errors of beam setting, etc. The final accuracy of the dose delivered can only be checked directly by means of *in vivo* dosimetry.

The most commonly used detector types for *in vivo* dosimetry are diodes and thermoluminescence dosimeters (TLD). The diode is superior to TLD, since the diode measurements can be obtained on line and allow an immediate check. Other advantages of diodes include high sensitivity, good spatial resolution, small size, simple instrumentation, no bias voltage, ruggedness, and independence from changes in air pressure [21]. The sensitivity relative to the ionization volume is high for a semiconductor, about 18,000 times higher than for an air ionization chamber. The average energy required to produce an e^- -hole pair in silicon is only 3.5eV compared with 34eV in air. The sensitive volume can thus be small, and hence the diode detector has high spatial resolution [3]. However, there are many factors that can affect the response of the diode to radiation, and diodes are different from one to another, even from the same batch, same model and same manufacturer. So the commissioning or characterization of every diode individually is necessary for accurate dosimetry [12,13].

The silicon diodes can be made of n-type or p-type silicon. A semiconductor with an excess of electrons is called an n-type semiconductor, while one with an excess of holes (electron deficits) is called a p-type semiconductor. Normally a pure silicon crystal has an equal number of electrons and holes. To make an n-type or a p-type silicon, certain impurities need be added into the pure crystal [31]. Silicon is in group IV in the periodic

table. If atoms in group V, each of which has five valence electrons, are added to the pure silicon, then there will be an excess number of electrons and finally results in n-type silicon. Similarly, a p-type silicon can be made by adding an impurity from group III to the pure silicon. Generally the impurities used are phosphorus from group IV and boron from group III.

One of the crucial keys to semiconductor detectors is the nature of the P-N junction. When p-type and n-type materials are placed in contact with each other, the junction behaves very differently than it does with either type of material alone. Specifically, current will flow readily in one direction but not in the other, creating the basic diode.

If the n region is connected to the positive terminal and the p region to the negative, which is known as reverse bias, almost no current (except for a very small current due to thermally generated holes and electrons) flows across the junction. Under this condition, the resistance of the p-n junction is very high, and almost all potential difference falls on the p-n junction, thus creating a strong electronic field in the p-n junction. The region around the junction is swept free by the potential difference. This region in a semiconductor that has a lower-than-usual number of mobile charge carriers is called the depletion layer. The depletion layer is the sensitive volume of the semiconductor detector [31]. The diodes are used without bias voltage in radiotherapy.

The charge collection process is described in the following way [21,22]:

- When an ionizing particle passes through the depletion layer, primary or secondary particles from the radiation source are absorbed, generating electron-hole pairs throughout the diode.

- By diffusion, those electrons and holes generated within one diffusion length from the junction will be able to reach the junction.
- The built-in potential across the p-n junction then sweeps the electrons and holes apart and to the opposite sides, giving rise to a pulse in the external circuit.

Some of the radiation generated electron-hole pairs will recombine through the recombination centers. When the instantaneous dose rate (dose per pulse) increases, the generated carrier concentration increase proportionally. Then the recombination centers are becoming saturated and recombination portion decreases. This portion, which is not recombined, will contribute to the signal, therefore the diode detector sensitivity increases. Generally p type diodes have lower instantaneous dose rate (dose per pulse) dependence than n type [21,22].

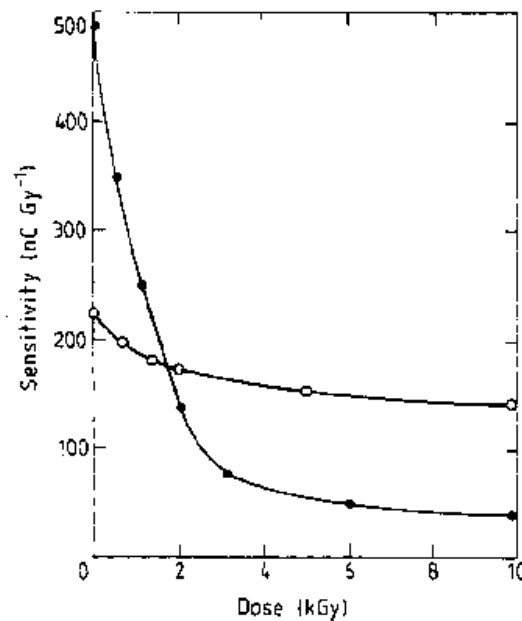


Figure 1.1 Sensitivity variation with pre-irradiation dose with 20 MeV electrons for an n type (●) and a p type (°) diode detector [3].

Not only is the diode detector dependent on the dose per pulse, but also it is dependent on the accumulated dose. Because radiation dose introduces defects in the semiconductor and thus forms more recombination centers and traps, the diode detector sensitivity decreases with the accumulated dose. From the Fig 1.1, one can see that generally the p type diode has lower sensitivity variation with the accumulated dose. For both types of diode detectors, the sensitivity degradation will slow down with accumulated radiation. These are the reasons why QED and Isorad-p detectors are pre-irradiated p type diode detectors. This will greatly reduce the calibration frequency of the detector [21].

Diode current generated by sources other than radiation, say, heat and light, is considered to be leakage current. The leakage current depends on the temperature. The diode current generated by radiation is also temperature dependent. The sensitivity of the diode detectors increases with the increase of temperature [32]. Ref [32] has shown that the sensitivity variation with temperature of a p type silicon detector increases linearly with increasing temperature.

Since the buildup materials and the encapsulation materials are not water equivalent, there are interface phenomena. The shape and geometry of the diode and p-n junction also affect diode's response to radiation. Both of the above two factors give rise to directional dependences [3].

The aim of the thesis is to characterize an *In Vivo* Diode Dosimetry System for Clinical Use. A model will be made to find the total correction factors (Correction Factor = Dose at Diode/(Diode reading)), for the diodes readings for given modality (photons or electrons), given energy, given SSD, given field size (cone size), given diode and

machine, and given wedge. The final diode correction factors will be made as lookup tables, and will also be programmed by using Microsoft Excel and FORTRAN.

Chapter 2

Literature Review

The first paper that introduced the silicon diode detectors into radiotherapy is Ref [2]. In recent years, encouraged by the work of Riker *et al* [3] the use of semiconductor diode detectors for in vivo dosimetry has been extensively investigated [2-20].

Diode in vivo dose measurements can be made at three positions:

(1) Beam entrance [5,9,13,15,19]

The diode is placed at the entrance points only. Entrance measurements give a check of correct settings of beam parameters such as energy, collimator jaw settings, monitor units given, source-to-distance (SSD), customer blocks, wedges used, and compensators. Entrance measurements minimize the extra workload for the staff and extra setup time. The basic idea is to calibrate the diode first and then use various calculation methods to obtain the target dose. Correction factors are needed. This method is the most popular and is the topic of this thesis.

(2) Beam exit [6,7,10]

The diode can be placed at the exit point. Theoretically exit measurements can check all of the parameters mentioned above for entrance measurements, plus changes in patient thickness, contour errors, problems with CT data transfer or CT miscalibration (inhomogeneities in tissue). However, there are some reasons for avoiding the exit position measurements. For example, there are much better more direct methods than in vivo diode measurements to provide quality assurance checks for CT and treatment planning system. These quality assurance methods should be applied long before an in vivo diode measurement is made [13]. In addition, there is

the problem of reduced backscattered radiation. Most computer treatment planning systems assume the exit dose as the dose on a depth dose curve without taking into account the finite extent of the patient. One way to solve this problem is described in Ref [11]. One can compare the readings of diode and ion chamber to get a calibration factor: $CF=D/R$, where D is the absorbed dose measured with the ion chamber, R is the diode reading (the inverse square factor is not employed). The exit factor is

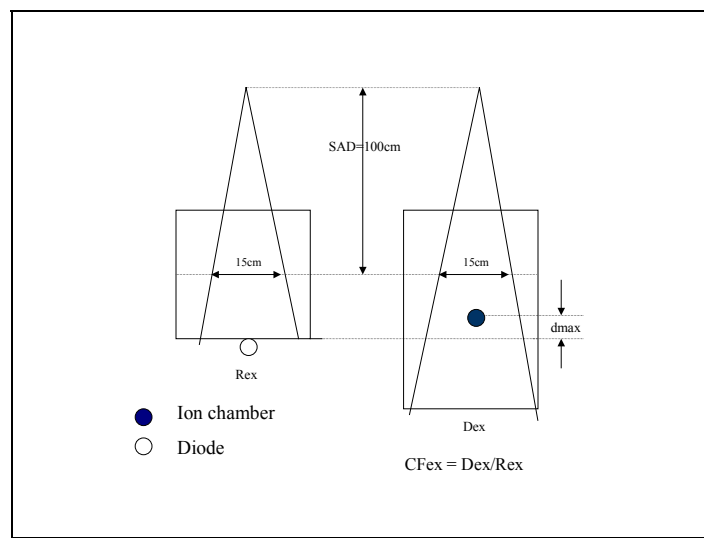


Figure 2.1 Determination of the exit calibration factor for the diode.

measured under condition of full backscatter for the chamber (Fig. 2.1) to take into account the loss of backscatter for patient while the computer dose calculations are valid for semiinfinite patients implying full backscatter at the exit surface.

(3) Both beam entrance and beam exit [8,10,11,15]

Theoretically this way is the best method. However, practically, not many institutions employ a diode in vivo system in this manner. The reason is evident: for a busy department, performing both entrance and exit measurements may increase the overall treatment time unacceptably.

Since diode response for radiation dose rate is nonlinear, and diodes have many characteristics that are very different from the ion chambers, the commissioning (or characterization) of the diodes is essential before clinical use. There are many papers [7-11,13-20] that address these aspects of diodes.

(1) Linearity:

Under the conditions of fixed SSD and FS, diode measurements are taken with different numbers of monitor units. The linearity of diodes is very good: the standard error of the line is less than 0.1% [15].

(2) Dose per pulse dependence

There is a relationship between diode response (or correction factor) and the dose-per-pulse. Dose-per-pulse is not the clinically used dose rate. The clinical dose rate is an average dose rate. For example, for 6 MV X rays with a pulse duration of 5 μ s, 1Gy at Source axis distance (SAD) = 100 cm was delivered with 3550 pulses, so the dose-per-pulse is 1Gy/3550pulses = 2.8×10^{-4} Gy/pulse. However, the clinical dose rate is about 1.0cGy/MU.

The dose-per-pulse and clinical dose rate is a function of the source-to-surface-distance (SSD). Sometimes the gun current can be adjusted on the Linear accelerator to deliver a different dose per pulse (especially for higher dose-per-pulse values).

Grussell and Rickner hypothesized [3] that dose rate dependence is associated with preirradiated n-type Si diodes and no dose rate dependence would be expected for p-type diodes. However, actual measurements indicated that both n- and p-type of

diodes have dose per pulse dependence, although the dependence for n-type diodes is greater [14].

(3) Field size dependence

For high energy photon beams, backscattering is negligible and almost all scattered photons come from the overlying layers [19]. So as the diode is placed on the phantom surface, the reading of the diode is virtually independent of the phantom scatter and only sees the head scatter. Therefore, the phantom scatter factor S_p should not be included in the calculation of the dose to the diode. Because S_p increases when the FS increases, we would expect that the FS correction factor of diode to increase when the FS increases. However, both increases and decreases were found with changes in field size [14].

(4) SSD dependence

Generally the diode correction factor increases when SSD increases [11,13-15]. That is, diodes tend to underestimate the dose when SSD increases.

(5) Energy dependence [11]

Diode response to radiation depends on energy. The calibration of the diode need be performed individually for each energy.

(6) Temperature dependence

Depending on the amount of pre-irradiation, the temperature correction of the Scanditronix diodes can be up to 3.5% if the diode is positioned on the patient skin and calibrated at room temperature [12]. For Sun Nuclear Corporation QED and Isorad diodes, the temperature dependence is small, just 0.3% per degree Celsius [12,13].

(7) Directional dependence [21,22]

Just as what described in the Chapter one, both of interface phenomena and the shape and geometry of the diode give rise to directional dependences. If the incident beam is not perpendicular to diode, the diode reading may be smaller or larger than that of perpendicular beam.

(8) Wedge correction factors

The wedges decrease the dose per pulse and also change the beam quality, consequently, they change the diode response. So wedge correction factors must be considered [12,14,15].

(9) Cumulative dose dependence [12]

As the cumulative dose to a diode increases, the diode sensitivity decreases. This will decide how often to re-calibrate the diode.

(10) Tray correction factor

The use of trays to support blocks modifies the incident photon fluence by producing scattered electrons. This correction is usually within 2% [14].

(11) Off-axis correction

Off-axis corrections are large for wedged fields and low energy photons [12,15].

There are primarily two published methods to obtain the actual dose from the diode reading.

One method is to make measurements varying each of above conditions, and find various diode correction factors, C_i , for each of the non-reference conditions, e.g., C_{SSD} ,

C_{FS} , etc. The correction factors are obtained by comparing readings from the diode and from the ion chamber under various non-reference conditions. That is

$$\text{Correction Factor} = \text{Dose at Diode}/(\text{Diode reading});$$

After obtaining all correction factors, for any actual clinical situation the “expected” diode reading R is calculated by

$$\begin{aligned} \text{Diode Expected Rdg} &= \text{Dose} * (\prod C_i)^{-1} \\ &= \text{Dose} * (C_{SSD} * C_{FS} * \dots)^{-1} \end{aligned}$$

Another method, which requires the similar measurements but is conceptually different. The basic idea is to find all or most physical quantities (or physical parameters) for the diode itself, not for ion chamber. This skips the step of determining diode correction factors that were obtained by comparing the readings of the diode and an ion chamber, and directly uses the physical quantities measured using the diode. One such example is detailed in Ref [13], which used the following formula

$$\begin{aligned} \text{Diode Rdg} &= MU * DCF * DWF * TEMPF * SSF * DOF(FS_{coll}) \\ &\quad * [(100/SSD)^2 * TBF * CF]^{n+1} \end{aligned}$$

where MU is the number of monitor units, DCF is the diode calibration factor, DWF is the surface-scatter-factor, SSF is the surface-scatter-factor, DOF is the output factor measured with the diode (Field size dependence), TBF is the block tray factor, and CF is the compensator factor. The “ n ” in the above formula is the fitting parameter that arose from the dose-per-pulse dependence the author found:

$$\text{Diode Rdg}/\text{dose-per-pulse} = (\text{dose-per-pulse})^n$$

Most of these quantities are for the diodes, and not applicable to ion chamber responses. In particular note that the DCF above is the “Diode Calibration Factor”.

However, in this thesis and in many publications the DCF also is used with a different meaning: “Diode Correction Factor”.

Summary, the second method tends to use quantities measured with and for the diode itself directly, in a similar way ion chamber corrections are determined.

All of above are for photons. There also are a few papers [12,16,17,20] on diode *in vivo* electron dosimetry. Similar to diode *in vivo* photon dosimetry, diodes for electrons need be calibrated under a reference condition and commissioned. The commissioning is similar to that of photons. One must determine the dose per pulse dependence, cumulative dose dependence, temperature dependence, directional dependence, field size dependence, energy dependence, the influence of the electron cut-out (insert), and the dose perturbation behind the diode detector. The dose reduction behind the diode detector for electrons can be as large as 25% [12] for some types of diodes, especially for low energies and small field size, say 6MeV and 3cm diameter circular field. Only entrance measurements are used for electron *in vivo* dosimetry.

Chapter 3

Materials and Methods

The Mary Bird Perkins Cancer Center has five Linear accelerators. They are Varian 600C, Varian 2100EX(Baton Rouge), Varian 2100C, Varian 2100EX(Covington), Varian 2000CR(Hammond) (Varian Oncology System, Palo Alto, CA). For photons, Varian 600C is used at a single energy: 6MV, and all other Linacs are used at dual energies. They are 6MV and 18MV for Varian 2100C and Varian 2100EX(Covington); 4MV and 10MV for Varian 2100EX(Baton Rouge); 6MV and 15MV for Varian 2000CR(Hammond). Except Varian 600C, all other four Linacs are operated at five electron energies: 6MeV, 9MeV, 12MeV, 16MeV and 20MeV.

The in vivo diode systems implemented at the Mary Bird Perkins Cancer Center are all IVD Model 1131 (Sun Nuclear Corporation, Melbourne, FL) (Fig. 3.1), and all



Figure 3.1 IVD Model 1131.

diodes are of p-type, since p-type diodes are generally better than n-type diodes in radiation measurements [3,21,22]. Except Varian 600C, which is equipped with one Sun Nuclear Corporation QED diode for photons, each other Linac is equipped with three Sun Nuclear Corporation diodes, two for photons and one for electrons. Except the Varian 2100C, which has two Sun Nuclear Corporation Isorad-p p-type photon diodes, all other

Linacs have two Sun Nuclear Corporation QED photon diodes. QED diodes and Isorad-p diodes are showed in Fig. 3.2. Every Linac has just one electron diode, QED electron diode, which is used for all five electron energies. This is different from the photon diodes, which each photon diode is used just for one photon energy.



Figure 3.2 QED diodes and Isorad-p diodes.

The QED photon diodes are constructed with internal build-up (aluminum or brass) for three energy ranges of 1-4MV, 6-12MV and 15-25MV, which are color-coded blue, gold and red, respectively. The only one QED electron diode is constructed with acrylic internal build-up for all electron energies. All diodes are connected to a dedicated IVD electrometer. The Isorad-p photon diode detectors are designed with cylindrical symmetry, which can be beneficial in some applications, such as tangential treatments. Besides aluminum and brass, the internal build-up materials of Isorad-p still include tungsten. There is no Isorad-p electron diode, otherwise the dose reduction behind the diode detector would be too large to be acceptable. All phantom measurements were made on the RMI 30x30 cm² Solid Water (GAMMEX RMI, WI). The diode was taped on the surface of the solid water, with the buildup side facing the beam.

To use the IVD for in vivo dosimetry, the calibration must be done first. That is, a calibration factor, CF, must be determined for each diode detector positioned in reference (standard) conditions in the beam. The calibration can be done as follows.

- (1) Determine the dose at the d_{\max} on the central axis using a calibrated ion chamber.

For convenience the phantom is usually a plastic phantom. For this work solid water phantom (GAMMEX RMI, WI) was used. Usually the reference setup is a Gantry of 180 degree, SSD of 100 cm, field size of $10 \times 10 \text{ cm}^2$ (or cone size of $10 \times 10 \text{ cm}^2$) and 100 monitor units. Since the Linacs at MBPCC are calibrated and the constancy check is done every day, using a calibrated chamber to determine the actual dose at d_{\max} was not performed. All Linacs here are calibrated to give 1.00cGy/MU at d_{\max} .

- (2) With the same setup, tape the diode on the top of the phantom and also on the central axis of the beam. The internal build-up in the diode should be sufficient to absorb electron contamination, and provide electron equilibrium. Flat diodes, such as QED diodes, should be positioned with the flat surface on the phantom and the build-up side facing the beam. Measure the diode reading for the same irradiation as in step (1).
- (3) The calibration factor can be obtained by finding the ratio of the readings from the ion chamber and the diode. This is done automatically by the IVD software.
- (4) Using this ratio, the diode has been calibrated to read the dose at d_{\max} below the surface, since no inverse square was used to compensate for the slight difference of the diode position. This is the method described in the IVD dosimeter manual [23], and many institutions use the diodes in this fashion.

(5) However, the protocol at the Mary Bird Perkins Cancer Center employs the inverse square factor account for the difference of the position of the diode being different than d_{\max} . Although conceptually more satisfying, the second method is equal to the first. Both methods suffer because the internal buildup of the diode is not accurate. For example, the 6-12MV use the same one diode, i.e. use the same buildup thickness.

(6) Since all Linacs at MBPCC are calibrated to give 1.00cGy/MU at d_{\max} , the dose at the diode, which is at the surface of the solid water, can easily obtained by hand calculation. For example, 6MV photons with d_{\max} of 1.5 cm, the dose rate at the diode is

$$((100 + 1.5)/100)^2 = 1.03 \text{ cGy/MU}.$$

For electron beams, the effective SSD, instead of the SSD, should be used. For example, 9 MeV electrons (on the 21EX BR) have an SSD_{eff} of 86.3 cm with a 10 x 10 cone and a d_{\max} of 2 cm, so the dose rate at the diode is

$$((86.3 + 2)/86.3)^2 = 1.047 \text{ cGy/MU}$$

(7) The calibration factor is verified on a regular basis, because radiation damage affects the diode sensitivity. For p-type diodes, a re-calibration will be necessary after about one kGy. Re-calibration has to be performed much more frequently for n-type diodes due to their faster decrease in sensitivity.

Besides a calibration factor, determined under reference conditions, correction factors have to be applied for accurate dosimetry. They originate from the variation in sensitivity of the diode with dose per pulse, the photon energy spectrum, the temperature, and from directional effects.

Since linearity, temperature dependence, directional (angular) response, radiation damage response, etc. of diodes have been extensively studied [4-20], and the sensitivity of the diode to these effects can be reliably obtained from the company's product manuals, this thesis centered on dose rate dependence and off-axis corrections. Because the dose per pulse can be altered by SSD, field size and choice of wedge, they were investigated one by one. The linacs and the modalities and energies that were used are tabulated in the Table 3.1.

For each photon energy of every Linac, measurements were made to obtain the diode correction factors for different SSDs and different FSs. A example for open fields (i.e. without wedge) is given in Table 3.2.

Table 3.1 Linacs, modalities and energies at MBPCC.

	<i>600C(BR)</i>	<i>2100C(BR)</i>	<i>2100EX(BR)</i>	<i>2000CR(Ham)</i>	<i>2100EX(Cov)</i>
<i>Photons</i>	6MV	6MV	4MV	6MV	6MV
		18MV	10MV	15MV	18MV
		6MeV	6MeV	6MeV	6MeV
		9MeV	9MeV	9MeV	9MeV
<i>Electrons</i>		12MeV	12MeV	12MeV	12MeV
		16MeV	16MeV	16MeV	16MeV
		20MeV	20MeV	20MeV	20MeV

The same SSDs were used for wedged fields. However, the different FSs were used for wedged fields, since the FSs can be obtained for wedged fields are different from those of open fields. The FSs used for wedged fields are showed as Table 3.3, and the data collection table used for electrons is showed as Table 3.4.

In order to get more accurate results, the following procedure was followed. Prior to making measurements, the Linac(s) that were used were checked, e.g., by checking the

Table 3.2 Diode correction factors data collection table for open fields of photons, where 5 x 5 is the field size in cm², and 70 is the SSD in cm.

	<i>5 x 5</i>	<i>10 x 10</i>	<i>20 x 20</i>	<i>40 x 40</i>
<i>70</i>				
<i>80</i>				
<i>90</i>				
<i>100</i>				
<i>110</i>				
<i>120</i>				

Table 3.3 The field sizes used for wedged fields.

<i>Wedge</i>	<i>Field Size</i>
<i>15° Narrow</i>	5x5 10x10 20x20
<i>15° Wide/upper/lower</i>	5x5 10x10 20x20 30x30
<i>30° Narrow</i>	5x5 10x10 20x20
<i>30° Wide/upper/lower</i>	5x5 10x10 20x20 30x30
<i>45° Narrow/upper/lower</i>	5x5 10x10 20x20
<i>60° Narrow/upper/lower</i>	5x5 10x10 15x15

constancy log book, to ensure that the outputs of Linac(s) were within specification. For Linac(s) restarted from standby status, the morning checkup and warm up procedure were done. Ideally, the diode *in vivo* system(s) that will be used should also would be checked

for its calibration. Even better would be to re-calibrate the diode system every time prior to making measurements.

Table 3.4 Data collection table used for electrons, where 6x6 is the cone size in cm² and 105 is the SSD in cm.

	<i>6 x 6</i>	<i>10 x 10</i>	<i>15 x 15</i>	<i>20 x 20</i>	<i>25 x 25</i>
<i>97/97.5</i>					
<i>100</i>					
<i>105</i>					
<i>110</i>					

In order to get accurate SSDs, the couch height readings on the console monitor should be used, since the optical distance indicator (ODI) is not accurate for SSDs far from 100 cm. The couch table readings are more accurate. Similarly, the couch table lateral/longitudinal (LAT/LNG) readings should be used for off-axis measurements. That is, the table is moved instead of the diode itself. This is very important for wedged fields, since, a 1 mm deviation of the diode's position could lead to a deviation as large as 1% in diode readings in a 60° wedged field.

Based upon experience, it is better to complete one entire group of data (the data in Table 3.3) as quickly as possible. This reduces the error caused by the drift of the diode system. The main source for the drift of the diode system is the relative short life of the system batteries. It was determined that the readings of a diode shortly before the death of the batteries and the first several readings of newly recharged system were not accurate. So it is recommended to finish one group of data before recharging the batteries.

Sometimes the data for several groups were measured in the same day. For example, the data for open, 15° wedged, 30° wedged, 45° wedged, 60° wedged fields of 2000CR(Ham) 6MV were taken in one day. Even though we re-calibrated the diode system before taking a single day's measurements, it was found that there were the drifts between measurements. Unfortunately the batteries can just last only one to three hours, and the recharging was needed several times per day. Therefore, the data of different groups were adjusted to remove the effect of the diode system's drifts. Because the data of every group were taken without recharging the batteries, the adjustments were needed only between data of different groups.

The method that was used to adjust the data is useful for all situation, both for data taken on the same day and data taken on different days. By way of example, suppose we want to adjust the data for open, 15° wedged, 30° wedged, 45° wedged, 60° wedged fields of 2000CR(Ham) 6MV that were taken over a period of several days. To adjust these data, readings are taken in one session with $FS = 10 \times 10 \text{ cm}^2$, $SSD = 100 \text{ cm}$, and $MU = 300$, and diode readings for open, 15° wedged, 30° wedged, 45° wedged, 60° wedged fields of 2000CR(Ham) 6MV. Usually these measurements can be finished in less than 10 minutes, and the drift of the diode system can be neglected. From the five readings obtained above, we can get the ratios between the reading of wedged fields to that of the open field. However, we can also have the similar ratios from the data of groups to be adjusted. We assume that the ratios from the data of groups may be inaccurate, and therefore use the ratios from the single session to adjust them. The rest of the data can then be adjusted accordingly.

In our experience this adjustment could be as large as 2%, even all data were collected in one day.

The Diode Correction Factor (DCF) used in this thesis is defined as

$$DCF = Dose\ at\ Diode / Diode\ Reading$$

Since for photons

$$Dose\ Rate = \dot{D}_{ref} * Sc * Sp * TMR * ISF * WF * OAF$$

where $\dot{D}_{ref} = 1.000\ cGy/MU$ at $100 + d_{max}$ cm, Sc is collimator scatter factor, Sp is phantom scatter factor, TMR is the tissue maximum ratio, ISF is the inverse square factor, WF is the wedge factor, and OAF is the off axis factor, one gets

$$\begin{aligned} Dose\ at\ Diode &= MU * 1.000 * Sc * Sp * 1.0 * ((100 + d_{max})/SSD)^2 * WF * OAF \\ &= MU * Sc * Sp * ((100 + d_{max})/SSD)^2 * WF * OAF \end{aligned}$$

Thus

$$DCF = MU * Sc * Sp * ((100 + d_{max})/SSD)^2 * WF * OAF / Diode\ Reading$$

Generally OAF will not be considered, therefore,

$$DCF = MU * Sc * Sp * ((100 + d_{max})/SSD)^2 * WF / Diode\ Reading$$

Since the solid water used for all measurements is $30 \times 30\ cm^2$, the largest effective FS used for Sp is $30 \times 30\ cm^2$. In this thesis the DCFs are a function of three variables: SSD, FS, and Wedge. Typically the correction factors are linearly independent. For example if one determines a correction factor for field size, C_{FS} , and one for SSD, C_{SSD} , the total diode correction factor for specific FS and SSD is

$$C_{SSD\&FS} = C_{SSD} * C_{FS}$$

However, the method used in this thesis does not rely on this assumption. Instead correction factors for FS, C_{FS} , were determined for different SSDs instead of just for one

fixed SSD, say, 100 cm. Similarly, C_{SSD} was also be found for different FSs instead of for just one fixed FS. This is due to considering the fact, that $C_{FS} * C_{SSD}$ is not necessarily equal to $C_{FS\&SSD}$.

In fact, due to the lack of overlying layers, contamination electrons and head scatter low energy photons, the diodes could overestimate or underestimate the dose as these complicating factors are dependent on FS and/or SSD. Thus the method used in this thesis is thought to be better.

Because the relationship between DCF and FS was found, the same relationship can be used (extrapolated) for blocked fields.

Since sometimes it is difficult to position the diode at the central axis of the beam accurately when taping the diode on the skin of the patients, it's necessary to find the deviation due to off-axis position, especially for the 60 degree wedge and low energies [12]. The off-axis diode corrections were investigated for 4MV with 60 degree wedge on the 21EX(BR).

According published data, the response of diode is dependent on dose per pulse instead of clinical dose rate (average dose rate). Measurements were taken to verify this. The method used was to change the repetition rate of the Linacs.

For electrons, only the dependencies of Cone Size and SSD were investigated. Since there was no dose data for insert factors available, the insert effect on DCF was not investigated. This is a topic for further investigation. The data collection table for electrons is as in Table 3.4. No assumption as to the linear combination of electron DCF was made.

The Diode Correction Factor (DCF) used in this thesis for electrons is the same as that for photons, that is

$$DCF = Dose\ at\ Diode / Diode\ Reading$$

Since for electrons

$$Dose\ Rate = \dot{D}_{ref} * Cone\ Ratio * ISF * Insert\ Factor * PDD$$

and

$$ISF = ((SSD_{eff} + d_{max}) / (SSD_{eff} + d_{max} + gap))^2$$

where \dot{D}_{ref} is calibrated as 1.000 cGy/MU at 100 + d_{max} cm. SSD_{eff} is the effective SSD.

If no insert was used:

$$\begin{aligned} Dose\ at\ Diode &= MU * 1.000 * Cone\ Ratio * ((SSD_{eff} + d_{max}) / (SSD_{eff} + gap))^2 \\ &\quad * 1.0 * 1.0 \\ &= MU * Cone\ Ratio * ((SSD_{eff} + d_{max}) / (SSD_{eff} + gap))^2 \\ &= MU * Cone\ Ratio * ((SSD_{eff} + d_{max}) / (SSD_{eff} + SSD - 100))^2 \\ &= MU * ((SSD_{eff} + d_{max} + SSD - 100) / (SSD_{eff} + SSD - 100))^2 \\ &\quad * (Cone\ Ratio * ISF) \end{aligned}$$

where $(Cone\ Ratio * ISF)$ are tabulated for each Linacs, and therefore

$$\begin{aligned} DCF &= MU * ((SSD_{eff} + d_{max} + SSD - 100) / (SSD_{eff} + SSD - 100))^2 \\ &\quad * (Cone\ Ratio * ISF) / Diode\ Reading \end{aligned}$$

After having obtained all the data, a model was created to fit the measured data. The Microsoft EXCEL was used since it is more available than other programs such as MATHEMATICA and MATLAB. In addition, a FORTRAN interpolation program [25] was also developed. This is attached as Appendix F and can be used to compare the EXCEL results if necessary.

The basic idea was to find some physically meaningful or like parameters, then perform a least squares fitting to describe the data. This also can be regarded as a multivariable (multidimensional) optimization problem. So generally any multidimensional optimization routine or software can be used to fit the data. One popular example is the Powell's method [25, pp406]. Because the number of variables used in the model is small, EXCEL worked effectively.

Chapter 4

Results and Discussions

I. Photons

Fig. 4.1 shows the diode correction factors (DCFs) for various source to surface distances (SSDs) for all diodes used at Mary Bird Cancer Center, but just for Field Size $10 \times 10 \text{ cm}^2$, where the DCF is defined as

$$DCF = \text{Dose at Diode} / \text{Diode Reading}.$$

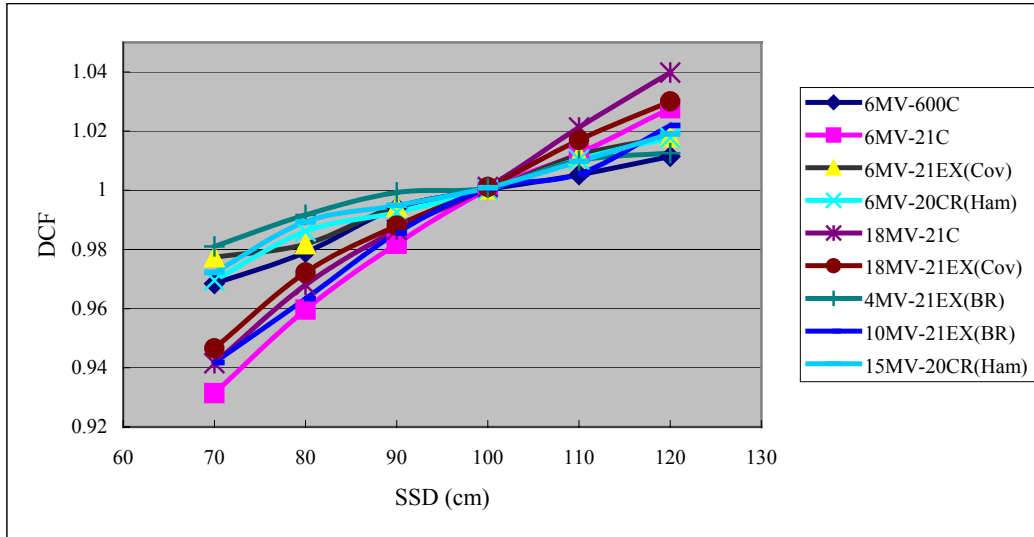


Figure 4.1 Diode correction factors as a function of the source to surface distance, SSD, for entrance measurements. All data in this figure are for open fields with field size $10 \times 10 \text{ cm}^2$.

Except the diodes for 21C(BR), which are Isorad-p photon diodes, all other diodes are QED photon diodes. Fig 4.1 shows that all diodes' DCFs, which were normalized to 1.0 for a 10×10 field at 100 SSD, decrease with decreasing SSD. This implies an over response of the diode with increased dose per pulse (decreased SSD). Two other factors also contribute to the diode response. First, the diodes and ion chambers have different energy responses, and second, when the SSD decreases, the number of contamination

electrons and head scattered low energy photons able to reach the sensitive part of the diode detector is larger, so the DCF, ratio of ion chamber and diode reading, decreases [11,14,15]. For 10 x 10 field size, the range for DCF is between 0.93 to 1.04, i.e. within 7%. For small SSD and FS, or large SSD and FS, the range is larger, say, DCFs for SSD = 70 cm and FS = 5 x 5 cm², and SSD = 120 cm and FS = 40 x 40 cm², 21C(BR)'s 18 MV Isorad-p photon diode, are 0.90 and 1.06, respectively.

Figure 4.2 shows the DCFs for various Field Sizes (FSs) for all diodes at SSD 100 cm.

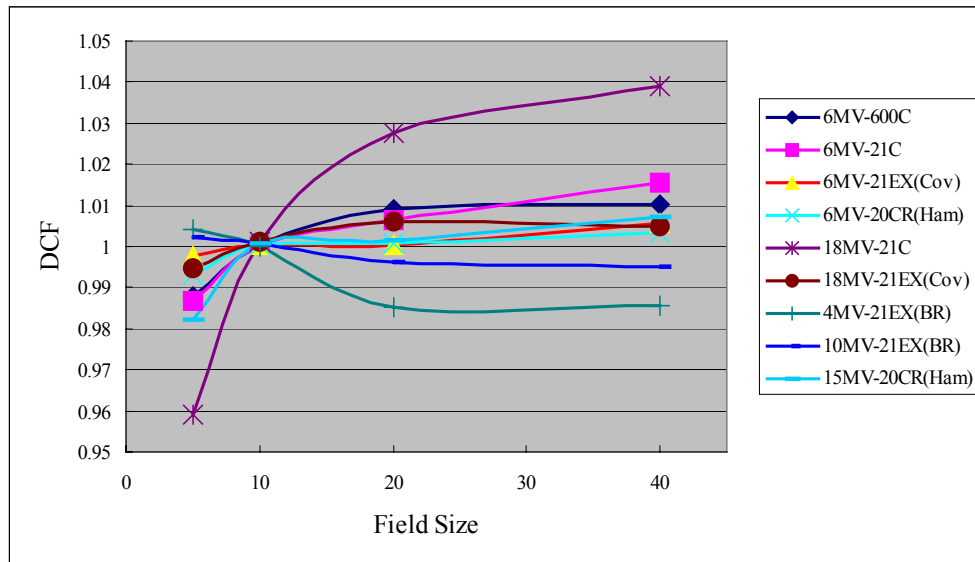


Figure 4.2 DCF as a function of the field size, FS, for entrance measurements. All data in this figure are for open fields with SSD 100 cm.

Generally the field size effect is due to the different irradiation conditions between the diodes and the ion chamber. Diode measurements are taken at the surface of phantom or skin, ion chamber measurements are carried out at depth. For low energy photon beams, scattered radiation from both overlaying and underlying material contribute to the diode and ion chamber readings. For high energy photon beams,

however, the backscattering is negligible and only scattered photons from the overlaying layer contribute to the diode and ion chamber readings. Since the diode is at the surface, and lacks of an overlaying layer, its reading is less dependent of the phantom scatter, and dependent heavily on head scatter. Therefore, DCF increases as the diode under responds with increase of field size [19, 11,14,15]. This happened for the majority of diodes used at MBPCC, except the two QED diodes for the 21EX(BR), one for 4MV and another for 10MV, this did not happen. In fact, the 4MV diode showed the opposite behavior, i.e. DCF decreased and diode over responded with increase of field size. For the 10MV diode, the DCF roughly remained a constant when FS changed. It was thought that the build up cap might not be thick enough to guarantee electronic equilibrium [14]. Some electrons scattered from accelerator head might reach the sensitive part of the diodes (the 4MV QED diode is blue colored, and is designed for 1-4MV photons. The total build up is 1.03 g/cm² Al [21]). In order to check this assumption, a small piece of solid water (5mm thick) was taped on the top of the 4MV QED diode, and then re-made the measurements. Because this time the total buildup was the solid water plus the build-in buildup of the diode, the total buildup thickness was great then d_{max} . However, the measurements indicated that the FS dependence of this 4MV QED diode was still the same as before, i.e., the DCF decreased with increasing of FS. So the above assumption is not right. The reason for this effect is unclear.

It was also noted that the 18MV Isorad-p photon diode of 21C(BR) is much more dependent on field size than other diodes. The change is up to 8% when Field size changes from 5x5 cm² to 40x40 cm² for open fields. This may be because Isorad-p diode gets less backscattering than QED diode due to the cylindrical shape.

Fig 4.3 shows the field size dependence of the QED photon diode of 20CR(Ham).

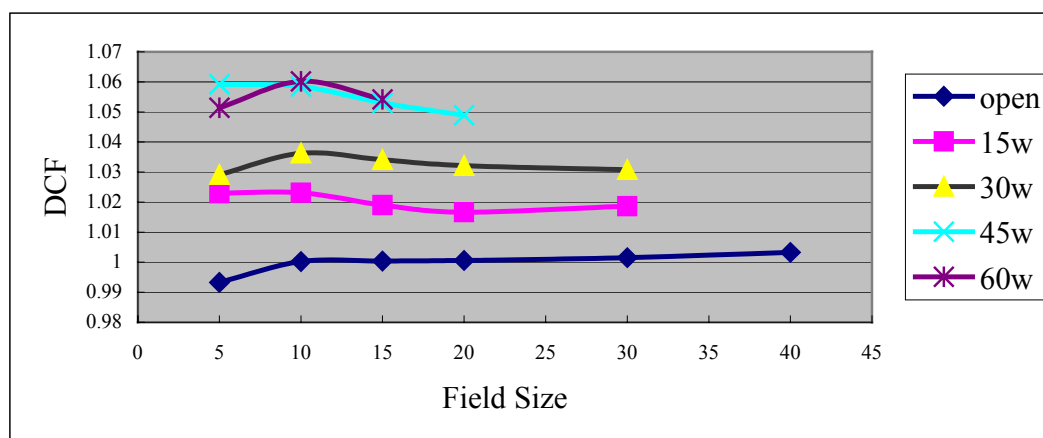


Figure 4.3 DCF of 6MV QED diode of 20CR(Ham) as a function of the field size, FS, for entrance measurements. All data in this figure are for SSD 100 cm.

The DCF of this diode doesn't change much when the field size changes. From this figure, one can see that DCF increases with wedge angle. This is because dose per pulse decreases with increase of wedge angle, and from Fig. 4.1, the decrease of dose per pulse (i.e. increase of SSD) leads to increase of DCF. Beam hardening also contributed to this effect. Fig 4.4 shows the field size dependence of another type of photon diode: 18MV Isorad-p photon diode. The field size effects are more significant than QED diode above. The field size dependences for open, 15 degree and 30 degree wedged fields are almost the same, but those for 45 degree and 60 degree wedged fields are larger, up to 6%.

However, it was found that DCF does not always increase with increasing of wedge angle, see Fig. 4.5. This might be due to the presence of contaminating electrons and head scattered low energy photons. Since the deviation was within 1%, it can be concluded that generally DCF increases with wedge angle increases, i.e. diodes under respond when wedge angle increases.

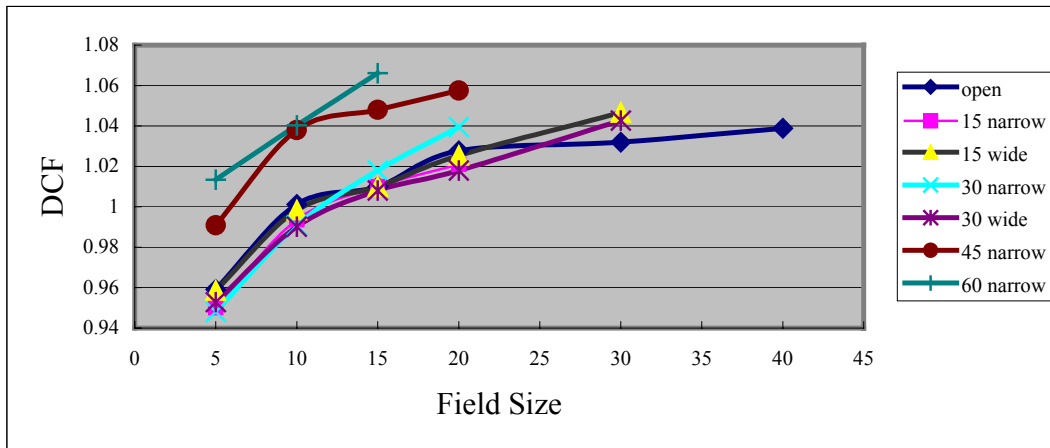


Figure 4.4 DCF of 18MV Isorad-p diode of 21C(BR) as a function of the field size, FS, for entrance measurements. All data in this figure are for SSD 100 cm.

Fig. 4.6 and 4.7 show the SSD dependence of open field and wedged fields for two energies: 6MV and 15MV. It can be seen that diodes still under respond with increase of SSD for wedged fields. This is primarily due to the dose per pulse change caused by SSD change.

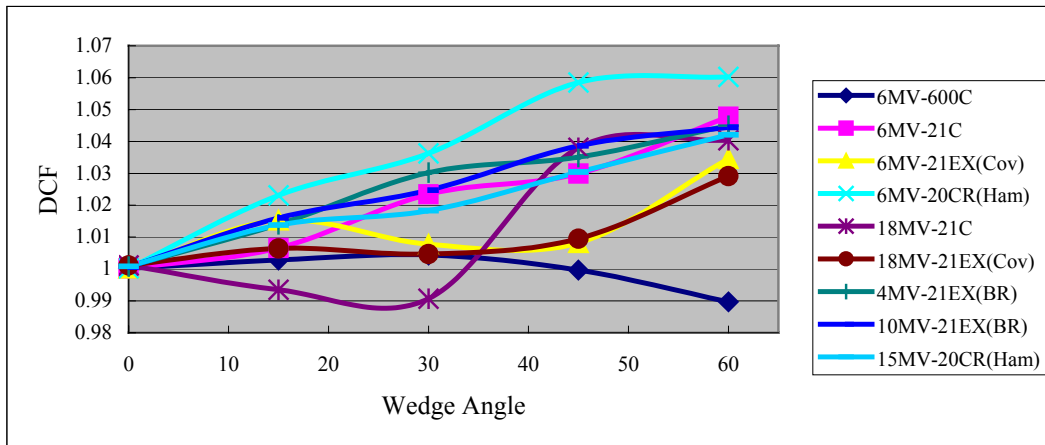


Figure 4.5 DCF as a function of the wedge angle for entrance measurements. All data in this figure are for SSD 100 cm and FS 10 x 10 cm², and only for narrow and upper wedges.

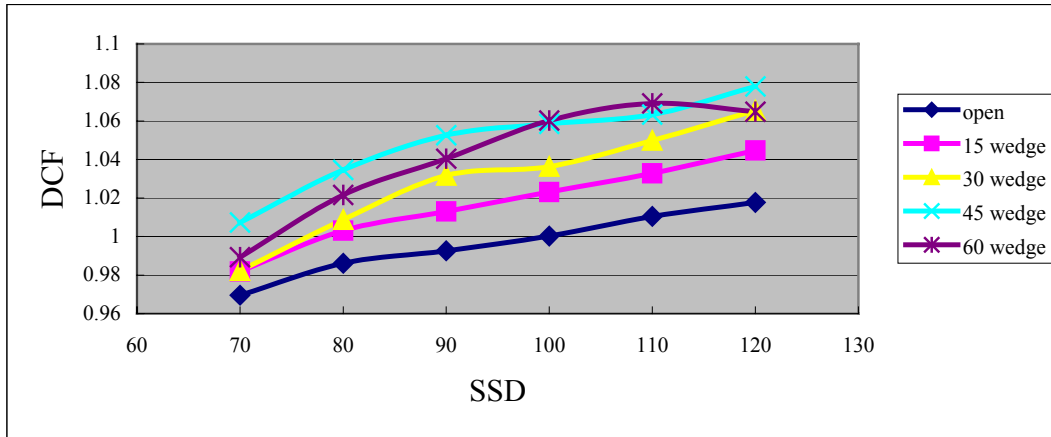


Figure 4.6 Diode correction factors as a function of the SSD for entrance measurements. All data in this figure are for field size $10 \times 10 \text{ cm}^2$. (6MV QED photon diode of 20CR(Ham)).

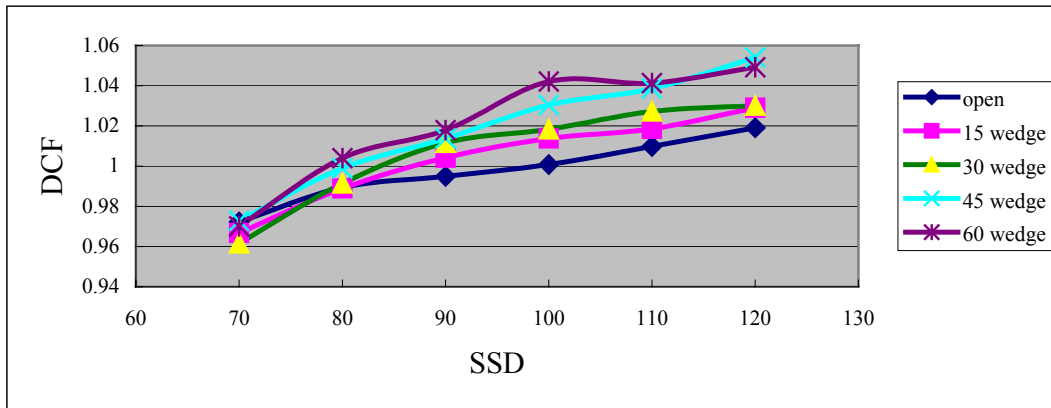


Figure 4.7 Diode correction factors as a function of the SSD for entrance measurements. All data in this figure are for field size $10 \times 10 \text{ cm}^2$. (15MV QED photon diode of 20CR(Ham)).

Fig. 4.8 shows the "wedge factors" for diode. They are not the ordinary wedge factors measured using ion chamber. The wedge factor for diodes used here is the ratio of diode reading with wedge over that without wedge. It is easy to see that wedge factors for diode decrease with increase of SSD. This property was used to fit the data and will be described later.

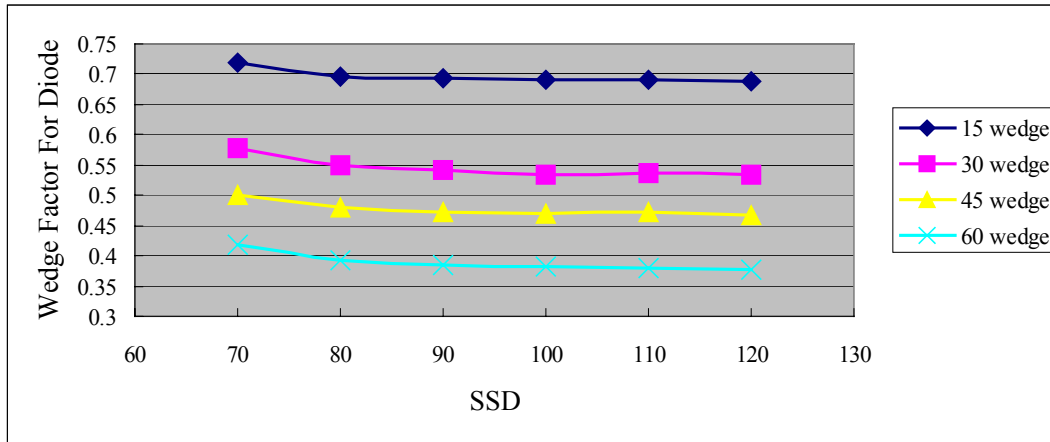


Figure 4.8 Wedge factors for diode as a function of the SSD for entrance measurements. All data in this figure are for field size $10 \times 10 \text{ cm}^2$ (QED 6MV photon diode at 21EX(COV)).

A model was created to fit the measured data. The Microsoft EXCEL was used since it is more available than other programs such as MATHEMATICA and MATLAB. In addition, a FORTRAN interpolation program [25] was developed. The FORTRAN routine is attached as Appendix F and can be used to compare the EXCEL results if necessary.

The basic idea was to find some physically meaningful or like parameters, then perform a least squares fitting to describe the data. This also can be regarded as a multivariable (multidimensional) optimization problem, so generally any multidimensional optimization routine or software can be used to fit the data. One popular example is the Powell's method [25, pp406]. Because the number of variables used in the model is small, EXCEL worked effectively.

As previously described, due to the lack of overlying layers, contamination electrons and head scattered low energy photons, the diodes could overestimate or underestimate the dose, dependent on FS and/or SSD. That is, the DCF for a specific FS (DCF_{FS}) is a function of SSD, and similarly DCF for a specific SSD (DCF_{SSD}) is a

function of FS. Thus $DCF_{FS} * DCF_{SSD}$ is not necessarily equal to $DCF_{FS\&SSD}$, especially for wedged fields. Therefore we used a two dimensional method fitting $DCF(FS,SSD)$. As an example, the data of a QED 6MV photon diode of 21EX(COV) are showed on Fig. 4.9 and Fig. 4.10.

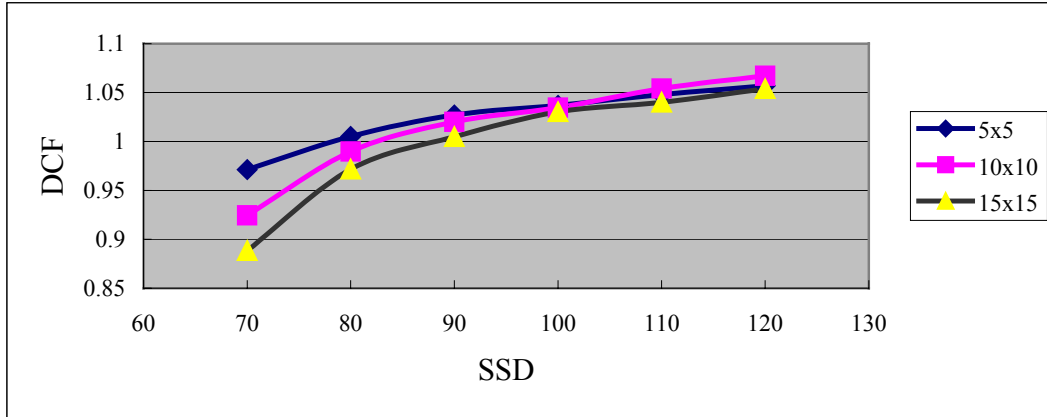


Figure 4.9 SSD dependence of QED 6MV photon diode of 21EX(COV) for different FSs (all for 60 degree wedged fields).

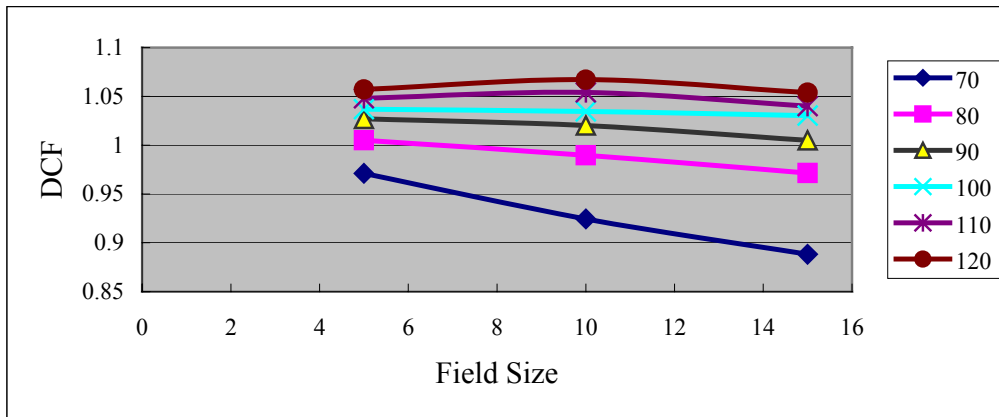


Figure 4.10 FS dependence of QED 6MV photon diode of 21EX(COV) for different SSDs (all for 60 degree wedged fields).

For illustration, consider the situation of $FS = 5 \times 5$ and $SSD = 70$. From Fig. 4.9 and 4.10, one gets for the 60 degree wedged fields, $DCF_{FS=5 \times 5} = 1.040$ for $SSD = 100$, and $DCF_{SSD=70} = 0.924$ for $FS = 10 \times 10$. Then $DCF_{FS} * DCF_{SSD} = 0.961$. However, from

the figures above, $DCF_{FS=5 \times 5 \& SSD=70} = 0.971$. The difference between $DCF_{FS} * DCF_{SSD}$ and $DCF_{FS \& SSD}$ is insignificantly (1%). Similarly, consider another situation of $FS = 15 \times 15$ and $SSD = 70$. $DCF_{FS=15 \times 15} = 1.030$ for $SSD = 100$, and $DCF_{SSD=70} = 0.924$ for $FS = 10 \times 10$. Then $DCF_{FS} * DCF_{SSD} = 0.952$. The value for $DCF_{FS=15 \times 15 \& SSD=70}$ is 0.888. The difference is 7%. This is mainly due to the electron contamination and low energy scattering photons from the wedge, since the distance between wedge and the diode for small SSDs is small.

To fit the data, several methods were tried. The first method used the dose per pulse as the parameter to fit the DCF data [13]. The result was poor for our data, since we did not use similar method as Ref [13], e.g., the Sp we used was from ion chamber measurements, not from diode itself. Finally, two corrections were introduced: field size correction and wedge correction. A second order polynomial was used to model the field size corrections. That is

$$FS \text{ correction} = b2 * FS^2 + b1 * FS + b0$$

where $b2$, $b1$ and $b0$ will be determined when fit the data using least squares.

It's desirable to put all data, open and wedged fields, together into a single model. Then the wedge corrections need to be introduced. Since the wedge factor (not the wedge correction here) decreases with increase of SSD (Fig. 4.8), a constant wedge correction is not enough to describe the real diode wedge factor shown in Fig. 4.8. Thus the following second order polynomial was used to model the wedge corrections:

$$Wedge \text{ correction} = WF * (w2 * (100/SSD)^2 + w1 * (100/SSD) + w0)$$

where the WF takes different value for different wedge angles. WF was named as $WF15$, $WF30$, $WF45$, $WF60$ for 15° , 30° , 45° , 60° wedges, respectively. The narrow wedge and

wide wedge of the same degree have the same WF value, say, $WF15$ is for both narrow and wide 15 degree wedges. This method worked well for all Linacs except 21EX(BR), since the DCF difference between upper wedged beam and lower wedged beam is somewhat large, especially for small SSDs. Fig. 4.11 shows the DCFs for upper and lower wedged fields. There are two groups of DCF curves, the upper one is for upper wedged fields, and the lower one is for lower wedged fields. The difference between two groups was too large (10%) to be ignored. So finally eight WFs were introduced to fit the data: $WF15u$, $WF30u$, $WF45u$, $WF60u$, $WF15l$, $WF30l$, $WF45l$, $WF60l$, where ‘ u ’ represent upper and ‘ l ’ represent lower. The $w2$, $w1$ and $w0$ are the same for all wedged beams for a specific photon diode. Using $100/SSD$ instead of SSD in above wedge correction formula is due to the fact that the real diode wedge factor decreases with increase in SSD (Fig. 4.8).

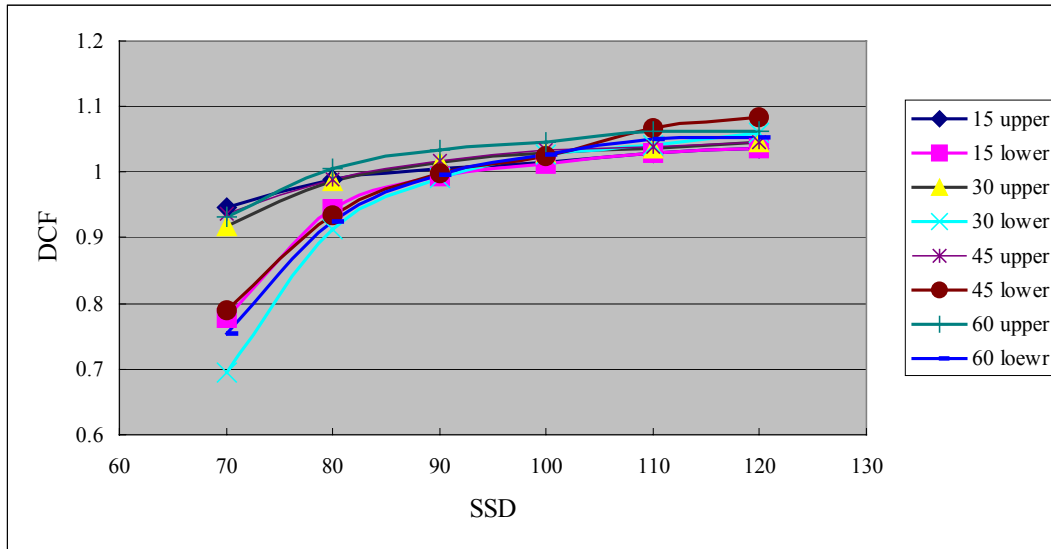


Figure 4.11 The SSD dependence for upper and lower wedged beams with $10 \times 10 \text{ cm}^2$ field size. The diode is 4MV QED photon diode at 21EX(BR).

A parameter named lambda was introduced. Lambda is essentially dose per pulse at the diode with the field correction and wedge correction included. That is

$$\text{Lambda} = ((100 + d_{\max}) / \text{SSD})^2 * (\text{FS correction}) * (\text{Wedge correction}).$$

Finally least square fitting was performed and the fitted relation curve between DCF and lambda was found. The fitting polynomial is of the form

$$\text{DCF} = a_0 + a_1 * \text{Lambda} + a_2 * (\text{Lambda})^2 + a_3 * (\text{Lambda})^3$$

The fitting was done using Microsoft EXCEL by adjusting all fourteen or eighteen variables listed above (i.e. $b_2, b_1, b_0, WF15, WF30, WF45, WF60, w_2, w_1, w_0, a_0, a_1, a_2$ and a_3). This is an optimization problem with fourteen or eighteen variables listed above and the cost function is the sum of squares of differences between fitted and measured DCF values. Fig. 4.12-4.20 show the fitted curves and polynomials.

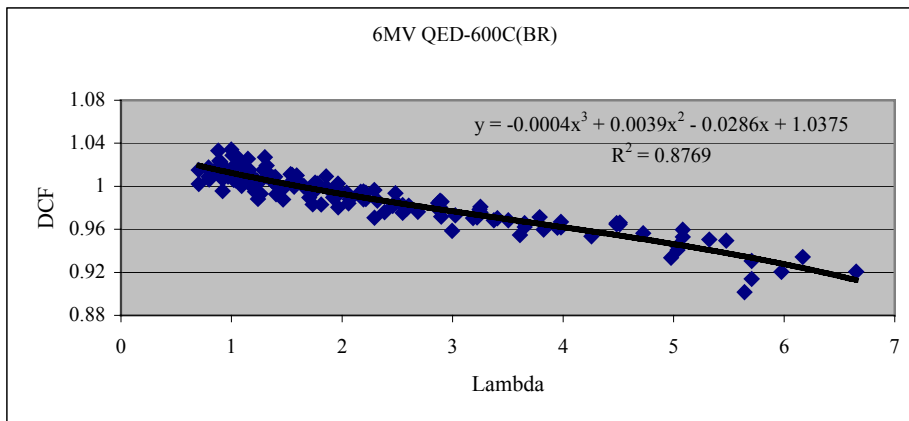


Figure 4.12 The fitted curve and polynomial of 6MV QED diode at 600C(BR).

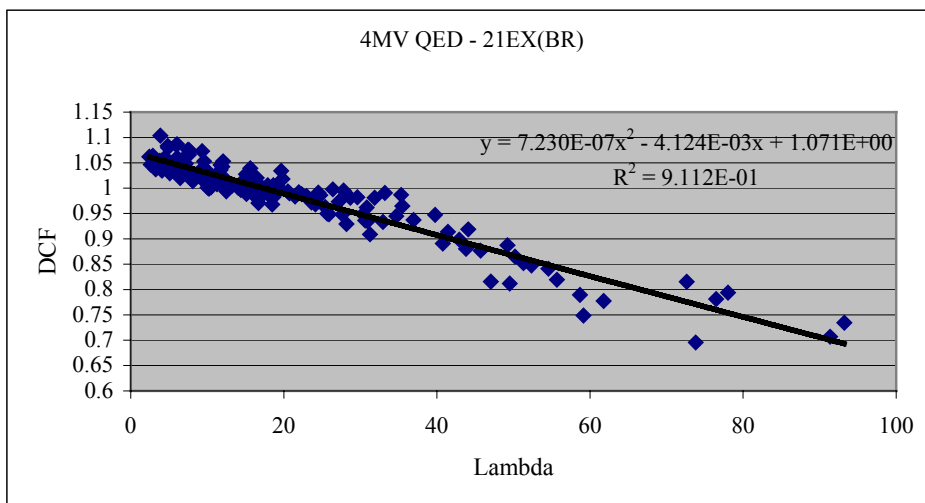


Figure 4.13 The fitted curve and polynomial of 4MV QED diode at 21EX(BR).

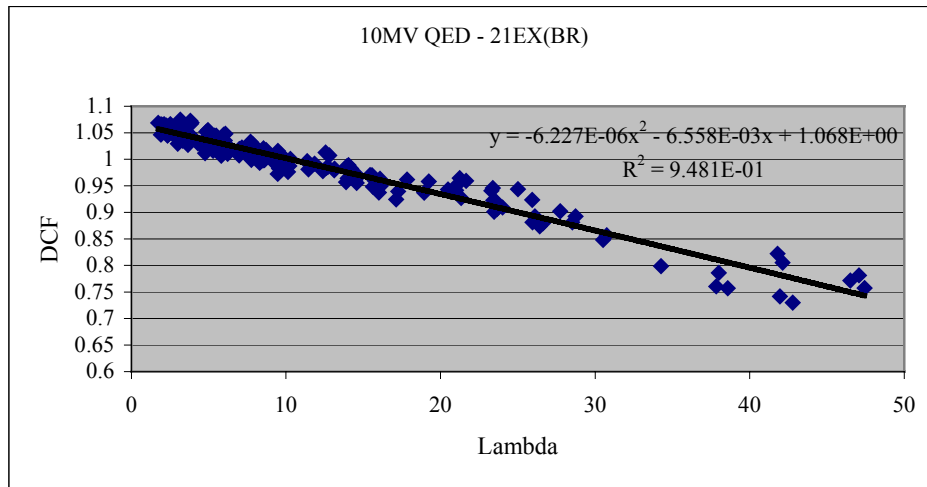


Figure 4.14 The fitted curve and polynomial of 10MV QED diode at 21EX(BR).

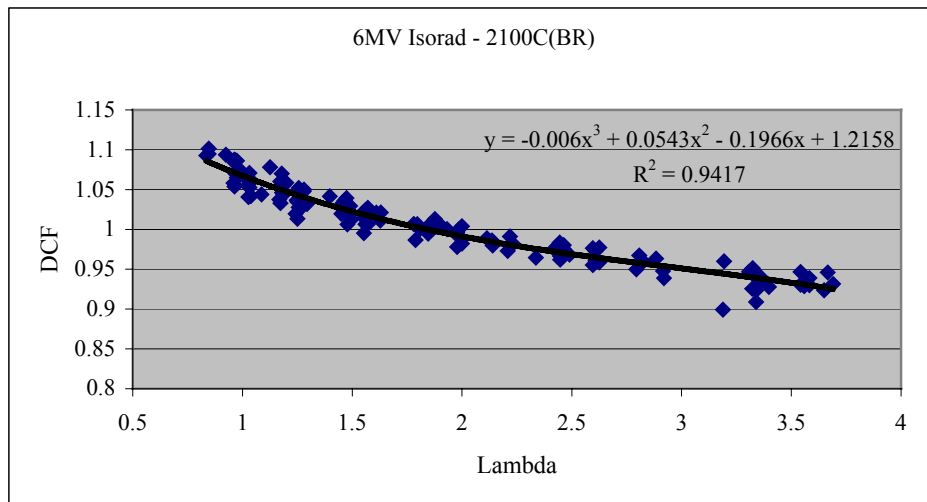


Figure 4.15 The fitted curve and polynomial of 6MV Isorad-p diode at 21C(BR).

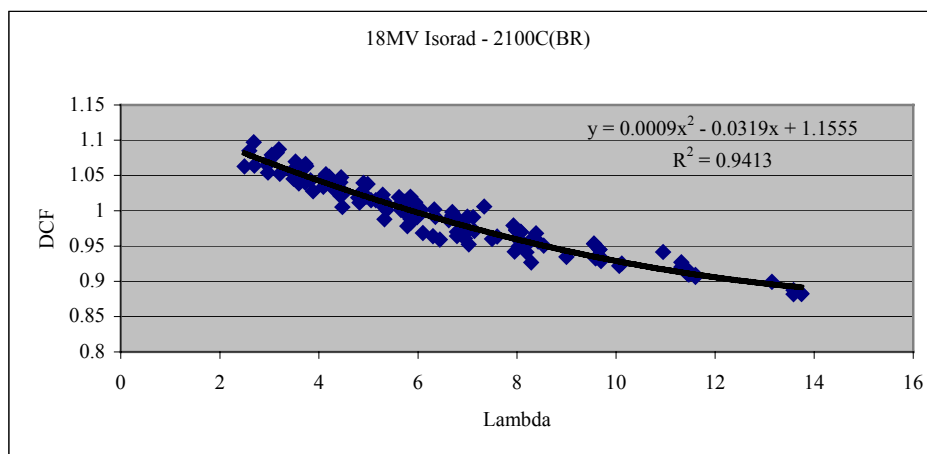


Figure 4.16 The fitted curve and polynomial of 18MV Isorad-p diode at 21C(BR).

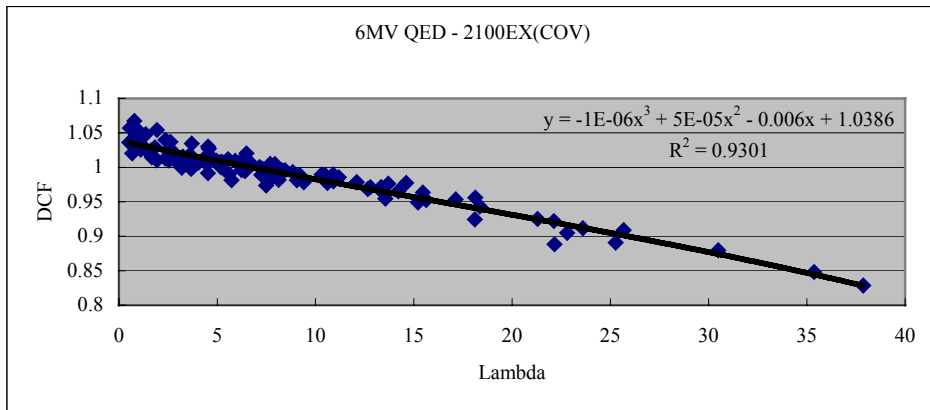


Figure 4.17 The fitted curve and polynomial of 6MV QED diode at 21EX(COV).

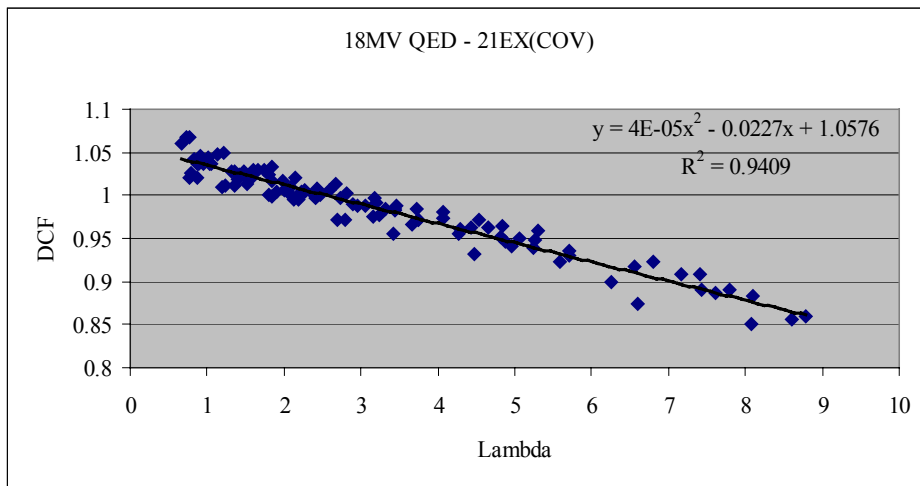


Figure 4.18 The fitted curve and polynomial of 18MV QED diode at 21EX(COV).

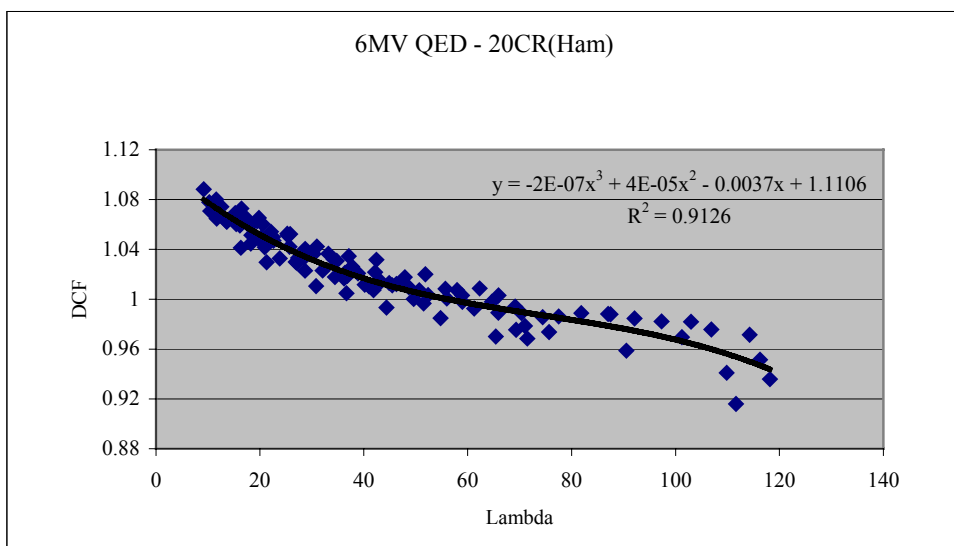


Figure 4.19 The fitted curve and polynomial of 6MV QED diode at 21CR(Ham).

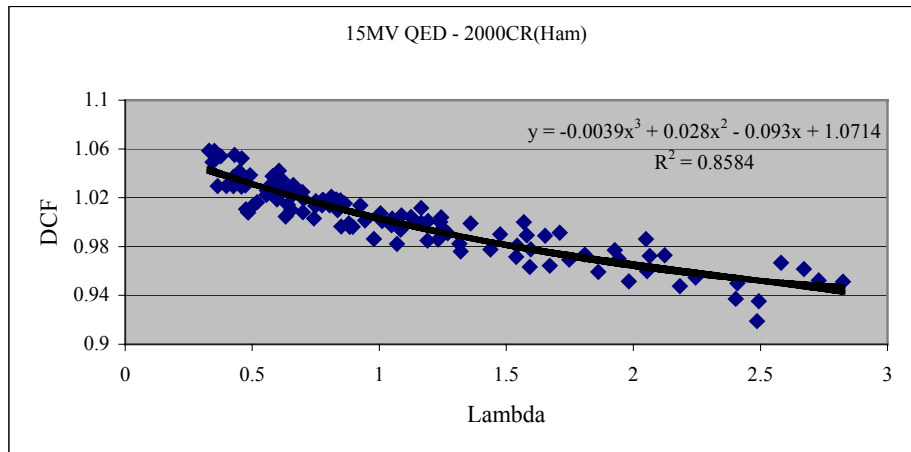


Figure 4.20 The fitted curve and polynomial of 15MV QED diode at 21CR(Ham).

The fitting routine consists of four steps.

1. Determine the field size correction.

$$FS \text{ correction} = b2*FS^2 + b1*FS + b0$$

where the FS (Field Size) is in cm^2 , and the values of $b2$, $b1$ and $b0$ are shown in the table below.

Table 4.1 Parameters for field size correction for each photon diode.

Energy & Diode	$b2$	$b1$	$b0$
6MV QED 600C(BR)	-0.00109	0.05231	1.19027
4MV QED 2100EX(BR)	-0.01458	0.76361	7.53744
10MV QED 2100EX(BR)	-0.00573	0.27829	7.58613
6MV Isorad-p 2100C(BR)	-0.00034	0.00893	1.69969
18MV Isorad-p 2100C(BR)	0.00416	-0.26328	7.22563
6MV QED 2100EX(COV)	-0.00707	0.40266	1.72589
18MV QED 2100EX(COV)	-0.001235	0.05640	1.79193
6MV QED 2000CR(Ham)	-0.02650	1.41491	36.65421
15MV QED 2000CR(Ham)	0.00031	-0.01553	1.07815

2. Determine the wedge correction.

$$\text{Wedge correction} = WF \cdot (w_2 \cdot (100/\text{SSD})^2 + w_1 \cdot (100/\text{SSD}) + w_0)$$

where WF will be replaced by $WF15$, $WF30$, $WF45$, $WF60$ for 15° , 30° , 45° , 60° wedges (narrow or wide), respectively. An exception is the 2100EX(BR), where WF will be replaced by $WF15u$, $WF30u$, $WF45u$, $WF60u$, $WF15l$, $WF30l$, $WF45l$, $WF60l$ for 15° upper, 15° lower, 30° upper, 30° lower, 45° upper, 45° lower, 60° upper, 60° lower wedges, respectively. The lookup table for the values of these parameters is shown below.

Table 4.2(a)(b)(c) Parameters for wedge correction for each photon diode.

(a)

Energy & Diode	$WF15$	$WF30$	$WF45$	$WF60$
6MV QED 600C(BR)	0.00346	0.00392	0.00411	0.00476
6MV Isorad-p 2100C(BR)	0.00740	0.00695	0.00691	0.00602
18MV Isorad-p 2100C(BR)	0.01528	0.01546	0.01138	0.01012
6MV QED 2100EX(COV)	0.73015	1.09422	0.94316	0.77166
18MV QED 2100EX(COV)	0.55297	0.62387	0.57349	0.48187
6MV QED 2000CR(Ham)	0.00265	0.00250	0.00149	0.001695
15MV QED 2000CR(Ham)	0.00326	0.00337	0.00268	0.00245

(b)

Energy & Diode	$WF15u$	$WF15l$	$WF30u$	$WF30l$	$WF45u$	$WF45l$	$WF60u$	$WF60l$
4MV QED 2100EX(BR)	0.00329	0.00512	0.00365	0.00611	0.00306	0.00486	0.00297	0.00598
10MV QED 2100EX(BR)	0.00293	0.004295	0.003135	0.00484	0.00265	0.00474	0.00260	0.00517

(table con'd)

(c)			
Energy & Diode	$w2$	$w1$	$w0$
6MV QED 600C(BR)	103.45	75.757	64.637
4MV QED 2100EX(BR)	221.07	37.197	-83.009
10MV QED 2100EX(BR)	221.06	37.171	-83.049
6MV Isorad-p 2100C(BR)	-2.6892	38.764	81.2555
18MV Isorad-p 2100C(BR)	-24.882	27.7205	78.817
6MV QED 2100EX(COV)	-1.4418	6.5061	-4.1401
18MV QED 2100EX(COV)	-1.6466	6.6566	-3.4922
6MV QED 2000CR(Ham)	103.07	75.868	65.138
15MV QED 2000CR(Ham)	103.07	75.868	65.138

3. Calculate lambda.

$$\text{Lambda} = ((100 + d_{\max}) / \text{SSD})^2 * (\text{FS correction}) * (\text{Wedge correction})$$

4. Determine the DCF from the following fitting polynomial, for the given photon diode and energy (Table 4.3).

$$\text{DCF} = a0 + a1 * \text{Lambda} + a2 * (\text{Lambda})^2 + a3 * (\text{Lambda})^3.$$

The method described above models every energy of every photon diode separately, i.e. find the parameters for every energy of each photon diode separately. However, it is desirable to put all diodes' data together and model the data just for each energy, no matter which diode is used. That is, model would be appropriate for this energy for all diodes. The principal advantage is that physicists do not have to perform all measurements for a newly purchased diode and find the corresponding parameters for it, provided the new diode is of the same model and from the same company as the one it replaces. There are five photon energies used at MBPCC. They are 4MV (1 machine),

6MV (4 machines), 10MV (1 machine), 15MV (1 machine) and 18MV (2 machines).

Only 6 MV and 18 MV occur on multiple linacs.

Table 4.3 Coefficients of fitting polynomials for each photon diode.

Energy & Diode	<i>a0</i>	<i>a1</i>	<i>a2</i>	<i>a3</i>
6MV QED 600C(BR)	1.0375	-0.0286	0.0039	-0.0004
4MV QED 2100EX(BR)	1.071	-4.124E-03	7.230E-07	0.0
10MV QED 2100EX(BR)	1.068	-6.558E-03	-6.227E-06	0.0
6MV Isorad-p 2100C(BR)	1.2158	-0.1966	0.0543	-0.006
18MV Isorad-p 2100C(BR)	1.1555	-0.0319	0.0009	0.0
6MV QED 2100EX(COV)	1.0386	-0.006	5E-05	-1E-06
18MV QED 2100EX(COV)	1.0576	-0.0227	4E-05	0.0
6MV QED 2000CR(Ham)	1.1106	-0.0037	4E-05	-2E-07
15MV QED 2000CR(Ham)	1.0714	-0.093	0.028	-0.0039

If all of the 6MV data from all four diodes is modeled together, using the same FS correction and the same wedge correction for any wedge angle, a single model can be developed for each energy (for simplicity, we ignore the difference between narrow and wide wedges). The steps employed to fit the data and then calculate DCF using fitting polynomial are the same as above. The parameters from this process are tabulated below.

Table 4.4 Parameters for field size correction for compiled 6MV and 18MV.

Energy	<i>b2</i>	<i>b1</i>	<i>b0</i>
6MV	-0.004309	0.21271	5.54807
18MV	0.00264	-0.17043	7.2321

Table 4.5(a)(b) Parameters for wedge correction for compiled 6MV and 18MV.

(a)				
Energy	<i>w2</i>	<i>w1</i>	<i>w0</i>	
6MV	144.81	98.480	74.021	
18MV	-12.308	33.921	80.604	

(b)				
Energy	<i>WF15</i>	<i>WF30</i>	<i>WF45</i>	<i>WF60</i>
6MV	0.002295	0.002456	0.002155	0.00201
18MV	0.01123	0.01165	0.00952	0.00819

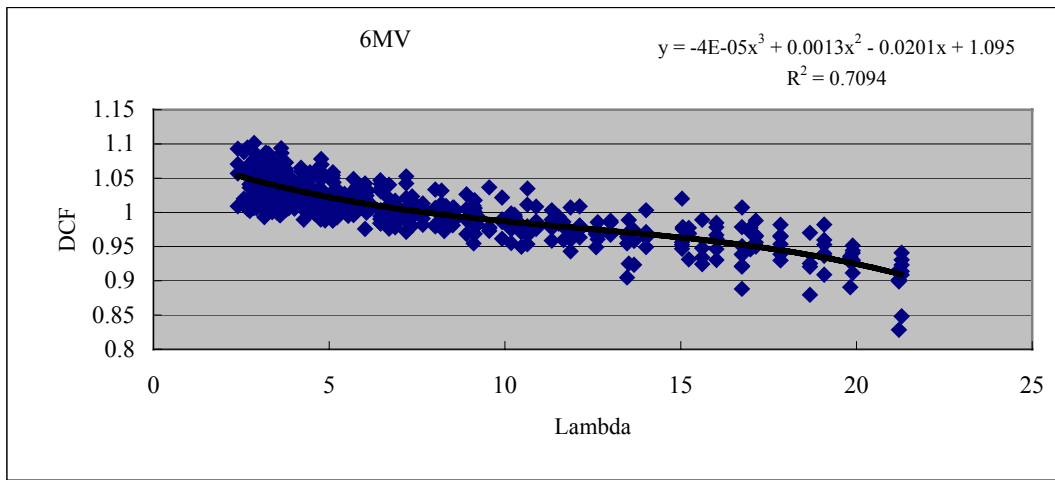
Table 4.6 Coefficients of fitting polynomials for compiled 6MV and 18MV.

Energy	<i>a0</i>	<i>a1</i>	<i>a2</i>	<i>a3</i>
6MV	1.095	-0.0201	0.0013	-4E-05
18MV	1.1497	-0.03	0.0013	-3E-05

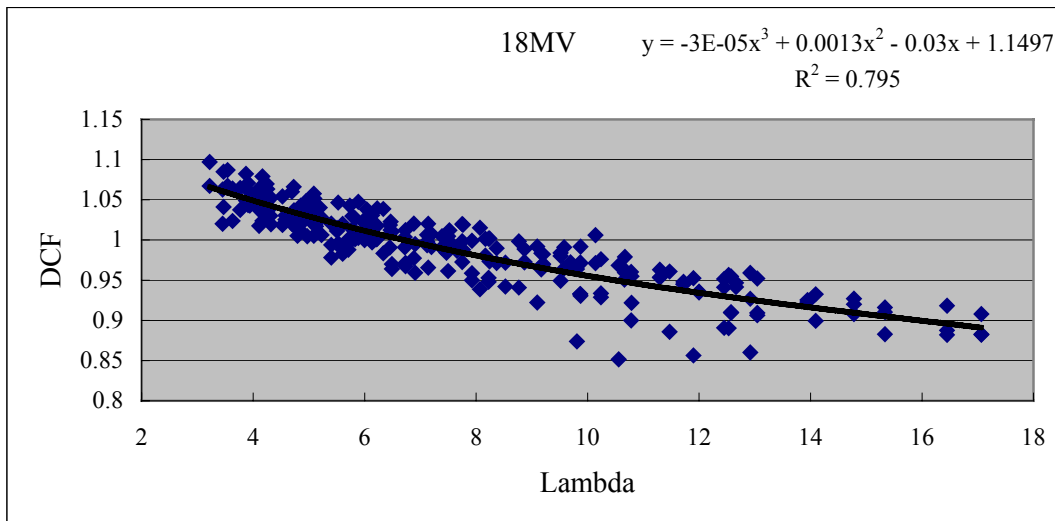
The fitted curves for compiled 6MV and 18MV are showed below (Fig. 4.21).

It's can be seen that the fitting results here are worse. The reasons are evident. First, the responses of QED diodes for given energy, SSD and field size are different to each other (Fig. 4.23 & 4.24). Second, the output and spectrum are a little different from Linac to Linac. Third, the differences between narrow and wide wedges (Fig. 4.11 & 4.27) were not considered when all 6MV/18MV data were put together and then were fitted. Fourth, the difference between QED diode and Isorad-p diode (Fig. 4.25 & 4.26) was also not considered. Since the situation is complicated when put all 6MV/18MV data together, and it would introduce too many parameters if all differences mentioned above were considered, and also it's not guarantee to get better results since some properties are opposite to each other between diodes. A simple method employed to enhance the accuracy was to introduce a diode factor into Lambda to account for the differences of

diodes. This improved the results marginally (Fig. 4.22). The improvement was not substantial enough to warrant inclusion in the final model, especially considering that physicists would have to re-take all measurements for a new diode to model the diode factor. This conflicts with the purpose of combining all the data to achieve a single model, and also increases the workload to physicists.

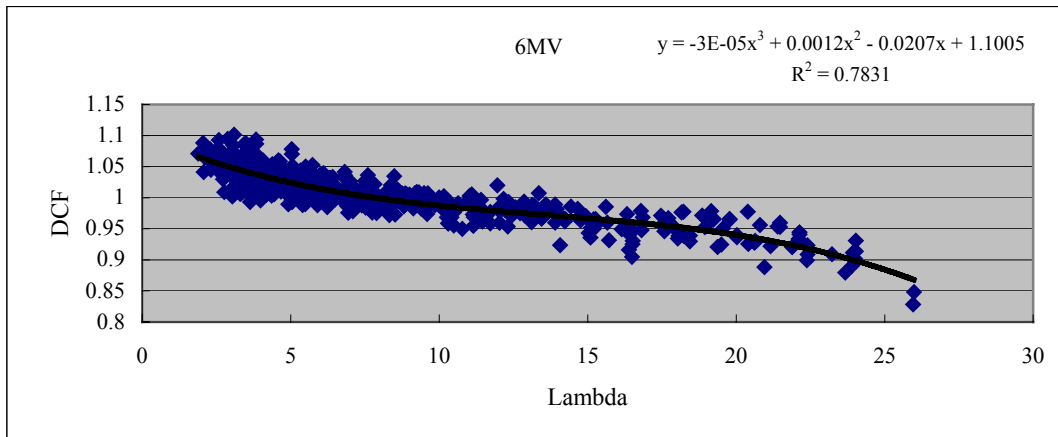


(a)

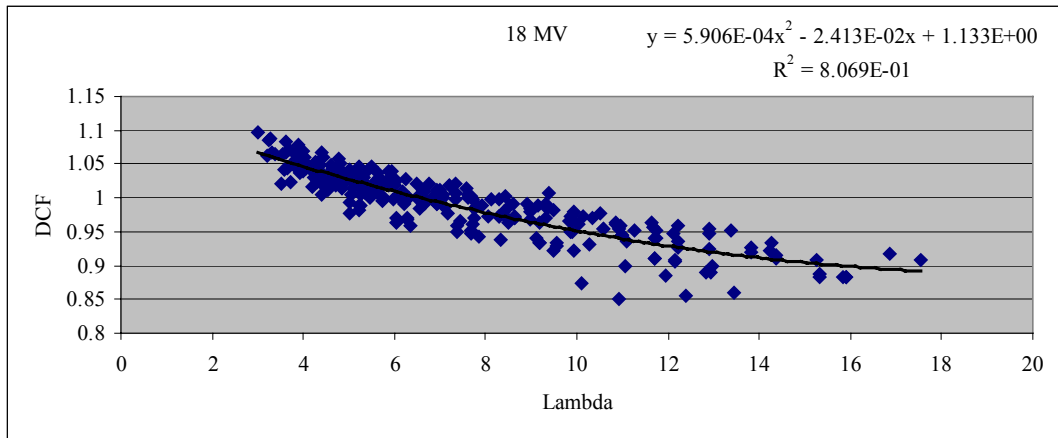


(b)

Figure 4.21 (a) The fitted curve and polynomial of all 6MV diodes at MBPCC. (b) The fitted curve and polynomial of all 18MV diodes at MBPCC.



(a)



(b)

Figure 4.22 (a) The fitted curve and polynomial of all 6MV diodes, with diode factors included. The diode factors are 1.0, 0.732, 1.072, 1.160 for 21C(BR), 20CR(Ham), 600C(BR), 21EX(COV), respectively. (b) The fitted curve and polynomial of all 18MV diodes, with diode factors included. The diode factors are 1.0, 0.908 for 21EX(COV) and 21C(BR), respectively.

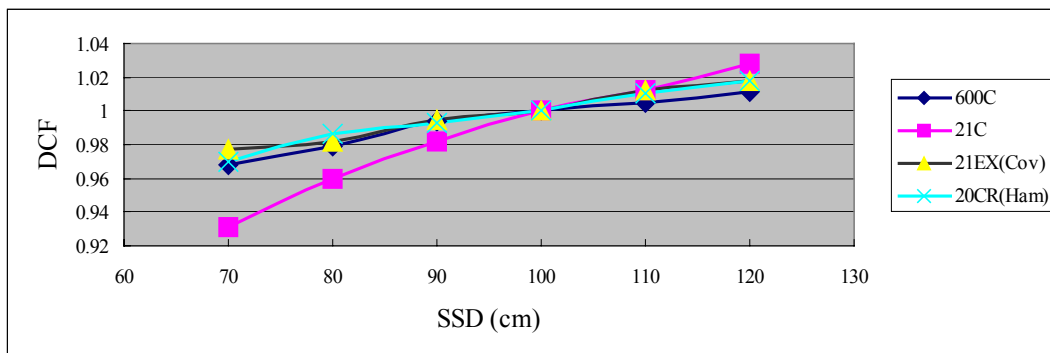


Figure 4.23 The SSD dependence of diodes for 6MV open field with 10x10 FS.

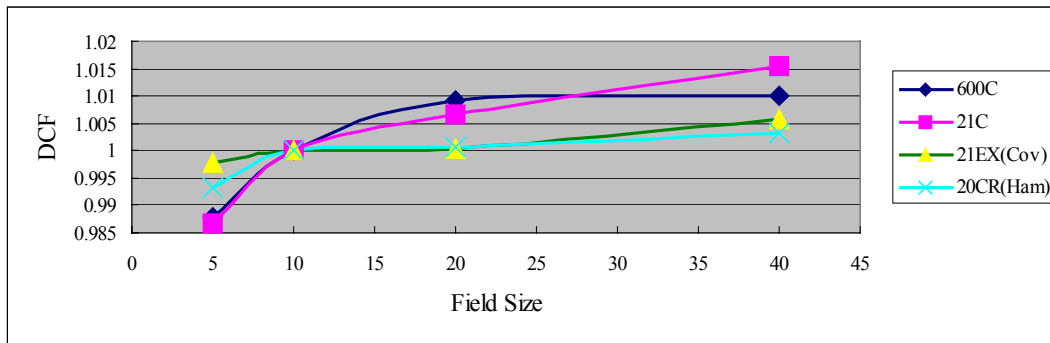


Figure 4.24 The FS dependence of diodes for 6MV open field with 100 SSD.

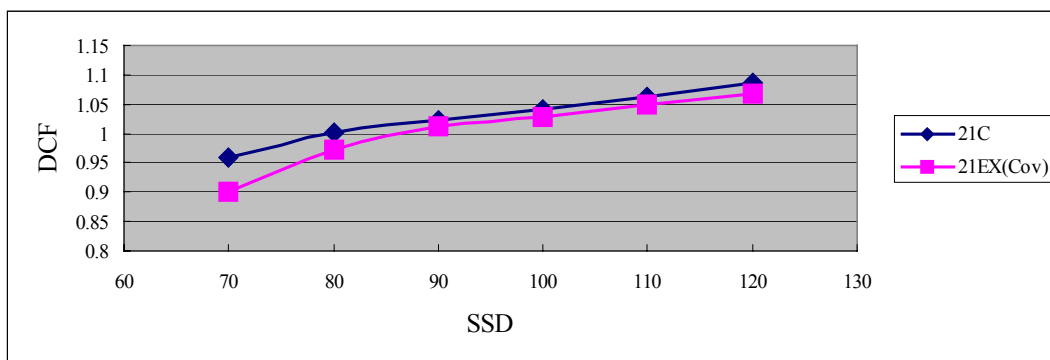


Figure 4.25 The SSD dependence of diodes for 18MV 60 degree wedged field with 10x10 FS.

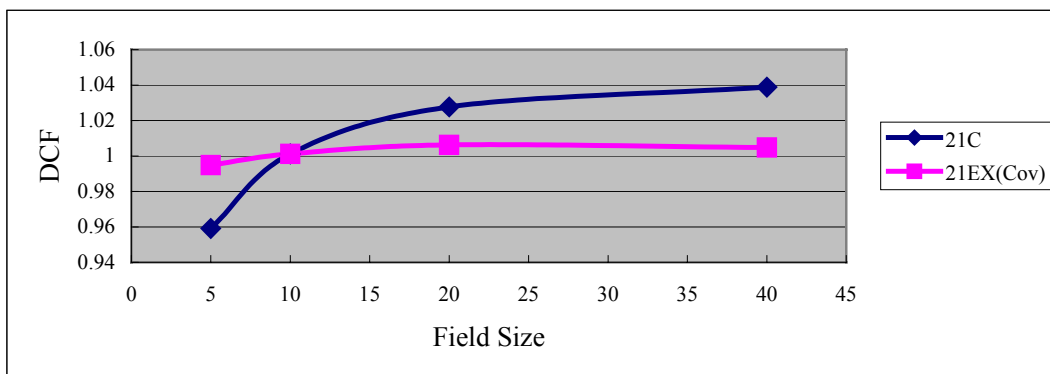


Figure 4.26 The FS dependence of diodes for 18MV open field with 100 SSD.

On the other hand, the fitting results above for 6MV and 18MV (Fig. 4.21 & 4.22) may be clinically acceptable. The large errors occurred at points with DCFs much different from one and usually with small or large lambdas. These lambdas usually correspond to SSDs far from 100 cm, say, 70 cm and 120 cm. Clinically these SSDs are

less likely to be used. Of course, highly accurate *in vivo* dosimetry needs modeling diodes separately, just as described before.

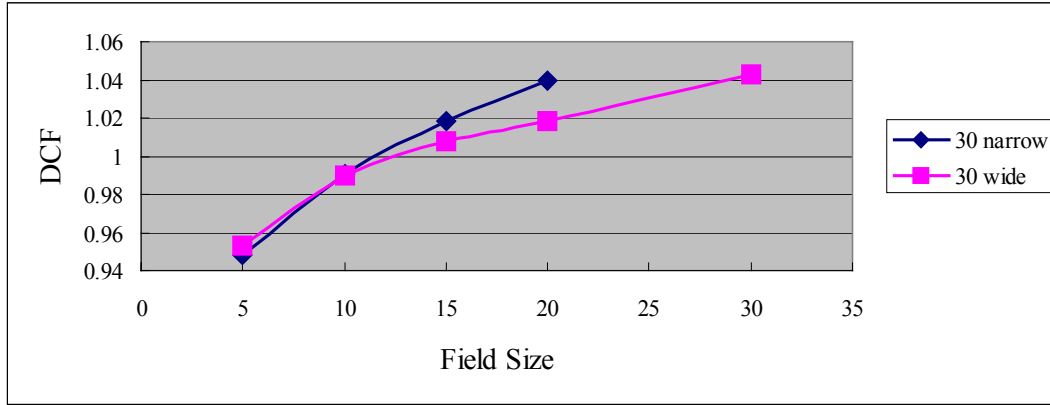


Figure 4.27 The FS dependence of Isorad-p diode (21C) for 18MV wedged fields with 100 SSD. One for 30 degree narrow wedge, another one for 30 degree wide wedge.

The model used in this thesis does not include the diode temperature dependence, directional dependence, radiation damage response, and off-axis correction. For the first three aspects, the data from the company's 'Technical Manual' [21,22] can be used directly.

Diode response increases with temperature. For QED and Isorad-p diodes, the temperature dependence is about 0.3%/°C [21,22]. The typical setup time for taping the diode on patient skin is around 1~2 minutes. The typical change of temperature of diode is some 5 °C for QED diode and 3 °C for Isorad-p diode. Then the increase of diode response is within 1.5% and can be ignored. Alternatively this 1.5% increase can be accounted for by multiplying 0.985 to the fitted DCF.

Diode response varies with incident beam angle. The diode response decreases are about 2% for 1-4MV QED diodes, 0.5% for 6-12MV QED diodes, 3% for 15-25MV QED diodes [21], respectively, if the beam incident angle deviates by 30° from the

perpendicular. For Isorad-p diodes, it is generally not necessary to consider the incident beam angle correction up to 60° [22], since they are designed with cylindrical symmetry. So keeping the incident beam angle deviation within 15° for QED diodes, makes it unnecessary to make an incident angle correction.

Diode sensitivity decreases with increase of cumulative dose to diode, due to radiation damage. Both QED photon diodes and Isorad-p photon diodes have superior radiation resistance. The radiation degradation rate is about 0.1%/kGy at 6MV photon beam [21,22]. Generally the radiation degradation rate is larger for higher photon energies. We can roughly estimate the radiation degradation rate for 18MV photon beam to be two times of that of 6MV beam [13], i.e. 0.2%/kGy. Since it is so low, monthly QA is sufficient to track this effect and recalibrate the diodes if necessary.

In order to find the range of the off-axis effects, off-axis diode corrections were investigated for 4MV with 60 degree wedge at 21EX(BR). Fig. 4.28 shows the result. The off-axis correction in this figure is defined as

$$\text{Off-axis correction} = (\text{OAF of diode})/(\text{OAF of ion chamber})$$

where OAF means off-axis factor. One can see that the off-axis correction is within 1.5%. Thus the off-axis correction of diode can usually be neglected and one may use the OAF from ion chamber measurements tabulated in the dosimetry book directly. However, since a displacement of the diode in the direction of the wedge profile of 1.0 cm resulted in a 9% error for this 4MV with 60 degree wedge, and also since it is difficult to put the diode detector at the central axis accurately, a larger tolerance is needed for wedged fields when performing the *in vivo* dosimetry.

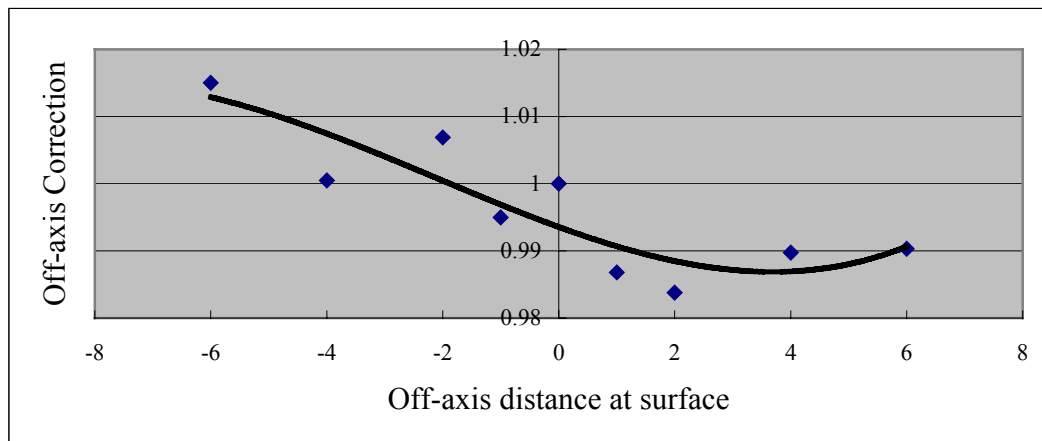


Figure 4.28 Off-axis correction for 4MV diode with 60° wedged field at 21EX(BR), where ‘-’ corresponds skinny side of the wedge. 100 SSD, 15x15 FS.

The off-axis correction above is for displacement of the diode in the direction of the wedge profile. The off-axis correction for displacement of the diode in the direction perpendicular to the direction of the wedge profile was also measured, for the 4MV diode and 60° wedged field on the 21EX(BR), with 100 cm SSD and 15x15 FS. It was found that the off-axis correction in this direction could be neglected, since it was small (with 0.5%).

Sometimes the Linac’s repetition rates are changed from default values. It’s useful to investigate its effect on the ion chamber (i.e. output of Linac) and the diode. The 4MV and 10MV of the 21EX(BR) and 6MV of the 600C(BR) were investigated. It was found that there was no difference between responses of ion chambers and diodes, i.e. for changes in repetition rate (in MU/min), no correction was needed to correct the diode’s reading to the ion chamber’s reading. For 6MV of the 600C(BR) and 10MV of the 21EX(BR), both the ion chamber’s reading and the diode’s reading remained unchanged when the repetition rate changed. However, for 4MV of the 21EX(BR), both the ion

chamber's reading and the diode's reading changed, at the same ratio, when the repetition rate changed. For example, when repetition rate changed from 250MU/min to 50MU/min, both ion chamber's reading and diode's reading increased 2%.

II. Electrons

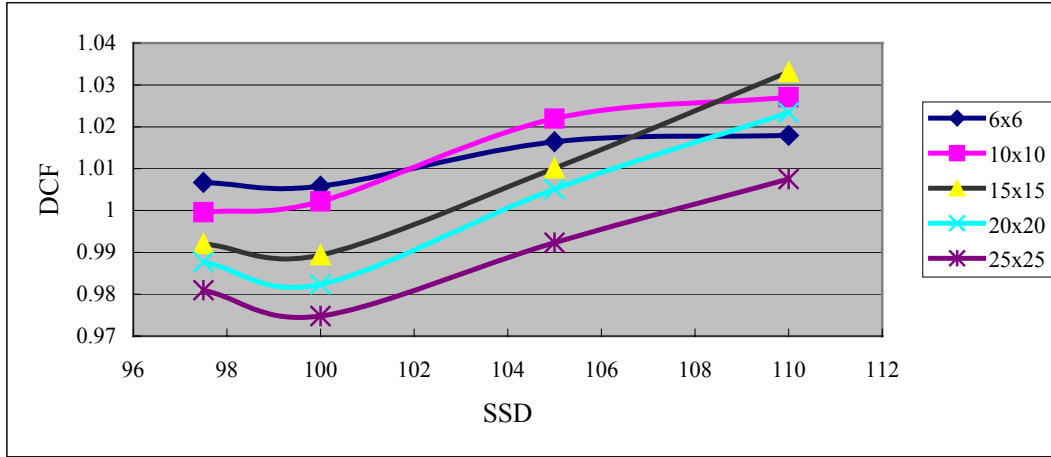


Figure 4.29 Diode correction factors of 6MeV electrons as a function of the SSD, for entrance measurements. QED electron diode at 2000CR(Ham).

Fig. 4.29 shows the diode correction factors (DCF) of 6MeV electrons for various source to surface distances (SSDs) of the QED electron diode at 2000CR(Ham). Just as for photons, the DCF is defined as

$$DCF = \text{Dose at Diode} / \text{Diode Reading}.$$

Generally the DCF increases with increasing SSD, i.e. diode under responds with increasing SSD. This is because dose per pulse decreases with increasing SSD, similar to photons. Almost all four electron diodes used at MBPCC showed the similar SSD dependence above, except the 6MeV with 6x6 cone size at 21EX(BR)(Fig. 4.30). From Fig. 4.30, the DCF of 6MeV and 6x6 cone size on the 21EX(BR) decreases with

increasing SSD, and the correction is as high as 17% for SSD = 97.5. But the DCF for other cone sizes of the same one electron diode behave normally.

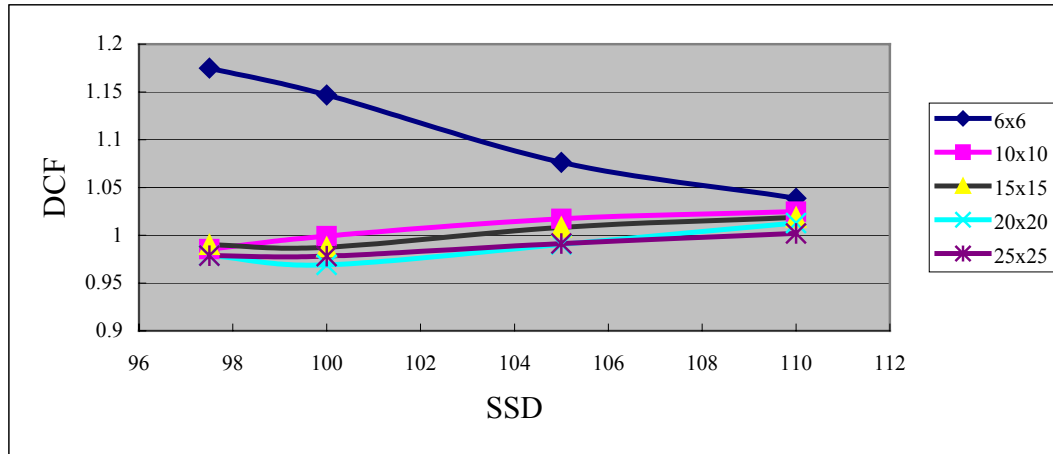


Figure 4.30 Diode correction factors of 6MeV electrons as a function of the SSD, for entrance measurements. QED electron diode at 21EX(BR).

Fig. 4.31 & 4.32 show the diode correction factors (DCF) of 9MeV electrons for various Linacs/SSDs. Generally the DCF showed a small dependence of cone size (within 2%). However, the electron diode on the 21C(BR) showed a larger dependence on cone size (4%). This difference may be attributable to linacs differences as well as diodes responses differences.

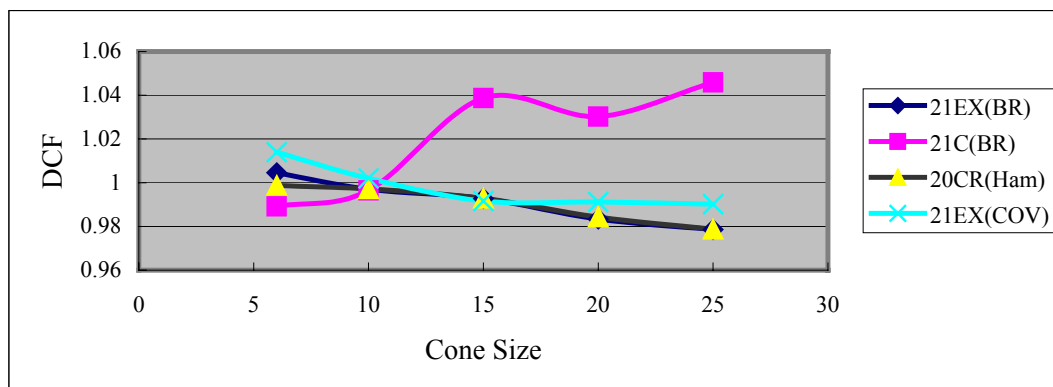


Figure 4.31 Diode correction factors of 9MeV electrons as a function of the cone size, for entrance measurements. SSD = 100 cm.

Since the correction due to cone size is small, it is usually not necessary to introduce cone size correction. On the other hand, the dose rate has already included the contribution of SSD, thus using just one parameter, dose rate, might be good enough to estimate the DCF. One example is shown as Fig. 4.33. The difference between the fitted values and measured values is within 1.5%. This is probably good enough for clinical use.

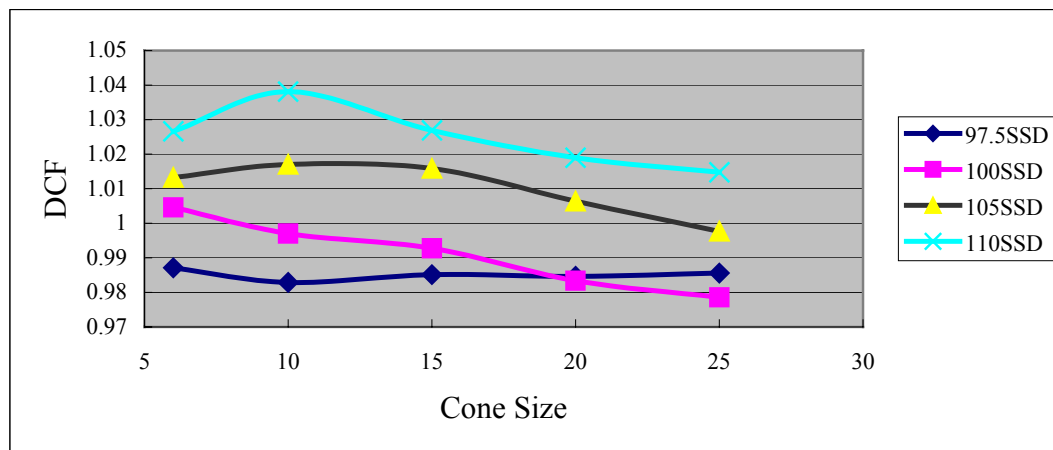


Figure 4.32 Diode correction factors of 9MeV electrons as a function of the cone size, for entrance measurements. QED electron diode at 21EX(BR).

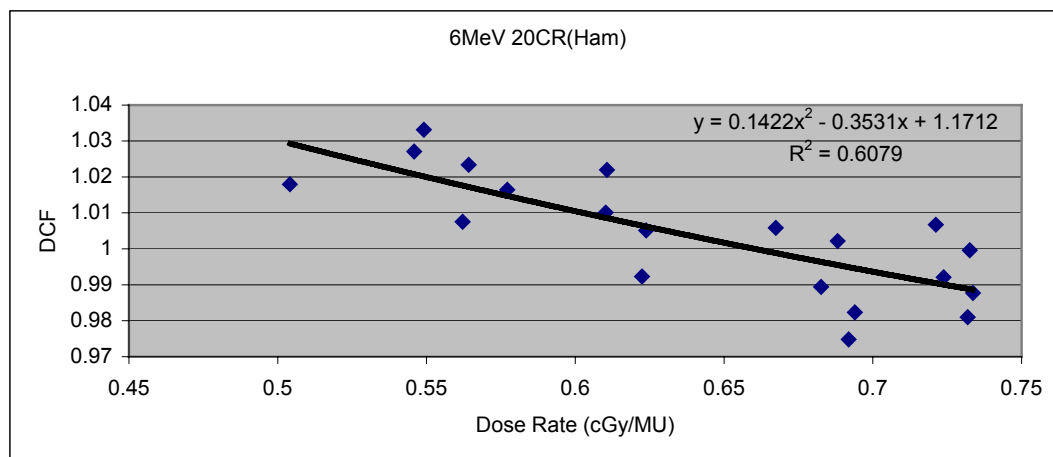


Figure 4.33 The fitted curve and polynomial of 6MeV QED diode at 20CR(Ham).

Similarly, one can derive all twenty fitted curves and polynomials for all four Linacs (each Linac has five electron energies). Again, it is desirable to put all data of one energy, say, 9MeV, together, and fit them together. Since even with the same energy and

cone size, different electron diodes on different Linacs give different responses, it is necessary to introduce a parameter to account for this difference.

In our model the dose rate was replaced by the dose rate multiplied by the diode factor. Each electron diode has it's own diode factor, found using EXCEL to create a fit to the data. The final fitted curves and polynomials for five electron energies are showed as below. Most measured values are within 3% of fitted values.

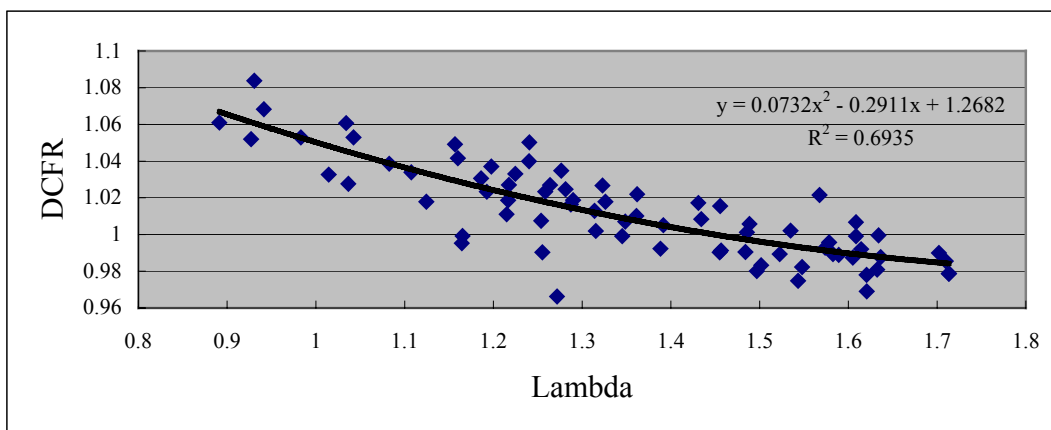


Figure 4.34 The fitted curve and polynomial of all 6MeV data.

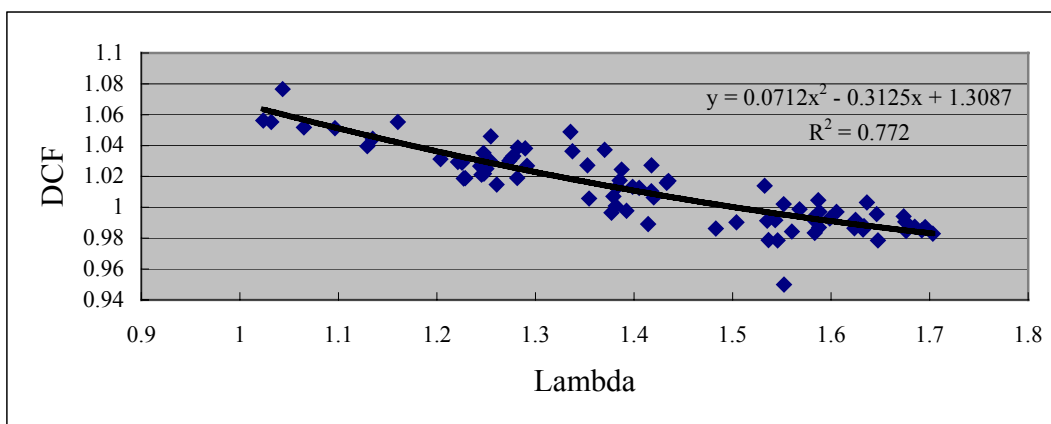


Figure 4.35 The fitted curve and polynomial of all 9MeV data.

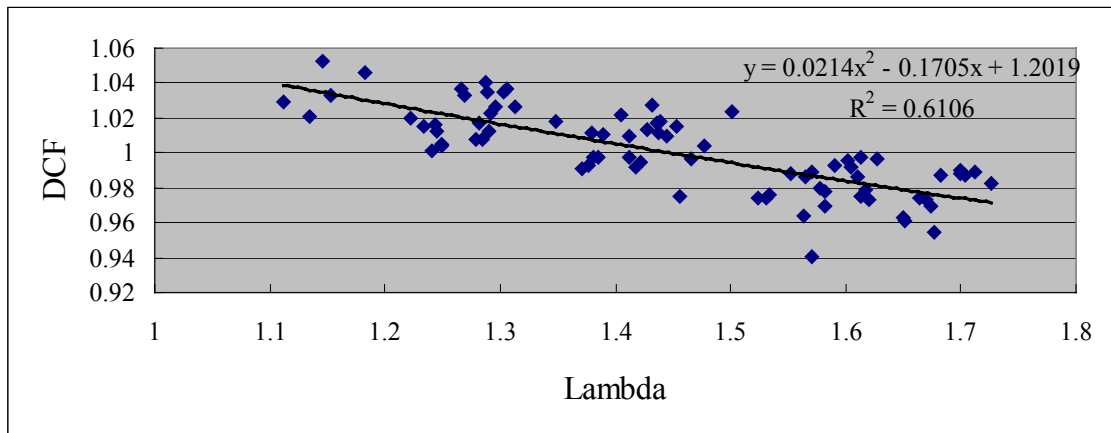


Figure 4.36 The fitted curve and polynomial of all 12MeV data

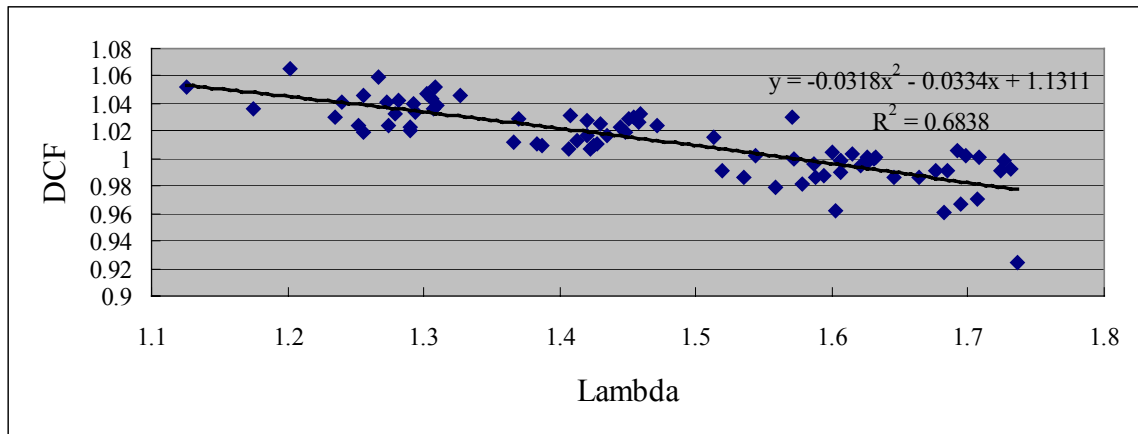


Figure 4.37 The fitted curve and polynomial of all 16MeV data.

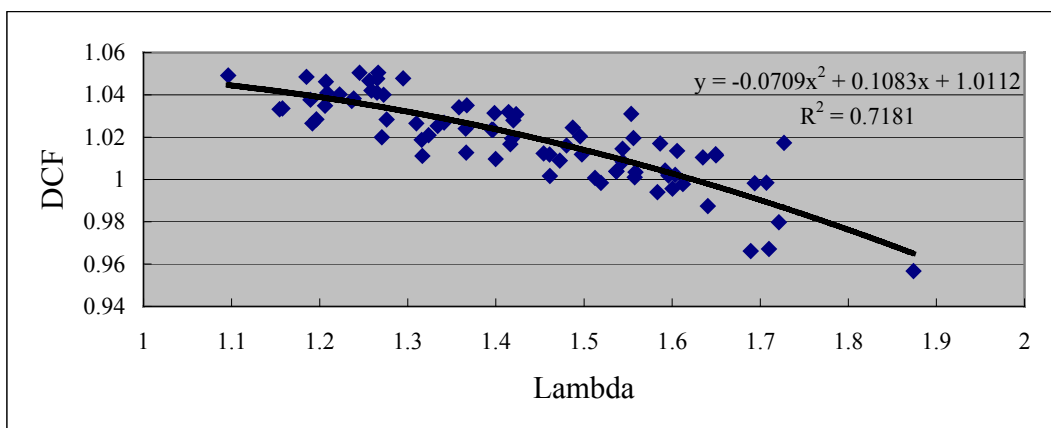


Figure 4.38 The fitted curve and polynomial of all 20MeV data.

In conclusion, the fitting routine for electrons consists of three steps.

1. Calculate the dose rate at the diode without considering the insert.

$$\begin{aligned} \text{Dose Rate at Diode} &= \text{Cone Ratio} * ((SSD_{eff} + d_{max}) / (SSD_{eff} + gap))^2 \\ &= ((SSD_{eff} + d_{max} + SSD - 100) / (SSD_{eff} + SSD - 100))^2 \\ &\quad * (\text{Cone Ratio} * ISF) \end{aligned}$$

where $(\text{Cone Ratio} * ISF)$ are tabulated for each Linacs in the dosimetry books.

2. Calculate lambda.

$$\text{Lambda} = (\text{Dose Rate at Diode}) * (\text{Diode factor})$$

The resultant diode factors are shown in the table below.

Table 4.7 Diode factors for each energy of each electron diode.

	20CR(Ham)	21C(BR)	21EX(BR)	21EX(COV)
6MeV	2.230	1.132	4.689	2.161
9MeV	2.275	1.316	4.601	2.234
12MeV	2.255	1.374	4.578	2.268
16MeV	2.263	1.457	4.551	2.266
20MeV	2.265	1.516	4.571	2.187

3. Determine the DCF from the following fitting polynomial, for the given electron diode and energy.

$$DCF = e0 + e1 * \text{Lambda} + e2 * (\text{Lambda})^2.$$

The resultant coefficients of fitting polynomials are shown in the table 4.8.

The data from 6MeV with 6x6 cone size on the 2100EX(BR) were not included in Fig. 4.34, since the behavior was abnormal (Fig. 4.30). For this special situation, one can easily get the expected diode reading by using the following formulae:

(1) $DCF = 0.282 \cdot (\text{Dose Rate at Diode}) + 0.820$; or

(2) $DCF = -0.011 \cdot SSD + 2.266$.

Table 4.8 Coefficients of fitting polynomials for electrons.

	<i>e0</i>	<i>e1</i>	<i>e2</i>
6MeV	1.2682	-0.2911	0.0732
9MeV	1.3087	-0.3125	0.0712
12MeV	1.2019	-0.1705	0.0214
16MeV	1.1311	-0.0334	-0.0318
20MeV	1.0112	0.1083	-0.0709

Chapter 5

Summary and Conclusion

The delivery of a treatment in radiotherapy requires many sequential, complex steps of prescription, imaging, calculation and patient positioning. Every step can contribute to the total uncertainty of delivered dose. So it is necessary to check each step. In vivo dosimetry is the only check that is performed during the patient treatment, and since it is independent of the calculation method. It is the only method that can trace a number of errors. In vivo dosimetry with diodes is relatively easy and accurate with results immediately available. There is an increasing trend to use diode in vivo dosimetry.

However, just as ion chamber responses are subject to designs and environmental aspects, say, temperature, atmospheric pressure, etc., silicon diode detector responses are also subject to their designs and operating environment. Diodes of different brands must be characterized individually due to different materials and designs. For accurate dosimetry, this characterization needs to be done individually, since even diodes from same batch can be very different. Additionally, diodes at different Linacs also need to be characterized individually, because the spectra from different Linacs might be different even with the same nominal energy.

For any one photon diode detector, the correction factors due to SSD, field size, wedge, temperature, beam incident direction, radiation damage, off-axis distance, etc., need be considered. For an electron diode detector, the correction factors due to SSD, cone size, insert, etc., need to be considered.

In this thesis, an in vivo dosimetry system that uses p-type semiconductor diodes with buildup caps was characterized for clinical use. The dose per pulse dependence was

investigated. This was done by altering the SSD, field size and wedge for photons. For SSD dependence of open fields with 10 x 10 field size, the range for DCF is between 0.93 to 1.04, i.e. within 7%. For small SSD and FS, or large SSD and FS, the range is larger, e.g., DCFs for SSD = 70 cm and FS = 5 x 5 cm², and SSD = 120 cm and FS = 40 x 40 cm², 21C(BR)'s 18 MV Isorad-p photon diode, are 0.90 and 1.06, respectively. For FS dependence of open fields with 100 cm SSD, the range for DCF is generally within 2%, i.e. from 0.98 to 1.02. But for the 18MV Isorad-p diode on the 21EX(BR), the range is much larger (0.96 to 1.04). The DCF for a wedged field is generally larger than that for corresponding open field, since dose per pulse becomes lower for a wedged field.

The off-axis correction and effect of changing repetition rate for photons were also investigated. It was found that the off-axis correction was within 1.5%. Thus the off-axis correction of diode can usually be neglected and one may use the OAF from ion chamber measurements tabulated in the dosimetry book directly. It was found that there was no difference between responses of ion chambers and diodes when change repetition rate (in MU/min), i.e., no correction is needed to correct the diode's reading to the ion chamber's reading.

The dose per pulse dependence for electrons was also investigated. This was done by altering SSD and cone size for electrons. The DCFs ranged from about 0.92 to 1.06. The effect of insert was not investigated due to lack of insert factor data. This is a topic for further study.

A model was made to fit the measured diode correction factors. The basic idea was to find some physically meaningful or like parameters, then perform a least squares fitting to describe the data. The fitted results were put into an EXCEL spreadsheet [33]

that is currently in clinical use, and a FORTRAN interpolation program [25] was produced to check the EXCEL spreadsheet results.

Some other characteristics were also considered. Every energy is calibrated individually to take into account the energy dependence of the diode. Since the temperature of the diode will increase when the diode is taped on the skin of patient, a factor of 0.985 can be included in the fitted DCF to compensate temperature dependence. The data for the directional dependence can be found in the technical manual [21,22]. The diode response decreases are about 2% for 1-4MV QED diodes, 0.5% for 6-12MV QED diodes, 3% for 15-25MV QED diodes [21], respectively, if the beam incident angle deviates by 30° from the perpendicular. For Isorad-p photon diodes, it is generally not necessary to consider the incident beam angle correction up to 60° [22], since they are designed with cylindrical symmetry. So keeping the incident photon beam angle deviation within 15° for QED photon diodes, makes it unnecessary to make an incident angle correction.

Another important aspect is the dose attenuation behind the diode. The dose attenuation is small for QED photon diodes, but is larger for Isorad diodes. The dose attenuation for Isorad photon diodes is up to 4%, 8%, and 13% for a 4MV, 6MV, and 15MV photon beam [12]. When an electron diode is used, a dose attenuation up to 25% for 6MeV electrons and 18% for 12MeV electrons has been observed [34]. Since each patient is usually treated with electrons in five fractions, treatment may only be monitored for one fraction [20].

The action level of *in vivo* dosimetry can be set to 5%. It is not effective and realistic to set tolerance ranges too tight for routine measurements. Therefore, generally

two ranges can be set: 5% and 10% [11]. If the reading is great than 5% but less than 10%, the therapist will check the setup, treatment parameters, read and record the SSD and take the chart to the physicist. The physicist might need to observe the next treatment in order to find and document in the chart the cause of the deviation. If the reading is great than 10%, the physicist is called and the source of discrepancy will be sought with the patient in the treatment position [11]. However, since a displacement of the diode in the direction of the wedge profile of 1.0 cm resulted in a 9% error for this 4MV with 60 degree wedge, and also since it is difficult to put the diode detector at the central axis accurately, a larger tolerance, e.g. 8%, is needed for wedged fields when performing the *in vivo* dosimetry.

The errors most likely to be found with *in vivo* diode dose measurements are incorrect daily dose (such as 2Gy instead of 1.8Gy), using the wrong energy, wrong wedge, wrong monitor units, wrong SSD. Since the action level is set as 5%, it is not good for determining small changes.

References

1. Khan M F, The Physics of Radiation Therapy, 2nd edition, (Lippincott Williams & Wilkins, 1994, USA).
2. Jones A R, "The application of some direct current properties of silicon junction detectors to γ -ray dosimetry," *Phys. Med. Biol.*, **8**, 451-9 (1963).
3. Rikner G and Grusell E, "General specifications for silicon semiconductors for use in radiation dosimetry," *Phys. Med. Biol.*, **32**, 1109-1117 (1987).
4. Gager D, Wright A E and Almond P, "Silicon diode detectors used in radiological physics measurements. Part I: Development of an energy compensating shield," *Med. Phys.*, **4**, 494-498 (1977).
5. Leunens G, Van Dam J, Dutreix A and van der Schueren E, "Quality assurance in radiotherapy by in vivo dosimetry. 1. Entrance dose measurements, a reliable procedure," *Radiother. Oncol.* **17**, 141-151 (1990).
6. Leunens G, Van Dam J, Dutreix A and van der Schueren E, "Quality assurance in radiotherapy by in vivo dosimetry. 2. Determination of target absorbed dose," *Radiother. Oncol.* **19**, 73-87 (1990).
7. Heukelom S, Lanson J H, and Mijnheer B J, "Comparison of entrance and exit dose measurements using ionization chambers and silicon diodes," *Phys. Med. Biol.* **36**, 47-59 (1991).
8. Lee P C, Sawicka J M and Glasgow G P, "Patient dosimetry quality assurance program with a commercial diode system," *Int. J. Radiat. Oncol., Biol., Phys.* **29**, 1175-1182 (1994).
9. Adeyemi A and Lord J, "An audit of radiotherapy patient doses measured with *in vivo* semiconductor detectors," *Br. J. Radiol.* **70**, 399-408 (1997).
10. Alecu R, Alecu M and Ochran T G, "A method to improve the effectiveness of diode *in vivo* dosimetry," *Med. Phys.* **25**, 746-749 (1998).
11. Alecu R, Loomis T, Alecu J and Ochran T, "Guidelines on the implementation of diode *in vivo* dosimetry programs for photon and electron external beam therapy," *Med. Dosimetry* **24**, 5-12 (1999).
12. Essers M. and Mijnheer B.J. "In Vivo dosimetry during external photon beam radiotherapy," *Int J Radiat Oncol Biol Phys* **43**, 245-259 (1999).

13. Jursinic PA. "Implementation of an in vivo diode dosimetry program and changes in diode characteristics over a 4 years clinical history," *Med Phys* **28**, 1718-1726 (2001).
14. Jornet N, *et al.* "In vivo dosimetry: intercomparison between p-type based and n-type based diodes for the 16-25 MV energy range," *Med Phys* **27**, 1287-1293 (2000).
15. Wolff T, Carter S, *et al.* "Characterization and use of a commercial n-type diode system," *Br J Radiol* **71**, 1168-1177 (1998).
16. Yaparalvli R, Fontenla DP, *et al.* "Clinical experience with routine diode dosimetry for electron beam radiotherapy," *Int J Radiat Oncol Biol Phys* **48**, 1259-1263(2000).
17. Verney JN and Morgan AM. "Evaluation of in vivo dose measurements for patients undergoing electron boost treatments," *Radiother Oncol* **59**, 293-296 (2001).
18. Millwater CJ, *et al.* "In vivo semiconductor dosimetry as part of routine quality assurance," *Br J Radiol* **71**, 661-668 (1998).
19. Wierzbick JG and Waid DS. "Large discrepancies between calculated D_{\max} and diode readings for small field sizes and small SSDs of 15 MV photon beams," *Med Phys* **25**, 245-246 (1998).
20. Eveling J N, Morgan A M, and Pitchford W G., "Commissioning a p-type silicon diode for use in clinical electron beams," *Med Phys* **26**, 100-107 (1999).
21. Sun Nuclear Corporation, Technical Manual for QED Diode Detector Series, Melbourne, FL (1997).
22. Sun Nuclear Corporation, Technical Manual for ISORAD-pTM Diode Detector Series, Melbourne, FL (1997).
23. Sun Nuclear Corporation, User's Guide, In Vivo Dosimetry (IVD Model 1131), Melbourne, FL (1999).
24. Shi J, Simon W E, Zhu T C, Sinai A, "Theoretical model for the SSD dependence of Si diode detectors in the application of dosimetry," *Med Phys* **23**, 1072 (1996).
25. Press W H, *et al*, Numerical Recipes in FORTRAN 77, 2nd edition, (Cambridge University Press, 1992, UK).
26. Dutreix A, "When and how can we improve precision in radiotherapy?" *Radiother Oncol* **2**, 275-292 (1984).

27. International Commission on radiation units and measurements (ICRU), "Determination of absorbed dose in a patient irradiated by beams of X and Gamma rays in radiotherapy procedures," ICRU Report 24, (Washington D.C., 1976).
28. Kutcher GJ, *et al*, Report of AAPM Radiation Therapy Committee Task Group 40, *Med Phys* 21, 581-618 (1994).
29. Shirato H, Shimizu S, Kunieda T, *et al*. "Physical aspects of a linear accelerator synchronized with real-time tumor tracking system," *Int J Radiat Oncol Biol Phys* 48, 1187–1195 (2000).
30. <http://www accuray.com>
31. Cember H, Introduction to Health Physics, 3rd Edition, (McGraw-Hill, New York, 1996).
32. Grusell E and Rikner G, "Evaluation of temperature effects in p-type silicon detectors," *Phys. Med. Biol.*, **31**, 527-534 (1986).
33. This EXCEL program was developed by Dr. Bice.
34. Sen A, *et al*. "Quantitative assessment of beam perturbations caused by silicon diodes used for in vivo dosimetry," *Int J Radiat Oncol Biol Phys* 36, 205–211 (1996).

Appendix A

600C (BR, S/N 039) Measurements

600C(BR), 6X, QED Diode				
energy	wedge	Eq Sq @ 100	SSD (diode distance)	Measured correction factor
6X	0	5	70	0.959
6X	0	5	80	0.971
6X	0	5	90	0.983
6X	0	5	100	0.988
6X	0	5	110	0.995
6X	0	5	120	1.006
6X	0	10	70	0.968
6X	0	10	80	0.979
6X	0	10	90	0.994
6X	0	10	100	1.000
6X	0	10	110	1.005
6X	0	10	120	1.011
6X	0	20	70	0.971
6X	0	20	80	0.986
6X	0	20	90	0.996
6X	0	20	100	1.009
6X	0	20	110	1.011
6X	0	20	120	1.015
6X	0	40	70	0.979
6X	0	40	80	0.994
6X	0	40	90	1.002
6X	0	40	100	1.010
6X	0	40	110	1.014
6X	0	40	120	1.018
6X	15N	5	70	0.962
6X	15N	5	80	0.975
6X	15N	5	90	0.983
6X	15N	5	100	0.988
6X	15N	5	110	0.996
6X	15N	5	120	1.002

6X	15N	10	70	0.966
6X	15N	10	80	0.979
6X	15N	10	90	0.991
6X	15N	10	100	1.003
6X	15N	10	110	1.006
6X	15N	10	120	1.009
6X	15N	20	70	0.944
6X	15N	20	80	0.971
6X	15N	20	90	0.988
6X	15N	20	100	1.000
6X	15N	20	110	1.002
6X	15N	20	120	1.019
6X	15W	5	70	0.967
6X	15W	5	80	0.983
6X	15W	5	90	0.994
6X	15W	5	100	1.003
6X	15W	5	110	1.007
6X	15W	5	120	1.015
6X	15W	10	70	0.965
6X	15W	10	80	0.985
6X	15W	10	90	0.998
6X	15W	10	100	1.009
6X	15W	10	110	1.018
6X	15W	10	120	1.018
6X	15W	20	70	0.941
6X	15W	20	80	0.972
6X	15W	20	90	0.995
6X	15W	20	100	1.007
6X	15W	20	110	1.015
6X	15W	20	120	1.024
6X	15W	30	70	0.934
6X	15W	30	80	0.970
6X	15W	30	90	0.995
6X	15W	30	100	1.011
6X	15W	30	110	1.026
6X	15W	30	120	1.033
6X	30N	5	70	0.965
6X	30N	5	80	0.980
6X	30N	5	90	0.980

6X	30N	5	100	0.993
6X	30N	5	110	1.006
6X	30N	5	120	1.006
6X	30N	10	70	0.960
6X	30N	10	80	0.981
6X	30N	10	90	0.988
6X	30N	10	100	1.004
6X	30N	10	110	1.008
6X	30N	10	120	1.012
6X	30N	20	70	0.931
6X	30N	20	80	0.966
6X	30N	20	90	0.985
6X	30N	20	100	1.001
6X	30N	20	110	1.009
6X	30N	20	120	1.017
6X	30W	5	70	0.966
6X	30W	5	80	0.986
6X	30W	5	90	0.993
6X	30W	5	100	1.001
6X	30W	5	110	1.009
6X	30W	5	120	1.015
6X	30W	10	70	0.953
6X	30W	10	80	0.976
6X	30W	10	90	0.994
6X	30W	10	100	1.006
6X	30W	10	110	1.010
6X	30W	10	120	1.022
6X	30W	20	70	0.914
6X	30W	20	80	0.962
6X	30W	20	90	0.985
6X	30W	20	100	1.002
6X	30W	20	110	1.019
6X	30W	20	120	1.029
6X	30W	30	70	0.902
6X	30W	30	80	0.955
6X	30W	30	90	0.982
6X	30W	30	100	1.003
6X	30W	30	110	1.027
6X	30W	30	120	1.034

6X	45N	5	70	0.956
6X	45N	5	80	0.973
6X	45N	5	90	0.984
6X	45N	5	100	0.998
6X	45N	5	110	1.000
6X	45N	5	120	1.012
6X	45N	10	70	0.951
6X	45N	10	80	0.970
6X	45N	10	90	0.987
6X	45N	10	100	1.000
6X	45N	10	110	1.006
6X	45N	10	120	1.017
6X	45N	20	70	0.920
6X	45N	20	80	0.960
6X	45N	20	90	0.982
6X	45N	20	100	0.999
6X	45N	20	110	1.008
6X	45N	20	120	1.027
6X	60N	5	70	0.949
6X	60N	5	80	0.968
6X	60N	5	90	0.976
6X	60N	5	100	0.990
6X	60N	5	110	0.993
6X	60N	5	120	1.009
6X	60N	10	70	0.934
6X	60N	10	80	0.962
6X	60N	10	90	0.976
6X	60N	10	100	0.990
6X	60N	10	110	1.000
6X	60N	10	120	1.005
6X	60N	15	70	0.921
6X	60N	15	80	0.954
6X	60N	15	90	0.972
6X	60N	15	100	0.988
6X	60N	15	110	1.004
6X	60N	15	120	1.007

Appendix B

21EX (BR, S/N 1412) Measurements

21EX(BR), 4X, QED Diode				
energy	wedge	Eq Sq @ 100	SSD (diode distance)	Measured correction factor
4X	0	5	70	0.984
4X	0	5	80	0.995
4X	0	5	90	1.004
4X	0	5	100	1.008
4X	0	5	110	1.018
4X	0	5	120	1.027
4X	0	10	70	0.981
4X	0	10	80	0.992
4X	0	10	90	0.999
4X	0	10	100	1.001
4X	0	10	110	1.010
4X	0	10	120	1.013
4X	0	20	70	0.965
4X	0	20	80	0.973
4X	0	20	90	0.983
4X	0	20	100	0.989
4X	0	20	110	0.997
4X	0	20	120	1.005
4X	0	40	70	0.962
4X	0	40	80	0.972
4X	0	40	90	0.983
4X	0	40	100	0.988
4X	0	40	110	0.994
4X	0	40	120	1.002
4X	15u	5	70	0.981
4X	15u	5	80	1.006
4X	15u	5	90	1.016
4X	15u	5	100	1.025
4X	15u	5	110	1.035
4X	15u	5	120	1.047

4X	15u	10	70	0.947
4X	15u	10	80	0.988
4X	15u	10	90	1.005
4X	15u	10	100	1.014
4X	15u	10	110	1.029
4X	15u	10	120	1.037
4X	15u	20	70	0.887
4X	15u	20	80	0.948
4X	15u	20	90	0.983
4X	15u	20	100	1.002
4X	15u	20	110	1.025
4X	15u	20	120	1.036
4X	15u	30	70	0.865
4X	15u	30	80	0.929
4X	15u	30	90	0.971
4X	15u	30	100	0.999
4X	15u	30	110	1.020
4X	15u	30	120	1.041
4X	15L	5	70	0.812
4X	15L	5	80	0.995
4X	15L	5	90	1.020
4X	15L	5	100	1.032
4X	15L	5	110	1.048
4X	15L	5	120	1.052
4X	15L	10	70	0.777
4X	15L	10	80	0.945
4X	15L	10	90	0.993
4X	15L	10	100	1.012
4X	15L	10	110	1.030
4X	15L	10	120	1.035
4X	15L	20	70	0.781
4X	15L	20	80	0.899
4X	15L	20	90	0.963
4X	15L	20	100	1.000
4X	15L	20	110	1.027
4X	15L	20	120	1.046
4X	15L	30	70	0.794
4X	15L	30	80	0.880
4X	15L	30	90	0.948

4X	15L	30	100	0.990
4X	15L	30	110	1.022
4X	15L	30	120	1.042
4X	30u	5	70	0.987
4X	30u	5	80	1.018
4X	30u	5	90	1.036
4X	30u	5	100	1.049
4X	30u	5	110	1.052
4X	30u	5	120	1.064
4X	30u	10	70	0.919
4X	30u	10	80	0.986
4X	30u	10	90	1.014
4X	30u	10	100	1.030
4X	30u	10	110	1.036
4X	30u	10	120	1.045
4X	30u	20	70	0.841
4X	30u	20	80	0.936
4X	30u	20	90	0.985
4X	30u	20	100	1.019
4X	30u	20	110	1.037
4X	30u	20	120	1.061
4X	30u	30	70	0.819
4X	30u	30	80	0.909
4X	30u	30	90	0.968
4X	30u	30	100	1.012
4X	30u	30	110	1.037
4X	30u	30	120	1.057
4X	30L	5	70	0.749
4X	30L	5	80	0.991
4X	30L	5	90	1.034
4X	30L	5	100	1.053
4X	30L	5	110	1.066
4X	30L	5	120	1.080
4X	30L	10	70	0.696
4X	30L	10	80	0.914
4X	30L	10	90	0.991
4X	30L	10	100	1.027
4X	30L	10	110	1.041
4X	30L	10	120	1.060

4X	30L	20	70	0.707
4X	30L	20	80	0.852
4X	30L	20	90	0.949
4X	30L	20	100	1.006
4X	30L	20	110	1.046
4X	30L	20	120	1.076
4X	30L	30	70	0.734
4X	30L	30	80	0.847
4X	30L	30	90	0.935
4X	30L	30	100	1.001
4X	30L	30	110	1.043
4X	30L	30	120	1.075
4X	45u	5	70	0.982
4X	45u	5	80	1.009
4X	45u	5	90	1.030
4X	45u	5	100	1.038
4X	45u	5	110	1.054
4X	45u	5	120	1.062
4X	45u	10	70	0.937
4X	45u	10	80	0.990
4X	45u	10	90	1.017
4X	45u	10	100	1.035
4X	45u	10	110	1.038
4X	45u	10	120	1.045
4X	45u	20	70	0.877
4X	45u	20	80	0.950
4X	45u	20	90	0.994
4X	45u	20	100	1.021
4X	45u	20	110	1.036
4X	45u	20	120	1.042
4X	45L	5	70	0.815
4X	45L	5	80	0.998
4X	45L	5	90	1.039
4X	45L	5	100	1.053
4X	45L	5	110	1.087
4X	45L	5	120	1.104
4X	45L	10	70	0.790
4X	45L	10	80	0.933
4X	45L	10	90	0.999

4X	45L	10	100	1.023
4X	45L	10	110	1.068
4X	45L	10	120	1.083
4X	45L	20	70	0.815
4X	45L	20	80	0.891
4X	45L	20	90	0.968
4X	45L	20	100	1.014
4X	45L	20	110	1.073
4X	45L	20	120	1.085
4X	60u	5	70	0.992
4X	60u	5	80	1.042
4X	60u	5	90	1.045
4X	60u	5	100	1.061
4X	60u	5	110	1.082
4X	60u	5	120	1.078
4X	60u	10	70	0.931
4X	60u	10	80	1.005
4X	60u	10	90	1.034
4X	60u	10	100	1.045
4X	60u	10	110	1.063
4X	60u	10	120	1.062
4X	60u	15	70	0.870
4X	60u	15	80	0.955
4X	60u	15	90	0.992
4X	60u	15	100	1.018
4X	60u	15	110	1.026
4X	60u	15	120	1.029
4X	60L	5	70	0.783
4X	60L	5	80	0.997
4X	60L	5	90	1.033
4X	60L	5	100	1.055
4X	60L	5	110	1.071
4X	60L	5	120	1.072
4X	60L	10	70	0.754
4X	60L	10	80	0.924
4X	60L	10	90	0.997
4X	60L	10	100	1.027
4X	60L	10	110	1.050
4X	60L	10	120	1.053

4X	60L	15	70	0.747
4X	60L	15	80	0.865
4X	60L	15	90	0.945
4X	60L	15	100	0.994
4X	60L	15	110	1.015
4X	60L	15	120	1.037

21EX(BR), 10X, QED Diode				
energy	wedge	Eq Sq @ 100	SSD (diode distance)	Measured correction factor
10X	0	5	70	0.937
10X	0	5	80	0.961
10X	0	5	90	0.981
10X	0	5	100	1.002
10X	0	5	110	1.004
10X	0	5	120	1.019
10X	0	10	70	0.942
10X	0	10	80	0.963
10X	0	10	90	0.986
10X	0	10	100	1.001
10X	0	10	110	1.006
10X	0	10	120	1.022
10X	0	20	70	0.941
10X	0	20	80	0.962
10X	0	20	90	0.980
10X	0	20	100	0.993
10X	0	20	110	0.997
10X	0	20	120	1.012
10X	0	40	70	0.943
10X	0	40	80	0.963
10X	0	40	90	0.978
10X	0	40	100	0.991
10X	0	40	110	0.993
10X	0	40	120	1.007
10X	15u	5	70	0.946
10X	15u	5	80	0.979
10X	15u	5	90	0.999
10X	15u	5	100	1.011
10X	15u	5	110	1.029
10X	15u	5	120	1.046
10X	15u	10	70	0.923
10X	15u	10	80	0.972
10X	15u	10	90	0.999
10X	15u	10	100	1.016

10X	15u	10	110	1.035
10X	15u	10	120	1.052
10X	15u	20	70	0.892
10X	15u	20	80	0.949
10X	15u	20	90	0.983
10X	15u	20	100	1.011
10X	15u	20	110	1.033
10X	15u	20	120	1.046
10X	15u	30	70	0.881
10X	15u	30	80	0.937
10X	15u	30	90	0.972
10X	15u	30	100	1.007
10X	15u	30	110	1.027
10X	15u	30	120	1.045
10X	15L	5	70	0.799
10X	15L	5	80	0.958
10X	15L	5	90	0.997
10X	15L	5	100	1.019
10X	15L	5	110	1.031
10X	15L	5	120	1.052
10X	15L	10	70	0.786
10X	15L	10	80	0.927
10X	15L	10	90	0.984
10X	15L	10	100	1.011
10X	15L	10	110	1.031
10X	15L	10	120	1.052
10X	15L	20	70	0.805
10X	15L	20	80	0.906
10X	15L	20	90	0.964
10X	15L	20	100	1.001
10X	15L	20	110	1.030
10X	15L	20	120	1.049
10X	15L	30	70	0.822
10X	15L	30	80	0.901
10X	15L	30	90	0.957
10X	15L	30	100	0.998
10X	15L	30	110	1.024
10X	15L	30	120	1.047
10X	30u	5	70	0.944

10X	30u	5	80	0.989
10X	30u	5	90	1.012
10X	30u	5	100	1.025
10X	30u	5	110	1.046
10X	30u	5	120	1.065
10X	30u	10	70	0.902
10X	30u	10	80	0.970
10X	30u	10	90	1.004
10X	30u	10	100	1.025
10X	30u	10	110	1.042
10X	30u	10	120	1.063
10X	30u	20	70	0.857
10X	30u	20	80	0.939
10X	30u	20	90	0.988
10X	30u	20	100	1.019
10X	30u	20	110	1.041
10X	30u	20	120	1.066
10X	30u	30	70	0.848
10X	30u	30	80	0.924
10X	30u	30	90	0.976
10X	30u	30	100	1.010
10X	30u	30	110	1.043
10X	30u	30	120	1.060
10X	30L	5	70	0.757
10X	30L	5	80	0.959
10X	30L	5	90	1.007
10X	30L	5	100	1.028
10X	30L	5	110	1.055
10X	30L	5	120	1.075
10X	30L	10	70	0.730
10X	30L	10	80	0.909
10X	30L	10	90	0.983
10X	30L	10	100	1.017
10X	30L	10	110	1.044
10X	30L	10	120	1.064
10X	30L	20	70	0.757
10X	30L	20	80	0.879
10X	30L	20	90	0.960
10X	30L	20	100	1.009

10X	30L	20	110	1.048
10X	30L	20	120	1.069
10X	30L	30	70	0.781
10X	30L	30	80	0.873
10X	30L	30	90	0.948
10X	30L	30	100	1.001
10X	30L	30	110	1.035
10X	30L	30	120	1.066
10X	45u	5	70	0.953
10X	45u	5	80	0.992
10X	45u	5	90	1.018
10X	45u	5	100	1.030
10X	45u	5	110	1.046
10X	45u	5	120	1.069
10X	45u	10	70	0.923
10X	45u	10	80	0.982
10X	45u	10	90	1.013
10X	45u	10	100	1.039
10X	45u	10	110	1.048
10X	45u	10	120	1.066
10X	45u	20	70	0.881
10X	45u	20	80	0.955
10X	45u	20	90	1.000
10X	45u	20	100	1.027
10X	45u	20	110	1.047
10X	45u	20	120	1.066
10X	45L	5	70	0.761
10X	45L	5	80	0.965
10X	45L	5	90	1.013
10X	45L	5	100	1.033
10X	45L	5	110	1.052
10X	45L	5	120	1.067
10X	45L	10	70	0.742
10X	45L	10	80	0.921
10X	45L	10	90	0.986
10X	45L	10	100	1.021
10X	45L	10	110	1.044
10X	45L	10	120	1.064
10X	45L	20	70	0.772

10X	45L	20	80	0.893
10X	45L	20	90	0.970
10X	45L	20	100	1.016
10X	45L	20	110	1.046
10X	45L	20	120	1.072
10X	60u	5	70	0.961
10X	60u	5	80	1.005
10X	60u	5	90	1.028
10X	60u	5	100	1.049
10X	60u	5	110	1.062
10X	60u	5	120	1.080
10X	60u	10	70	0.916
10X	60u	10	80	0.990
10X	60u	10	90	1.020
10X	60u	10	100	1.044
10X	60u	10	110	1.070
10X	60u	10	120	1.075
10X	60u	15	70	0.874
10X	60u	15	80	0.959
10X	60u	15	90	0.997
10X	60u	15	100	1.031
10X	60u	15	110	1.053
10X	60u	15	120	1.059
10X	60L	5	70	0.743
10X	60L	5	80	0.969
10X	60L	5	90	1.023
10X	60L	5	100	1.078
10X	60L	5	110	1.061
10X	60L	5	120	1.086
10X	60L	10	70	0.718
10X	60L	10	80	0.913
10X	60L	10	90	0.994
10X	60L	10	100	1.028
10X	60L	10	110	1.057
10X	60L	10	120	1.078
10X	60L	15	70	0.718
10X	60L	15	80	0.873
10X	60L	15	90	0.960
10X	60L	15	100	1.004

10X	60L	15	110	1.035
10X	60L	15	120	1.054

21EX(BR), Electrons, QED Diode						
Cone Size	SSD (diode distance)	DCF (6MeV)	DCF (9MeV)	DCF (12MeV)	DCF (16MeV)	DCF (20MeV)
6	97.5	1.175	0.987	0.955	0.970	0.980
6	100	1.147	1.005	0.978	0.990	0.998
6	105	1.076	1.013	1.009	1.025	1.031
6	110	1.039	1.027	1.033	1.043	1.048
10	97.5	0.986	0.983	0.982	0.998	0.998
10	100	0.999	0.997	0.996	1.002	1.002
10	105	1.017	1.017	1.015	1.029	1.031
10	110	1.025	1.038	1.037	1.047	1.040
15	97.5	0.990	0.985	0.987	1.005	1.011
15	100	0.987	0.993	0.986	1.004	1.003
15	105	1.008	1.016	1.010	1.017	1.024
15	110	1.019	1.027	1.035	1.039	1.042
20	97.5	0.979	0.985	0.970	0.986	1.013
20	100	0.969	0.983	0.969	0.979	0.998
20	105	0.990	1.006	0.994	1.007	1.013
20	110	1.013	1.019	1.007	1.024	1.037
25	97.5	0.979	0.986	0.973	0.999	1.015
25	100	0.978	0.979	0.976	0.992	1.002
25	105	0.991	0.998	0.997	1.012	1.011
25	110	1.002	1.015	1.004	1.030	1.027

Appendix C

21C (BR, S/N 090) Measurements

21C(BR), 6X, Isorad-p Diode				
energy	wedge	Eq Sq @ 100	SSD (diode distance)	Measured correction factor
6X	0	5	70	0.924
6X	0	5	80	0.950
6X	0	5	90	0.973
6X	0	5	100	0.987
6X	0	5	110	1.006
6X	0	5	120	1.020
6X	0	10	70	0.931
6X	0	10	80	0.960
6X	0	10	90	0.982
6X	0	10	100	1.000
6X	0	10	110	1.012
6X	0	10	120	1.028
6X	0	20	70	0.946
6X	0	20	80	0.967
6X	0	20	90	0.991
6X	0	20	100	1.007
6X	0	20	110	1.017
6X	0	20	120	1.037
6X	0	40	70	0.960
6X	0	40	80	0.983
6X	0	40	90	1.000
6X	0	40	100	1.015
6X	0	40	110	1.032
6X	0	40	120	1.044
6X	15N	5	70	0.931
6X	15N	5	80	0.955
6X	15N	5	90	0.978
6X	15N	5	100	0.995
6X	15N	5	110	1.013
6X	15N	5	120	1.041

6X	15N	10	70	0.930
6X	15N	10	80	0.959
6X	15N	10	90	0.982
6X	15N	10	100	1.007
6X	15N	10	110	1.026
6X	15N	10	120	1.042
6X	15N	20	70	0.929
6X	15N	20	80	0.961
6X	15N	20	90	0.990
6X	15N	20	100	1.007
6X	15N	20	110	1.038
6X	15N	20	120	1.053
6X	15W	5	70	0.947
6X	15W	5	80	0.976
6X	15W	5	90	0.996
6X	15W	5	100	1.015
6X	15W	5	110	1.035
6X	15W	5	120	1.057
6X	15W	10	70	0.939
6X	15W	10	80	0.977
6X	15W	10	90	1.004
6X	15W	10	100	1.027
6X	15W	10	110	1.042
6X	15W	10	120	1.062
6X	15W	20	70	0.930
6X	15W	20	80	0.973
6X	15W	20	90	1.000
6X	15W	20	100	1.024
6X	15W	20	110	1.052
6X	15W	20	120	1.071
6X	15W	30	70	0.928
6X	15W	30	80	0.968
6X	15W	30	90	1.007
6X	15W	30	100	1.030
6X	15W	30	110	1.059
6X	15W	30	120	1.076
6X	30N	5	70	0.951
6X	30N	5	80	0.976
6X	30N	5	90	1.001

6X	30N	5	100	1.026
6X	30N	5	110	1.033
6X	30N	5	120	1.054
6X	30N	10	70	0.940
6X	30N	10	80	0.975
6X	30N	10	90	1.003
6X	30N	10	100	1.023
6X	30N	10	110	1.044
6X	30N	10	120	1.065
6X	30N	20	70	0.923
6X	30N	20	80	0.966
6X	30N	20	90	1.001
6X	30N	20	100	1.032
6X	30N	20	110	1.050
6X	30N	20	120	1.070
6X	30W	5	70	0.950
6X	30W	5	80	0.979
6X	30W	5	90	1.005
6X	30W	5	100	1.033
6X	30W	5	110	1.053
6X	30W	5	120	1.084
6X	30W	10	70	0.936
6X	30W	10	80	0.980
6X	30W	10	90	1.013
6X	30W	10	100	1.039
6X	30W	10	110	1.055
6X	30W	10	120	1.086
6X	30W	20	70	0.909
6X	30W	20	80	0.962
6X	30W	20	90	1.006
6X	30W	20	100	1.036
6X	30W	20	110	1.070
6X	30W	20	120	1.087
6X	30W	30	70	0.899
6X	30W	30	80	0.965
6X	30W	30	90	1.007
6X	30W	30	100	1.042
6X	30W	30	110	1.078
6X	30W	30	120	1.094

6X	45N	5	70	0.947
6X	45N	5	80	0.977
6X	45N	5	90	0.995
6X	45N	5	100	1.020
6X	45N	5	110	1.037
6X	45N	5	120	1.058
6X	45N	10	70	0.938
6X	45N	10	80	0.971
6X	45N	10	90	1.005
6X	45N	10	100	1.030
6X	45N	10	110	1.046
6X	45N	10	120	1.071
6X	45N	20	70	0.925
6X	45N	20	80	0.971
6X	45N	20	90	1.007
6X	45N	20	100	1.032
6X	45N	20	110	1.060
6X	45N	20	120	1.088
6X	60N	5	70	0.963
6X	60N	5	80	0.989
6X	60N	5	90	1.021
6X	60N	5	100	1.035
6X	60N	5	110	1.066
6X	60N	5	120	1.093
6X	60N	10	70	0.948
6X	60N	10	80	0.986
6X	60N	10	90	1.011
6X	60N	10	100	1.048
6X	60N	10	110	1.064
6X	60N	10	120	1.095
6X	60N	15	70	0.939
6X	60N	15	80	0.980
6X	60N	15	90	1.021
6X	60N	15	100	1.050
6X	60N	15	110	1.060
6X	60N	15	120	1.101

21C(BR), 18X, Isorad-p Diode				
energy	wedge	Eq Sq @ 100	SSD (diode distance)	Measured correction factor
18X	0	5	70	0.899
18X	0	5	80	0.922
18X	0	5	90	0.942
18X	0	5	100	0.959
18X	0	5	110	0.988
18X	0	5	120	1.005
18X	0	10	70	0.942
18X	0	10	80	0.968
18X	0	10	90	0.987
18X	0	10	100	1.001
18X	0	10	110	1.021
18X	0	10	120	1.040
18X	0	20	70	0.979
18X	0	20	80	1.001
18X	0	20	90	1.019
18X	0	20	100	1.028
18X	0	20	110	1.052
18X	0	20	120	1.064
18X	0	40	70	1.006
18X	0	40	80	1.019
18X	0	40	90	1.031
18X	0	40	100	1.039
18X	0	40	110	1.054
18X	0	40	120	1.063
18X	15N	5	70	0.887
18X	15N	5	80	0.910
18X	15N	5	90	0.933
18X	15N	5	100	0.950
18X	15N	5	110	0.964
18X	15N	5	120	0.978
18X	15N	10	70	0.927
18X	15N	10	80	0.953
18X	15N	10	90	0.972
18X	15N	10	100	0.994

18X	15N	10	110	1.001
18X	15N	10	120	1.012
18X	15N	20	70	0.951
18X	15N	20	80	0.984
18X	15N	20	90	1.006
18X	15N	20	100	1.021
18X	15N	20	110	1.034
18X	15N	20	120	1.045
18X	15W	5	70	0.882
18X	15W	5	80	0.910
18X	15W	5	90	0.933
18X	15W	5	100	0.959
18X	15W	5	110	0.970
18X	15W	5	120	0.994
18X	15W	10	70	0.920
18X	15W	10	80	0.954
18X	15W	10	90	0.973
18X	15W	10	100	0.998
18X	15W	10	110	1.011
18X	15W	10	120	1.023
18X	15W	20	70	0.941
18X	15W	20	80	0.980
18X	15W	20	90	1.001
18X	15W	20	100	1.025
18X	15W	20	110	1.044
18X	15W	20	120	1.057
18X	15W	30	70	0.961
18X	15W	30	80	0.998
18X	15W	30	90	1.020
18X	15W	30	100	1.047
18X	15W	30	110	1.054
18X	15W	30	120	1.065
18X	30N	5	70	0.882
18X	30N	5	80	0.909
18X	30N	5	90	0.929
18X	30N	5	100	0.948
18X	30N	5	110	0.967
18X	30N	5	120	0.988
18X	30N	10	70	0.916

18X	30N	10	80	0.945
18X	30N	10	90	0.970
18X	30N	10	100	0.991
18X	30N	10	110	1.005
18X	30N	10	120	1.023
18X	30N	20	70	0.959
18X	30N	20	80	0.992
18X	30N	20	90	1.020
18X	30N	20	100	1.039
18X	30N	20	110	1.052
18X	30N	20	120	1.070
18X	30W	5	70	0.883
18X	30W	5	80	0.906
18X	30W	5	90	0.934
18X	30W	5	100	0.953
18X	30W	5	110	0.971
18X	30W	5	120	0.983
18X	30W	10	70	0.910
18X	30W	10	80	0.945
18X	30W	10	90	0.970
18X	30W	10	100	0.990
18X	30W	10	110	1.013
18X	30W	10	120	1.025
18X	30W	20	70	0.927
18X	30W	20	80	0.971
18X	30W	20	90	0.999
18X	30W	20	100	1.018
18X	30W	20	110	1.038
18X	30W	20	120	1.049
18X	30W	30	70	0.952
18X	30W	30	80	0.992
18X	30W	30	90	1.020
18X	30W	30	100	1.043
18X	30W	30	110	1.060
18X	30W	30	120	1.071
18X	45N	5	70	0.925
18X	45N	5	80	0.951
18X	45N	5	90	0.971
18X	45N	5	100	0.991

18X	45N	5	110	1.015
18X	45N	5	120	1.030
18X	45N	10	70	0.956
18X	45N	10	80	0.991
18X	45N	10	90	1.012
18X	45N	10	100	1.038
18X	45N	10	110	1.048
18X	45N	10	120	1.065
18X	45N	20	70	0.968
18X	45N	20	80	1.015
18X	45N	20	90	1.039
18X	45N	20	100	1.058
18X	45N	20	110	1.079
18X	45N	20	120	1.085
18X	60N	5	70	0.935
18X	60N	5	80	0.963
18X	60N	5	90	0.991
18X	60N	5	100	1.013
18X	60N	5	110	1.025
18X	60N	5	120	1.043
18X	60N	10	70	0.960
18X	60N	10	80	1.002
18X	60N	10	90	1.023
18X	60N	10	100	1.040
18X	60N	10	110	1.063
18X	60N	10	120	1.087
18X	60N	15	70	0.964
18X	60N	15	80	1.005
18X	60N	15	90	1.047
18X	60N	15	100	1.066
18X	60N	15	110	1.082
18X	60N	15	120	1.097

21C(BR), Electrons, QED Diode						
Cone Size	SSD (diode distance)	DCF (6MeV)	DCF (9MeV)	DCF (12MeV)	DCF (16MeV)	DCF (20MeV)
6	97	0.966	0.950	0.940	0.924	0.957
6	100	0.995	0.989	0.975	0.962	0.967
6	105	1.033	1.029	1.012	1.013	1.016
6	110	1.061	1.052	1.033	1.046	1.048
10	97	0.990	0.986	0.989	0.992	1.017
10	100	0.999	0.997	0.997	0.999	0.996
10	105	1.028	1.029	1.026	1.031	1.019
10	110	1.052	1.051	1.046	1.059	1.051
15	97	1.050	1.037	1.024	1.030	1.031
15	100	1.049	1.039	1.022	1.024	1.012
15	105	1.061	1.055	1.037	1.046	1.027
15	110	1.084	1.077	1.052	1.066	1.049
20	97	1.040	1.036	1.004	1.015	1.025
20	100	1.042	1.030	0.997	1.007	1.010
20	105	1.053	1.040	1.005	1.021	1.020
20	110	1.068	1.056	1.020	1.037	1.034
25	97	1.035	1.049	1.017	1.032	1.028
25	100	1.037	1.046	1.018	1.029	1.025
25	105	1.039	1.044	1.020	1.041	1.035
25	110	1.053	1.055	1.029	1.052	1.049

Appendix D

21EX (COV, S/N 1251) Measurements

21EX(COV), 6X, QED Diode				
energy	wedge	Eq Sq @ 100	SSD (diode distance)	Measured correction factor
6X	0	5	70	0.974
6X	0	5	80	0.981
6X	0	5	90	0.992
6X	0	5	100	0.998
6X	0	5	110	1.005
6X	0	5	120	1.010
6X	0	10	70	0.977
6X	0	10	80	0.982
6X	0	10	90	0.994
6X	0	10	100	1.000
6X	0	10	110	1.012
6X	0	10	120	1.018
6X	0	20	70	0.977
6X	0	20	80	0.985
6X	0	20	90	0.993
6X	0	20	100	1.000
6X	0	20	110	1.009
6X	0	20	120	1.009
6X	0	40	70	0.976
6X	0	40	80	0.989
6X	0	40	90	0.996
6X	0	40	100	1.006
6X	0	40	110	1.012
6X	0	40	120	1.016
6X	15u	5	70	0.978
6X	15u	5	80	0.998
6X	15u	5	90	1.009
6X	15u	5	100	1.014
6X	15u	5	110	1.029
6X	15u	5	120	1.036

6X	15u	10	70	0.953
6X	15u	10	80	0.990
6X	15u	10	90	1.007
6X	15u	10	100	1.015
6X	15u	10	110	1.029
6X	15u	10	120	1.041
6X	15u	20	70	0.912
6X	15u	20	80	0.965
6X	15u	20	90	0.996
6X	15u	20	100	1.010
6X	15u	20	110	1.026
6X	15u	20	120	1.036
6X	15u	30	70	0.891
6X	15u	30	80	0.949
6X	15u	30	90	0.981
6X	15u	30	100	1.008
6X	15u	30	110	1.024
6X	15u	30	120	1.041
6X	30u	5	70	0.956
6X	30u	5	80	0.987
6X	30u	5	90	0.998
6X	30u	5	100	1.006
6X	30u	5	110	1.010
6X	30u	5	120	1.029
6X	30u	10	70	0.909
6X	30u	10	80	0.963
6X	30u	10	90	0.989
6X	30u	10	100	1.008
6X	30u	10	110	1.016
6X	30u	10	120	1.026
6X	30u	20	70	0.848
6X	30u	20	80	0.925
6X	30u	20	90	0.969
6X	30u	20	100	0.989
6X	30u	20	110	1.012
6X	30u	20	120	1.022
6X	30u	30	70	0.828
6X	30u	30	80	0.905
6X	30u	30	90	0.955

6X	30u	30	100	0.984
6X	30u	30	110	1.007
6X	30u	30	120	1.025
6X	45u	5	70	0.952
6X	45u	5	80	0.978
6X	45u	5	90	0.990
6X	45u	5	100	0.999
6X	45u	5	110	1.015
6X	45u	5	120	1.020
6X	45u	10	70	0.922
6X	45u	10	80	0.966
6X	45u	10	90	0.995
6X	45u	10	100	1.008
6X	45u	10	110	1.013
6X	45u	10	120	1.029
6X	45u	20	70	0.880
6X	45u	20	80	0.943
6X	45u	20	90	0.980
6X	45u	20	100	0.996
6X	45u	20	110	1.016
6X	45u	20	120	1.027
6X	60u	5	70	0.971
6X	60u	5	80	1.005
6X	60u	5	90	1.027
6X	60u	5	100	1.037
6X	60u	5	110	1.048
6X	60u	5	120	1.057
6X	60u	10	70	0.924
6X	60u	10	80	0.990
6X	60u	10	90	1.020
6X	60u	10	100	1.035
6X	60u	10	110	1.054
6X	60u	10	120	1.067
6X	60u	15	70	0.888
6X	60u	15	80	0.972
6X	60u	15	90	1.005
6X	60u	15	100	1.030
6X	60u	15	110	1.040
6X	60u	15	120	1.054

21EX(COV), 18X, QED Diode				
energy	wedge	Eq Sq @ 100	SSD (diode distance)	Measured correction factor
18X	0	5	70	0.933
18X	0	5	80	0.955
18X	0	5	90	0.972
18X	0	5	100	0.995
18X	0	5	110	1.001
18X	0	5	120	1.013
18X	0	10	70	0.947
18X	0	10	80	0.972
18X	0	10	90	0.988
18X	0	10	100	1.001
18X	0	10	110	1.017
18X	0	10	120	1.030
18X	0	20	70	0.959
18X	0	20	80	0.980
18X	0	20	90	0.991
18X	0	20	100	1.006
18X	0	20	110	1.020
18X	0	20	120	1.024
18X	0	40	70	0.971
18X	0	40	80	0.988
18X	0	40	90	0.997
18X	0	40	100	1.005
18X	0	40	110	1.018
18X	0	40	120	1.020
18X	15u	5	70	0.918
18X	15u	5	80	0.955
18X	15u	5	90	0.972
18X	15u	5	100	0.999
18X	15u	5	110	1.010
18X	15u	5	120	1.020
18X	15u	10	70	0.908
18X	15u	10	80	0.963
18X	15u	10	90	0.989
18X	15u	10	100	1.006

18X	15u	10	110	1.027
18X	15u	10	120	1.043
18X	15u	20	70	0.891
18X	15u	20	80	0.949
18X	15u	20	90	0.984
18X	15u	20	100	1.000
18X	15u	20	110	1.024
18X	15u	20	120	1.046
18X	15u	30	70	0.886
18X	15u	30	80	0.941
18X	15u	30	90	0.977
18X	15u	30	100	0.996
18X	15u	30	110	1.019
18X	15u	30	120	1.037
18X	30u	5	70	0.908
18X	30u	5	80	0.952
18X	30u	5	90	0.976
18X	30u	5	100	1.002
18X	30u	5	110	1.012
18X	30u	5	120	1.020
18X	30u	10	70	0.883
18X	30u	10	80	0.948
18X	30u	10	90	0.982
18X	30u	10	100	1.005
18X	30u	10	110	1.027
18X	30u	10	120	1.037
18X	30u	20	70	0.860
18X	30u	20	80	0.931
18X	30u	20	90	0.972
18X	30u	20	100	1.001
18X	30u	20	110	1.026
18X	30u	20	120	1.037
18X	30u	30	70	0.856
18X	30u	30	80	0.922
18X	30u	30	90	0.966
18X	30u	30	100	0.997
18X	30u	30	110	1.020
18X	30u	30	120	1.043
18X	45u	5	70	0.923

18X	45u	5	80	0.963
18X	45u	5	90	0.990
18X	45u	5	100	1.004
18X	45u	5	110	1.011
18X	45u	5	120	1.026
18X	45u	10	70	0.890
18X	45u	10	80	0.965
18X	45u	10	90	0.998
18X	45u	10	100	1.010
18X	45u	10	110	1.027
18X	45u	10	120	1.037
18X	45u	20	70	0.851
18X	45u	20	80	0.939
18X	45u	20	90	0.983
18X	45u	20	100	1.005
18X	45u	20	110	1.024
18X	45u	20	120	1.041
18X	60u	5	70	0.936
18X	60u	5	80	0.984
18X	60u	5	90	1.007
18X	60u	5	100	1.030
18X	60u	5	110	1.037
18X	60u	5	120	1.059
18X	60u	10	70	0.900
18X	60u	10	80	0.973
18X	60u	10	90	1.012
18X	60u	10	100	1.029
18X	60u	10	110	1.048
18X	60u	10	120	1.067
18X	60u	15	70	0.874
18X	60u	15	80	0.961
18X	60u	15	90	1.003
18X	60u	15	100	1.033
18X	60u	15	110	1.049
18X	60u	15	120	1.067

21EX(COV), Electrons, QED Diode						
Cone Size	SSD (diode distance)	DCF (6MeV)	DCF (9MeV)	DCF (12MeV)	DCF (16MeV)	DCF (20MeV)
6	97.5	1.022	1.003	0.974	0.960	0.987
6	100	1.016	1.014	0.986	0.987	1.004
6	105	1.027	1.027	1.010	1.017	1.034
6	110	1.034	1.031	1.016	1.033	1.046
10	97.5	0.996	0.996	0.989	0.993	1.010
10	100	1.001	1.002	0.997	1.001	1.004
10	105	1.027	1.024	1.018	1.027	1.035
10	110	1.031	1.035	1.023	1.039	1.040
15	97.5	0.993	0.988	0.990	1.001	1.017
15	100	0.991	0.992	0.992	1.003	1.012
15	105	1.018	1.017	1.011	1.020	1.027
15	110	1.023	1.025	1.026	1.036	1.041
20	97.5	0.989	0.986	0.973	0.991	1.008
20	100	0.983	0.991	0.980	0.996	1.012
20	105	1.007	1.007	0.992	1.011	1.019
20	110	1.019	1.021	1.008	1.023	1.038
25	97.5	0.989	0.987	0.975	1.000	1.020
25	100	0.980	0.990	0.974	1.002	1.017
25	105	0.999	1.006	0.991	1.009	1.028
25	110	1.011	1.019	1.001	1.020	1.033

Appendix E

2000CR (Ham, S/N 951) Measurements

20CR(Ham), 6X, QED Diode				
energy	wedge	Eq Sq @ 100	SSD (diode distance)	Measured correction factor
6X	0	5	70	0.959
6X	0	5	80	0.975
6X	0	5	90	0.985
6X	0	5	100	0.993
6X	0	5	110	1.005
6X	0	5	120	1.011
6X	0	10	70	0.970
6X	0	10	80	0.986
6X	0	10	90	0.993
6X	0	10	100	1.000
6X	0	10	110	1.010
6X	0	10	120	1.018
6X	0	20	70	0.972
6X	0	20	80	0.988
6X	0	20	90	0.994
6X	0	20	100	1.001
6X	0	20	110	1.012
6X	0	20	120	1.021
6X	0	40	70	0.976
6X	0	40	80	0.989
6X	0	40	90	0.998
6X	0	40	100	1.003
6X	0	40	110	1.014
6X	0	40	120	1.021
6X	15	5	70	0.985
6X	15	5	80	0.998
6X	15	5	90	1.012
6X	15	5	100	1.023
6X	15	5	110	1.030
6X	15	5	120	1.041

6X	15	10	70	0.982
6X	15	10	80	1.003
6X	15	10	90	1.013
6X	15	10	100	1.023
6X	15	10	110	1.033
6X	15	10	120	1.045
6X	15	20	70	0.951
6X	15	20	80	0.986
6X	15	20	90	1.007
6X	15	20	100	1.017
6X	15	20	110	1.030
6X	15	20	120	1.045
6X	15	30	70	0.936
6X	15	30	80	0.974
6X	15	30	90	0.997
6X	15	30	100	1.019
6X	15	30	110	1.033
6X	15	30	120	1.042
6X	30	5	70	0.988
6X	30	5	80	1.008
6X	30	5	90	1.023
6X	30	5	100	1.029
6X	30	5	110	1.049
6X	30	5	120	1.060
6X	30	10	70	0.982
6X	30	10	80	1.009
6X	30	10	90	1.032
6X	30	10	100	1.036
6X	30	10	110	1.050
6X	30	10	120	1.065
6X	30	20	70	0.941
6X	30	20	80	0.989
6X	30	20	90	1.018
6X	30	20	100	1.032
6X	30	20	110	1.051
6X	30	20	120	1.063
6X	30	30	70	0.916
6X	30	30	80	0.968
6X	30	30	90	1.010

6X	30	30	100	1.031
6X	30	30	110	1.052
6X	30	30	120	1.065
6X	45	5	70	1.020
6X	45	5	80	1.037
6X	45	5	90	1.047
6X	45	5	100	1.059
6X	45	5	110	1.069
6X	45	5	120	1.088
6X	45	10	70	1.007
6X	45	10	80	1.035
6X	45	10	90	1.053
6X	45	10	100	1.058
6X	45	10	110	1.063
6X	45	10	120	1.078
6X	45	20	70	0.970
6X	45	20	80	1.007
6X	45	20	90	1.033
6X	45	20	100	1.049
6X	45	20	110	1.065
6X	45	20	120	1.080
6X	60	5	70	1.003
6X	60	5	80	1.026
6X	60	5	90	1.042
6X	60	5	100	1.051
6X	60	5	110	1.062
6X	60	5	120	1.071
6X	60	10	70	0.989
6X	60	10	80	1.022
6X	60	10	90	1.040
6X	60	10	100	1.060
6X	60	10	110	1.069
6X	60	10	120	1.065
6X	60	15	70	0.979
6X	60	15	80	1.011
6X	60	15	90	1.042
6X	60	15	100	1.054
6X	60	15	110	1.073
6X	60	15	120	1.074

20CR(Ham), 15X, QED Diode				
energy	wedge	Eq Sq @ 100	SSD (diode distance)	Measured correction factor
15X	0	5	70	0.948
15X	0	5	80	0.964
15X	0	5	90	0.976
15X	0	5	100	0.982
15X	0	5	110	0.996
15X	0	5	120	1.003
15X	0	10	70	0.972
15X	0	10	80	0.989
15X	0	10	90	0.995
15X	0	10	100	1.001
15X	0	10	110	1.010
15X	0	10	120	1.019
15X	0	20	70	0.977
15X	0	20	80	0.990
15X	0	20	90	1.000
15X	0	20	100	1.001
15X	0	20	110	1.018
15X	0	20	120	1.022
15X	0	40	70	0.986
15X	0	40	80	1.000
15X	0	40	90	1.000
15X	0	40	100	1.007
15X	0	40	110	1.018
15X	0	40	120	1.025
15X	15	5	70	0.952
15X	15	5	80	0.969
15X	15	5	90	0.985
15X	15	5	100	0.996
15X	15	5	110	1.005
15X	15	5	120	1.008
15X	15	10	70	0.967
15X	15	10	80	0.989
15X	15	10	90	1.004

15X	15	10	100	1.014
15X	15	10	110	1.019
15X	15	10	120	1.029
15X	15	20	70	0.950
15X	15	20	80	0.981
15X	15	20	90	1.003
15X	15	20	100	1.017
15X	15	20	110	1.026
15X	15	20	120	1.037
15X	15	30	70	0.937
15X	15	30	80	0.972
15X	15	30	90	0.997
15X	15	30	100	1.013
15X	15	30	110	1.022
15X	15	30	120	1.029
15X	30	5	70	0.951
15X	30	5	80	0.973
15X	30	5	90	0.986
15X	30	5	100	0.999
15X	30	5	110	1.010
15X	30	5	120	1.013
15X	30	10	70	0.962
15X	30	10	80	0.991
15X	30	10	90	1.012
15X	30	10	100	1.018
15X	30	10	110	1.027
15X	30	10	120	1.030
15X	30	20	70	0.935
15X	30	20	80	0.978
15X	30	20	90	1.005
15X	30	20	100	1.018
15X	30	20	110	1.032
15X	30	20	120	1.035
15X	30	30	70	0.919
15X	30	30	80	0.963
15X	30	30	90	0.994
15X	30	30	100	1.014
15X	30	30	110	1.028

15X	30	30	120	1.038
15X	45	5	70	0.955
15X	45	5	80	0.978
15X	45	5	90	0.986
15X	45	5	100	1.008
15X	45	5	110	1.016
15X	45	5	120	1.030
15X	45	10	70	0.973
15X	45	10	80	0.999
15X	45	10	90	1.014
15X	45	10	100	1.030
15X	45	10	110	1.039
15X	45	10	120	1.054
15X	45	20	70	0.952
15X	45	20	80	0.991
15X	45	20	90	1.015
15X	45	20	100	1.035
15X	45	20	110	1.052
15X	45	20	120	1.058
15X	60	5	70	0.960
15X	60	5	80	0.982
15X	60	5	90	0.996
15X	60	5	100	1.014
15X	60	5	110	1.011
15X	60	5	120	1.030
15X	60	10	70	0.970
15X	60	10	80	1.004
15X	60	10	90	1.018
15X	60	10	100	1.042
15X	60	10	110	1.041
15X	60	10	120	1.049
15X	60	15	70	0.959
15X	60	15	80	1.001
15X	60	15	90	1.021
15X	60	15	100	1.038
15X	60	15	110	1.055
15X	60	15	120	1.059

20CR(Ham), Electrons, QED Diode						
Cone Size	SSD (diode distance)	DCF (6MeV)	DCF (9MeV)	DCF (12MeV)	DCF (16MeV)	DCF (20MeV)
6	97.5	1.007	0.991	0.961	0.966	0.966
6	100	1.006	0.999	0.988	0.987	0.994
6	105	1.016	1.013	1.011	1.027	1.031
6	110	1.018	1.019	1.015	1.041	1.050
10	97.5	1.000	0.987	0.988	0.991	0.998
10	100	1.002	0.997	0.996	0.998	1.004
10	105	1.022	1.027	1.028	1.030	1.032
10	110	1.027	1.032	1.040	1.052	1.041
15	97.5	0.992	0.994	0.987	1.002	1.012
15	100	0.989	0.993	0.993	0.999	1.001
15	105	1.010	1.010	1.014	1.023	1.024
15	110	1.033	1.033	1.035	1.044	1.047
20	97.5	0.988	0.979	0.963	0.986	1.002
20	100	0.982	0.984	0.964	0.981	1.001
20	105	1.005	1.013	0.997	1.009	1.024
20	110	1.023	1.030	1.017	1.034	1.038
25	97.5	0.981	0.992	0.979	0.995	1.020
25	100	0.975	0.979	0.974	0.986	1.009
25	105	0.992	1.001	0.993	1.011	1.021
25	110	1.008	1.022	1.012	1.024	1.028

Appendix F

The FORTRAN Program for Calculating DCF

```

PROGRAM MAIN
C   This program is for the diode systems at MBPCC.
C   The DCF(Diode Correction Factor) for photons and electrons
C   of all diodes at MBPCC can be obtained by using this routine.
C   The interpolation routines used are from Ref [25].
C   Only take 4 significant numbers for all results.
REAL x1a(1:6), x2a1(1:4), x2a2(1:4), x2a3(1:3), x2a4(1:3)
REAL ya01(1:6,1:4), ya02(1:6,1:3), ya03(1:6,1:4), ya04(1:6,1:3)
REAL ya05(1:6,1:4), ya06(1:6,1:3), ya07(1:6,1:3), ya08(1:6,1:4)
REAL ya09(1:6,1:4), ya10(1:6,1:4), ya11(1:6,1:4), ya12(1:6,1:4)
REAL ya13(1:6,1:3), ya14(1:6,1:3), ya15(1:6,1:3), ya16(1:6,1:3)
REAL ya17(1:6,1:4), ya18(1:6,1:4), ya19(1:6,1:4), ya20(1:6,1:4)
REAL ya21(1:6,1:4), ya22(1:6,1:3), ya23(1:6,1:3), ya24(1:6,1:3)
REAL ya25(1:6,1:3), ya26(1:6,1:4), ya27(1:6,1:3), ya28(1:6,1:4)
REAL ya29(1:6,1:3), ya30(1:6,1:4), ya31(1:6,1:3), ya32(1:6,1:3)
REAL ya33(1:6,1:4), ya34(1:6,1:3), ya35(1:6,1:4), ya36(1:6,1:3)
REAL ya37(1:6,1:4), ya38(1:6,1:3), ya39(1:6,1:3), ya40(1:6,1:4)
REAL ya41(1:6,1:4), ya42(1:6,1:4), ya43(1:6,1:3), ya44(1:6,1:3)
REAL ya45(1:6,1:4), ya46(1:6,1:4), ya47(1:6,1:4), ya48(1:6,1:3)
REAL ya49(1:6,1:3), ya50(1:6,1:4), ya51(1:6,1:4), ya52(1:6,1:4)
REAL ya53(1:6,1:3), ya54(1:6,1:3), ya55(1:6,1:4), ya56(1:6,1:4)
REAL ya57(1:6,1:4), ya58(1:6,1:3), ya59(1:6,1:3)
REAL SSD,FS,DCF, dDCF
INTEGER Linac, Energy, wedge
REAL Another
DATA x1a/70.0,80.0,90.0,100.0,110.0,120.0/
DATA x2a1/5.0,10.0,20.0,40.0/
DATA x2a2/5.0,10.0,20.0,30.0/
DATA x2a3/5.0,10.0,20.0/
DATA x2a4/5.0,10.0,15.0/
DATA ya01/0.958653993, 0.970782983, 0.98301443, 0.987715356,
$ 0.99499795, 1.006052683, 0.968438488, 0.979016642,
$ 0.994089279, 1.000218447, 1.005226643, 1.011455324,
& 0.971293762, 0.985673562, 0.99646844, 1.009197417,
& 1.011288508, 1.015349567, 0.978623175, 0.993562782,
$ 1.002461795, 1.010041385, 1.014060527, 1.017986646/
DATA ya02/0.961785288, 0.975418296, 0.983184835, 0.988207944,
$ 0.995563664, 1.002192681, 0.965730326, 0.978748783,
$ 0.991114011, 1.002829896, 1.005592512, 1.00887104,
$ 0.944215301, 0.971097574, 0.987876212, 0.999749149,
$ 1.002000717, 1.018894486/
DATA ya03/0.967008855, 0.982663739, 0.993983001, 1.002676861,
$ 1.00670287, 1.015149919, 0.964590994, 0.984518176,
$ 0.997700289, 1.008741238, 1.018377903, 1.017542336,
$ 0.940838183, 0.971828359, 0.995257871, 1.006542062,
$ 1.01523119, 1.023598348, 0.933542831, 0.970440314,
$ 0.994850698, 1.010557019, 1.025572789, 1.033048712/
DATA ya04/0.964844806, 0.98043392, 0.980489717, 0.99260536,
$ 1.006219827, 1.00638324, 0.959661728, 0.980840416,
$ 0.988112539, 1.004427699, 1.007509466, 1.011860964,

```

\$ 0.930707762, 0.965674637, 0.984580579, 1.000833622,
 \$ 1.009211489, 1.017413261/
 DATA ya05/0.966257775, 0.986461732, 0.993245998,1.001094479,
 \$ 1.009148037, 1.014940397, 0.95290213, 0.975651936,
 \$ 0.993989613, 1.00635312, 1.010052947, 1.022494846,
 \$ 0.913852815, 0.962204579, 0.985279913, 1.002359141,
 \$ 1.019234024, 1.028733245, 0.901628149, 0.95471933,
 \$ 0.98172468, 1.003403274, 1.026963014, 1.034151302/
 DATA ya06/0.956474783, 0.973064357, 0.984256464,0.998247213,
 \$ 1.000439756, 1.012374022, 0.950546786, 0.970307188,
 \$ 0.986615328, 0.99968853, 1.005650308, 1.016670418,
 \$ 0.920459314, 0.959805794, 0.982034392, 0.998945046,
 \$ 1.007936856, 1.026664098/
 DATA ya07/0.949406526, 0.968388801, 0.975904557,0.989505428,
 \$ 0.993046602, 1.008928389, 0.934237985, 0.961547377,
 \$ 0.976225208, 0.989696464, 0.999818359, 1.005290819,
 \$ 0.920724275, 0.953583511, 0.971794674, 0.987896883,
 \$ 1.003541757, 1.006501627/
 DATA ya08/0.984062194, 0.995245947, 1.003775722,1.00789375,
 \$ 1.017736929, 1.026798811, 0.98105183, 0.991703355,
 \$ 0.999271017, 1.000792182, 1.010045375, 1.012584462,
 \$ 0.964924532, 0.973191667, 0.983483368, 0.989358451,
 \$ 0.996532277, 1.004544051, 0.961646955, 0.971980294,
 \$ 0.982515291, 0.988416112, 0.99357226, 1.001852028/
 DATA ya09/0.981100265, 1.005769279, 1.016141754,1.024946955,
 \$ 1.034822197, 1.046614073, 0.947357079, 0.988146548,
 \$ 1.00450601, 1.014030384, 1.029166234, 1.037284,
 \$ 0.887326416, 0.948128053, 0.982561478, 1.001514036,
 \$ 1.024507639, 1.035725614, 0.865052953, 0.929052092,
 \$ 0.970590269, 0.998960549, 1.01984305, 1.040583906/
 DATA ya10/0.811759305, 0.995329961, 1.020333804,1.032463139,
 \$ 1.047897171, 1.05174767, 0.777447105, 0.944714117,
 \$ 0.993357362, 1.01174202, 1.029613483, 1.035276553,
 \$ 0.781224307, 0.898523158, 0.96290587, 0.999746715,
 \$ 1.026527348, 1.045904478, 0.793676887, 0.880484747,
 \$ 0.948472787, 0.990165625, 1.021838374, 1.042234082/
 DATA ya11/0.986679734, 1.017807857, 1.03593156, 1.048501643,
 \$ 1.052152506, 1.064141862, 0.918854906, 0.986101684,
 \$ 1.014070003, 1.030203218, 1.036423419, 1.045418266,
 \$ 0.840957379, 0.936210384, 0.985149561, 1.018691097,
 \$ 1.037276858, 1.060660278, 0.819392674, 0.908888801,
 \$ 0.968038067, 1.012114718, 1.036737228, 1.057289829/
 DATA ya12/0.748733611, 0.990627656, 1.034190707,1.052825361,
 \$ 1.06584076, 1.079897417, 0.695627755, 0.913707227,
 \$ 0.991313859, 1.027461942, 1.04069733, 1.060226561,
 \$ 0.706944636, 0.8522306, 0.94860339, 1.005559196,
 \$ 1.045979613, 1.075894075, 0.73437058, 0.847459187,
 \$ 0.934738645, 1.000988929, 1.042578756, 1.074824714/
 DATA ya13/0.981989209, 1.008936946, 1.029865297,1.038422613,
 \$ 1.054058345, 1.061735803, 0.937241431, 0.990086005,
 \$ 1.017034894, 1.035087045, 1.038475919, 1.045199965,
 \$ 0.87682477, 0.949834664, 0.993962607, 1.020666167,
 \$ 1.035851164, 1.042129549/
 DATA ya14/0.815491697, 0.997620023, 1.039237881,1.053102522,
 \$ 1.086585749, 1.103663917, 0.78953925, 0.933446549,
 \$ 0.99930244, 1.023476805, 1.067900774, 1.083282378,

\$ 0.815214272, 0.890943069, 0.968269595, 1.013964294,
 \$ 1.072808137, 1.085029003/
 DATA ya15/0.991569322, 1.041521512, 1.045037861,1.060793203,
 \$ 1.082287649, 1.07803524, 0.931020364, 1.005285496,
 \$ 1.034036331, 1.044945944, 1.063403916, 1.06161532,
 \$ 0.870086897, 0.955048935, 0.992329347, 1.018151792,
 \$ 1.02615996, 1.029434499/
 DATA ya16/0.782623888, 0.997288478, 1.033065383,1.055405644,
 \$ 1.070592293, 1.07151269, 0.75429023, 0.924118485,
 \$ 0.996635144, 1.027293159, 1.050247674, 1.053311205,
 \$ 0.746718191, 0.864680228, 0.945338789, 0.993593826,
 \$ 1.015120801, 1.037266927/
 DATA ya17/0.936981989, 0.961491638, 0.98101193, 0.992490958,
 \$ 1.003756796, 1.01929283, 0.941759217, 0.963363931,
 \$ 0.985544713, 1.000595238, 1.005550482, 1.021919293,
 \$ 0.940861405, 0.961993845, 0.980056582, 0.993203303,
 \$ 0.996858632, 1.012274762, 0.943236824, 0.962524674,
 \$ 0.977802843, 0.990595999, 0.993286747, 1.007198815/
 DATA ya18/0.945736581, 0.979047232, 0.998814433,1.011311631,
 \$ 1.029409027, 1.046307817, 0.923348521, 0.971709893,
 \$ 0.998598761, 1.016020723, 1.034837742, 1.052099771,
 \$ 0.892241376, 0.949468185, 0.982678443, 1.010894371,
 \$ 1.032850906, 1.045554585, 0.881352635, 0.937247285,
 \$ 0.972365937, 1.006729178, 1.02731453, 1.044703968/
 DATA ya19/0.798522522, 0.958135206, 0.996520275,1.019239792,
 \$ 1.030614708, 1.052211921, 0.785970877, 0.926842304,
 \$ 0.983831095, 1.011194764, 1.031299649, 1.051750109,
 \$ 0.805366815, 0.906054945, 0.964124484, 1.000591881,
 \$ 1.029683211, 1.04940917, 0.822074852, 0.901103511,
 \$ 0.956780637, 0.997844254, 1.024241055, 1.047120514/
 DATA ya20/0.943630414, 0.988841633, 1.012365897,1.024988507,
 \$ 1.045528582, 1.065176368, 0.902103213, 0.969939035,
 \$ 1.003643769, 1.024706356, 1.041937231, 1.063316483,
 \$ 0.856871457, 0.939233616, 0.987529077, 1.018772368,
 \$ 1.041284705, 1.066397906, 0.848203581, 0.924468982,
 \$ 0.976308293, 1.010321933, 1.042514392, 1.059778252/
 DATA ya21/0.756754762, 0.959357459, 1.007205468,1.028082266,
 \$ 1.05478134, 1.074603005, 0.729802842, 0.909059796,
 \$ 0.98274568, 1.017190217, 1.044196892, 1.064144847,
 \$ 0.757324243, 0.879467018, 0.959552509, 1.009115397,
 \$ 1.048045067, 1.069139727, 0.781179873, 0.873479077,
 \$ 0.947957424, 1.000985216, 1.035231028, 1.066498708/
 DATA ya22/0.952954331, 0.991738226, 1.018290383,1.030205614,
 \$ 1.046204925, 1.068606217, 0.922627749, 0.982462528,
 \$ 1.012662125, 1.038617857, 1.047806987, 1.065709012,
 \$ 0.881130748, 0.955320645, 0.999861892, 1.027024489,
 \$ 1.047239437, 1.065687659/
 DATA ya23/0.760528191, 0.964537011, 1.012508385,1.032744818,
 \$ 1.05199923, 1.067438234, 0.74158793, 0.921382756,
 \$ 0.986492874, 1.020607143, 1.044290395, 1.063841195,
 \$ 0.771581611, 0.892509983, 0.970293638, 1.015745942,
 \$ 1.046381825, 1.072475479/
 DATA ya24/0.960708726, 1.005324701, 1.027534953,1.048635042,
 \$ 1.062186311, 1.080284572, 0.915605904, 0.989997082,
 \$ 1.019634173, 1.044438113, 1.069950546, 1.075055732,
 \$ 0.873900795, 0.958970553, 0.997291785, 1.030537412,

\$ 1.053246563, 1.059426723/
 DATA ya25/0.742701746, 0.969470464, 1.02265456, 1.078235309,
 \$ 1.061343974, 1.086309236, 0.718057682, 0.912625002,
 \$ 0.994286795, 1.027996154, 1.056971856, 1.078325132,
 \$ 0.718382803, 0.872612548, 0.960129877, 1.003540547,
 \$ 1.034978924, 1.054347181/
 DATA ya26/0.923555486, 0.94992878, 0.972856525, 0.986572476,
 \$ 1.006330761, 1.019616713, 0.931433823, 0.959687207,
 \$ 0.98194285, 1.000218447, 1.012413623, 1.027726424,
 \$ 0.946014509, 0.967302925, 0.991118565, 1.006566769,
 \$ 1.017065452, 1.036632856, 0.959950798, 0.98348752,
 \$ 1.0002794, 1.015483647, 1.031855759, 1.043877104/
 DATA ya27/0.930621137, 0.955413882, 0.978100746,0.995214932,
 \$ 1.013353934, 1.040686726, 0.929869261, 0.958637583,
 \$ 0.982040072, 1.006608783, 1.026400457, 1.041867529,
 \$ 0.928701792, 0.960637294, 0.990495366, 1.006590357,
 \$ 1.037775499, 1.052564285/
 DATA ya28/0.946513518, 0.976476799, 0.995566831,1.014666538,
 \$ 1.03460382,1.056654935, 0.939010833, 0.977176426,
 \$ 1.003968866, 1.027006124, 1.041700836, 1.061712625,
 \$ 0.930456056, 0.972955842, 1.000229212, 1.024426382,
 \$ 1.051963624, 1.070838387, 0.927830279, 0.968172106,
 \$ 1.006802711, 1.029505713, 1.058514366, 1.075806235/
 DATA ya29/0.95125968, 0.97586105, 1.00083498, 1.025546152,
 \$ 1.032876828, 1.053815812, 0.939856468, 0.975023936,
 \$ 1.003160496, 1.023440171, 1.043945106, 1.0650885,
 \$ 0.923374211, 0.966276483, 1.000541394, 1.031577757,
 \$ 1.050378694, 1.069995493/
 DATA ya30/0.94998769, 0.979130065, 1.005150673,1.03340163,
 \$ 1.053328077, 1.084196397, 0.936389276, 0.980113508,
 \$ 1.012968127, 1.039464275, 1.055356911, 1.086023612,
 \$ 0.908786245, 0.961939661, 1.006342062, 1.036158145,
 \$ 1.070007705, 1.086688091, 0.899228918, 0.964553225,
 \$ 1.006785206, 1.041503232, 1.078106693, 1.093719519/
 DATA ya31/0.946850116, 0.976597988, 0.994736663,1.019592713,
 \$ 1.03735099, 1.058206486, 0.938436599, 0.970951983,
 \$ 1.004893633, 1.029927905, 1.046164974, 1.070541836,
 \$ 0.925408252, 0.971133827, 1.0065348, 1.031980088,
 \$ 1.060054569, 1.087534817/
 DATA ya32/0.963274888, 0.988889027, 1.021057874,1.034854524,
 \$ 1.065984223, 1.092816919, 0.947767217, 0.986049492,
 \$ 1.01110947, 1.047729128, 1.063748128, 1.094658662,
 \$ 0.93879454, 0.979755037, 1.021201933, 1.050021284,
 \$ 1.060078236, 1.101315427/
 DATA ya33/0.899310952, 0.921874469, 0.942136953,0.959146563,
 \$ 0.987853398, 1.00539472, 0.941557506, 0.968045823,
 \$ 0.986584049, 1.00114486, 1.021274831, 1.039807078,
 \$ 0.979047652, 1.001434608, 1.018610106, 1.027678703,
 \$ 1.052360414, 1.064003214, 1.006094067, 1.019127533,
 \$ 1.030702809, 1.038864483, 1.054127873, 1.062912272/
 DATA ya34/0.887491161, 0.909519152, 0.932840156,0.949986101,
 \$ 0.964034551, 0.978232824, 0.927082368, 0.953163465,
 \$ 0.972115168, 0.99353729, 1.001044538, 1.011523334,
 \$ 0.951481504, 0.984081843, 1.005646952, 1.021016785,
 \$ 1.034021551, 1.045214596/
 DATA ya35/0.881896522, 0.909960693, 0.932735495,0.958542378,

\$ 0.970075966, 0.993818456, 0.92012876, 0.953582349,
 \$ 0.972816413, 0.998319543, 1.010987748, 1.02287857,
 \$ 0.941104874, 0.980218721, 1.001406278, 1.02540114,
 \$ 1.044062082, 1.056819488, 0.960824563, 0.998309782,
 \$ 1.020339234, 1.046625465, 1.054391342, 1.06473229/
 DATA ya36/0.882070844, 0.909189526, 0.928866593,0.948048317,
 \$ 0.967443383, 0.988151396, 0.916025174, 0.944852981,
 \$ 0.970265245, 0.990702455, 1.004712389, 1.02337833,
 \$ 0.958975361, 0.991694126, 1.019932555, 1.039456638,
 \$ 1.051680858, 1.069749649/
 DATA ya37/0.882681882, 0.906320045, 0.933663034,0.952759585,
 \$ 0.971462508, 0.982756676, 0.910278875, 0.945017856,
 \$ 0.969536224, 0.990132266, 1.012996751, 1.024535845,
 \$ 0.926857169, 0.971092045, 0.998548916, 1.017986833,
 \$ 1.038273825, 1.049035668, 0.952475649, 0.99195157,
 \$ 1.020166571, 1.042737672, 1.060049267, 1.070778194/
 DATA ya38/0.925257259, 0.950627216, 0.971420997, 0.990883753,
 \$ 1.014985628, 1.030400129, 0.956456398, 0.990904991,
 \$ 1.012006235, 1.038009446, 1.04807637, 1.064638734,
 \$ 0.968478277, 1.015135484, 1.038549138, 1.057587729,
 \$ 1.079126537, 1.084830805/
 DATA ya39/0.934715942, 0.963453164, 0.991450948, 1.013404505,
 \$ 1.024758251, 1.042954893, 0.960218002, 1.001749392,
 \$ 1.022726289, 1.040356367, 1.063408939, 1.087063399,
 \$ 0.963795038, 1.004701663, 1.047499085, 1.066151411,
 \$ 1.082311779, 1.097076707/
 DATA ya40/0.973709636, 0.981489059, 0.991674663,0.997711141,
 \$ 1.005029415, 1.010120637, 0.977409978, 0.981841478,
 \$ 0.994479515, 1.000218447, 1.011901873, 1.017990977,
 \$ 0.977289049, 0.985439645, 0.993100083, 1.000397717,
 \$ 1.009319515, 1.009359424, 0.976294269, 0.988855273,
 \$ 0.995760565, 1.005807078, 1.011951066, 1.015966745/
 DATA ya41/0.978406437, 0.998223711, 1.008992515,1.014082256,
 \$ 1.028641358, 1.036090371, 0.953491995, 0.989517382,
 \$ 1.007165526, 1.01530118, 1.029167773, 1.040693368,
 \$ 0.911529208, 0.965277201, 0.995925904, 1.010451721,
 \$ 1.025636156, 1.036093048, 0.890769819, 0.949176507,
 \$ 0.981288963, 1.007852928, 1.02417168, 1.041206086/
 DATA ya42/0.956184997, 0.986641432, 0.998447414,1.005621252,
 \$ 1.010356909, 1.029480289, 0.908989704, 0.963449662,
 \$ 0.989115869, 1.007747364, 1.016131792, 1.025624132,
 \$ 0.848181965, 0.925058332, 0.968592548, 0.989073575,
 \$ 1.012039601, 1.022041586, 0.828422824, 0.904829074,
 \$ 0.954533395, 0.983648374, 1.006987405, 1.024633723/
 DATA ya43/0.952491626, 0.97822479, 0.990410188, 0.999446371,
 \$ 1.014609205, 1.020158438, 0.92191957, 0.966416232,
 \$ 0.994948438, 1.0081995, 1.012782225, 1.028782144,
 \$ 0.87953726, 0.943144478, 0.979508673, 0.99594718,
 \$ 1.015503298, 1.026954052/
 DATA ya44/0.971215683, 1.005171885, 1.027047754,1.036915448,
 \$ 1.047968682, 1.05707281, 0.924463717, 0.989716357,
 \$ 1.020166744, 1.03459036, 1.054131435, 1.06715481,
 \$ 0.888274803, 0.971566414, 1.004901597, 1.030298252,
 \$ 1.040020276, 1.053861366/
 DATA ya45/0.932546409, 0.955038561, 0.971823041,0.994856723,
 \$ 1.001041693, 1.013390665, 0.94654525, 0.972231846,

\$ 0.988077878, 1.00114486, 1.01702443, 1.030037347,
 \$ 0.959330118, 0.980464638, 0.990785681, 1.006244273,
 \$ 1.01969838, 1.023700998, 0.971291296, 0.98796397,
 \$ 0.996949814, 1.004770713, 1.017518939,1.020250374/
 DATA ya46/0.918123943, 0.954694707, 0.972060996,0.999175976,
 \$ 1.010092861, 1.020390499, 0.90789767, 0.963136077,
 \$ 0.98871783, 1.006467402, 1.026903288, 1.042701251,
 \$ 0.890594574, 0.949315206, 0.984244498, 0.999865729,
 \$ 1.024191523, 1.045580944, 0.885884843, 0.940902682,
 \$ 0.977455623, 0.995966967, 1.018740995, 1.03746559/
 DATA ya47/0.90792975, 0.951977214, 0.976157633,1.001671925,
 \$ 1.01231869, 1.020006744, 0.882671616, 0.947920402,
 \$ 0.982330978, 1.004672089, 1.027427704, 1.036989666,
 \$ 0.86000385, 0.930585198, 0.972484525, 1.001394886,
 \$ 1.025577878, 1.037118928, 0.856413785, 0.922201883,
 \$ 0.965593825, 0.997316156, 1.020260888, 1.043427448/
 DATA ya48/0.922703601, 0.963104525, 0.989866816,1.003631597,
 \$ 1.011383491, 1.02552188, 0.890198514, 0.964673344,
 \$ 0.997680395, 1.009546187, 1.027009027, 1.036927011,
 \$ 0.851473272, 0.938765476, 0.983468954, 1.005259497,
 \$ 1.023652755, 1.041121407/
 DATA ya49/0.935790827, 0.983624128, 1.007400335,1.029664803,
 \$ 1.03683878, 1.05949192, 0.900033426, 0.973262061,
 \$ 1.012459574, 1.029165275, 1.048342766, 1.067417867,
 \$ 0.873892507, 0.961365048, 1.002517698, 1.032553159,
 \$ 1.049129743, 1.06725545/
 DATA ya50/0.958731425, 0.975409702, 0.984817876,0.993261103,
 \$ 1.004765249, 1.010600353, 0.969539755, 0.98613696,
 \$ 0.992541394, 1.000218447, 1.010473786, 1.017745639,
 \$ 0.971500386, 0.987939988, 0.994057495, 1.000568523,
 \$ 1.012219126, 1.020826947, 0.975732562, 0.988844256,
 \$ 0.997927899, 1.003269748, 1.014066575, 1.021047996/
 DATA ya51/0.984563906, 0.997896793, 1.011642503,1.022967468,
 \$ 1.029730335, 1.041325755, 0.981905722, 1.003054623,
 \$ 1.013013547, 1.023099591, 1.032849245, 1.044700267,
 \$ 0.951464095, 0.985609642, 1.007131338, 1.01665536,
 \$ 1.029945579, 1.044765004, 0.935839101, 0.973753746,
 \$ 0.996746695, 1.018627905, 1.033168799, 1.041778539/
 DATA ya52/0.988132231, 1.008283864, 1.023261141,1.029123816,
 \$ 1.049018226, 1.060416314, 0.98222274, 1.008717981,
 \$ 1.031659088, 1.036268489, 1.049876055, 1.065471367,
 \$ 0.9409996, 0.988952436, 1.017688021, 1.032121385,
 \$ 1.051208626, 1.062623394, 0.915965961, 0.96848479,
 \$ 1.009596414, 1.03079319, 1.052341127, 1.065288237/
 DATA ya53/1.020051152, 1.036538587, 1.047017611,1.059199911,
 \$ 1.069013656, 1.088213015, 1.007263531, 1.034590036,
 \$ 1.052596078, 1.058495063, 1.063306404, 1.077959311,
 \$ 0.970094285, 1.007272853, 1.033262005, 1.048903509,
 \$ 1.065180225, 1.079959811/
 DATA ya54/1.003053722, 1.02622691, 1.042107739, 1.051375457,
 \$ 1.06214194, 1.070718166, 0.989236204, 1.021633186,
 \$ 1.040465638, 1.060223218, 1.069111858, 1.064802434,
 \$ 0.978542962, 1.011191467, 1.042264361, 1.054196721,
 \$ 1.072798946, 1.074290236/
 DATA ya55/0.947613295, 0.964310247, 0.976077844,0.982186872,
 \$ 0.99613966, 1.003044446, 0.972262591, 0.989342093,

```

$ 0.994923716, 1.000849057, 1.009777528, 1.019057997,
$ 0.976989079, 0.990114647, 0.999598541, 1.001420384,
$ 1.018034874, 1.021543819, 0.986114427, 1.00000847,
$ 1.000094804, 1.007312879, 1.018471788, 1.024778672/
DATA ya56/0.952348124, 0.969213158, 0.984997563,0.996406662,
$ 1.004546208, 1.007966525, 0.966699213, 0.988905689,
$ 1.004255907, 1.013752565, 1.018576331, 1.029112452,
$ 0.949892512, 0.980756781, 1.002888257, 1.017211543,
$ 1.026114766, 1.037211052, 0.937120616, 0.971507227,
$ 0.997433092, 1.013446332, 1.022399548, 1.029499545/
DATA ya57/0.951278926, 0.973414566, 0.985834931,0.998917954,
$ 1.010010681, 1.013071097, 0.961602056, 0.991382475,
$ 1.011558237, 1.018299758, 1.027247394, 1.030098877,
$ 0.935141197, 0.977637496, 1.00544668, 1.018055344,
$ 1.031536937, 1.035032554, 0.918822577, 0.963286687,
$ 0.993906209, 1.013775082, 1.027926675, 1.038237668/
DATA ya58/0.95462905, 0.977596964, 0.986203232,1.008127626,
$ 1.016362919, 1.029536074, 0.9727693, 0.998923079,
$ 1.013787537, 1.030439377, 1.03857799, 1.054112427,
$ 0.951556487, 0.99099299, 1.015327662, 1.034666499,
$ 1.052289031, 1.058370623/
DATA ya59/0.959848119, 0.98229636, 0.996141917, 1.014309575,
$ 1.010564833, 1.029545959, 0.970037833, 1.00400919,
$ 1.017900832, 1.042078063, 1.041299424, 1.049196082,
$ 0.959212423, 1.000876174, 1.020783524, 1.03764468,
$ 1.055055698, 1.058524014/

```

```

WRITE(*,*)'*****'
WRITE(*,*)'***DIODE CORRECTION FACTOR CALCULATOR (MBPCC)--2002***'
WRITE(*,*)'*****'
  WRITE(*,*) ' '
  WRITE(*,*) ' '
12  WRITE(*,*)'Please select the Linac (1=600C, 2=21EX(BR), 3=21C,'
    WRITE(*,*)'4=21EX(COV), 5=20CR(Ham)):'
    READ(*,*) Linac
    IF((Linac .ne.1) .and.(Linac .ne. 2) .and.(Linac .ne.3) .and.
$(Linac .ne. 4) .and. (Linac .ne. 5)) then
      WRITE(*,*)'Linac is wrong!'
      GOTO 12
    ELSE
      GOTO 13
    END IF
13  WRITE(*,*)'Select the energy (1=4X, 2=6X, 3=10X, 4=15X, 5=18X):'
    READ(*,*) Energy
    IF((Energy .ne.1) .and.(Energy .ne. 2) .and.(Energy .ne.3) .and.
$(Energy .ne.4).and. (Energy .ne.5))then
      WRITE(*,*)'Energy is wrong!'
      GO TO 13
    ELSE
      GOTO 14
    END IF
14  WRITE(*,*)'Please select the wedge (see the following):'
    WRITE(*,*)'1 = open (none)'
    WRITE(*,*)'2 = 15degree (normal/narrow/upper)'
    WRITE(*,*)'3 = 15degree (wide/lower)'

```



```

        WRITE(*,*)'4 = 30degree (normal/narrow/upper)'
        WRITE(*,*)'5 = 30degree (wide/lower)'
WRITE(*,*)'6 = 45degree (normal/upper)'
        WRITE(*,*)'7 = 45degree (lower)'
        WRITE(*,*)'8 = 60degree (normal/upper)'
        WRITE(*,*)'9 = 60degree (lower)'
        READ(*,*)Wedge
        IF((wedge .ne. 1) .and.(wedge .ne. 2) .and.(wedge .ne.3) .and.
$ (wedge .ne. 4) .and. (wedge .ne. 5) .and.(wedge .ne. 6).and.
$ (wedge .ne.7).and.(wedge.ne.8).and.(wedge.ne.9))then
        WRITE(*,*)'Wedge is wrong!'
        GOTO 14
    ELSE
        GOTO 15
    END IF
15    WRITE(*,*)'Please input the SSD:'
        READ(*,*)SSD
        WRITE(*,*)'Please input the Blocked Equivalent Square FS:'
        READ(*,*)FS

    IF (Linac .eq. 1) then
        IF(Energy .eq. 2)then
            IF(wedge.eq. 1)then
                CALL POLIN2(x1a,x2a1,ya01,6,4,SSD,FS,DCF,dDCF)
            else if (wedge .eq. 2) then
                CALL POLIN2(x1a,x2a3,ya02,6,3,SSD,FS,DCF ,dDCF)
            else if (wedge .eq. 3) then
                CALL POLIN2(x1a,x2a2,ya03,6,4,SSD,FS,DCF ,dDCF)
            else if (wedge .eq. 4) then
                CALL POLIN2(x1a,x2a3,ya04,6,3,SSD,FS,DCF ,dDCF)
            else if (wedge .eq. 5) then
                CALL POLIN2(x1a,x2a2,ya05,6,4,SSD,FS,DCF ,dDCF)
            else if (wedge .eq. 6) then
                CALL POLIN2(x1a,x2a3,ya06,6,3,SSD,FS,DCF ,dDCF)
            else if (wedge .eq. 8) then
                CALL POLIN2(x1a,x2a4,ya07,6,3,SSD,FS,DCF ,dDCF)
            else
                write(*,*)'Wedge was wrong!'
            END IF
        ELSE
            write(*,*)'Energy was wrong!'
        END IF
    ELSE IF (Linac .eq. 2) then
        IF (Energy .eq. 1)then
            IF(wedge.eq. 1)then
                CALL POLIN2(x1a,x2a1,ya08,6,4,SSD,FS,DCF,dDCF)
            else if (wedge .eq. 2) then
                CALL POLIN2(x1a,x2a2,ya09,6,4,SSD,FS,DCF ,dDCF)
            else if (wedge .eq. 3) then
                CALL POLIN2(x1a,x2a2,ya10,6,4,SSD,FS,DCF ,dDCF)
            else if (wedge .eq. 4) then
                CALL POLIN2(x1a,x2a2,ya11,6,4,SSD,FS,DCF ,dDCF)
            else if (wedge .eq. 5) then
                CALL POLIN2(x1a,x2a2,ya12,6,4,SSD,FS,DCF ,dDCF)
            else if (wedge .eq. 6) then
                CALL POLIN2(x1a,x2a3,ya13,6,3,SSD,FS,DCF ,dDCF)

```

```

        else if (wedge .eq. 7) then
            CALL POLIN2(x1a,x2a3,ya14,6,3,SSD,FS,DCF ,dDCF)
        else if (wedge .eq. 8) then
            CALL POLIN2(x1a,x2a4,ya15,6,3,SSD,FS,DCF ,dDCF)
        else if (wedge .eq. 9) then
            CALL POLIN2(x1a,x2a4,ya16,6,3,SSD,FS,DCF ,dDCF)
        else
            write(*,*)'Wedge was wrong!'
    END IF
ELSE IF (Energy .eq. 3)then
    IF(wedge.eq. 1)then
        CALL POLIN2(x1a,x2a1,ya17,6,4,SSD,FS,DCF,dDCF)
    else if (wedge .eq. 2) then
        CALL POLIN2(x1a,x2a2,ya18,6,4,SSD,FS,DCF ,dDCF)
    else if (wedge .eq. 3) then
        CALL POLIN2(x1a,x2a2,ya19,6,4,SSD,FS,DCF ,dDCF)
    else if (wedge .eq. 4) then
        CALL POLIN2(x1a,x2a2,ya20,6,4,SSD,FS,DCF ,dDCF)
    else if (wedge .eq. 5) then
        CALL POLIN2(x1a,x2a2,ya21,6,4,SSD,FS,DCF ,dDCF)
    else if (wedge .eq. 6) then
        CALL POLIN2(x1a,x2a3,ya22,6,3,SSD,FS,DCF ,dDCF)
    else if (wedge .eq. 7) then
        CALL POLIN2(x1a,x2a3,ya23,6,3,SSD,FS,DCF ,dDCF)
    else if (wedge .eq. 8) then
        CALL POLIN2(x1a,x2a4,ya24,6,3,SSD,FS,DCF ,dDCF)
    else if (wedge .eq. 9) then
        CALL POLIN2(x1a,x2a4,ya25,6,3,SSD,FS,DCF ,dDCF)
    else
        write(*,*)'Wedge was wrong!'
    END IF
ELSE
    write(*,*)'Energy was wrong!'
END IF
ELSE IF (Linac .eq. 3) then
    IF (Energy .eq. 2)then
        IF(wedge.eq. 1)then
            CALL POLIN2(x1a,x2a1,ya26,6,4,SSD,FS,DCF,dDCF)
        else if (wedge .eq. 2) then
            CALL POLIN2(x1a,x2a3,ya27,6,3,SSD,FS,DCF ,dDCF)
        else if (wedge .eq. 3) then
            CALL POLIN2(x1a,x2a2,ya28,6,4,SSD,FS,DCF ,dDCF)
        else if (wedge .eq. 4) then
            CALL POLIN2(x1a,x2a3,ya29,6,3,SSD,FS,DCF ,dDCF)
        else if (wedge .eq. 5) then
            CALL POLIN2(x1a,x2a2,ya30,6,4,SSD,FS,DCF ,dDCF)
        else if (wedge .eq. 6) then
            CALL POLIN2(x1a,x2a3,ya31,6,3,SSD,FS,DCF ,dDCF)
        else if (wedge .eq. 8) then
            CALL POLIN2(x1a,x2a4,ya32,6,3,SSD,FS,DCF ,dDCF)
        else
            write(*,*)'Wedge was wrong!'
        END IF
    ELSE IF (Energy .eq. 5)then
        IF(wedge.eq. 1)then
            CALL POLIN2(x1a,x2a1,ya33,6,4,SSD,FS,DCF,dDCF)

```

```

else if (wedge .eq. 2) then
    CALL POLIN2(x1a,x2a3,ya34,6,3,SSD,FS,DCF ,dDCF)
else if (wedge .eq. 3) then
    CALL POLIN2(x1a,x2a2,ya35,6,4,SSD,FS,DCF ,dDCF)
else if (wedge .eq. 4) then
    CALL POLIN2(x1a,x2a3,ya36,6,3,SSD,FS,DCF ,dDCF)
else if (wedge .eq. 5) then
    CALL POLIN2(x1a,x2a2,ya37,6,4,SSD,FS,DCF ,dDCF)
else if (wedge .eq. 6) then
    CALL POLIN2(x1a,x2a3,ya38,6,3,SSD,FS,DCF ,dDCF)
else if (wedge .eq. 8) then
    CALL POLIN2(x1a,x2a4,ya39,6,3,SSD,FS,DCF ,dDCF)
else
    write(*,*)'Wedge was wrong!'
END IF
ELSE
    write(*,*)'Energy was wrong!'
END IF
ELSE IF (Linac .eq. 4) then
    IF (Energy .eq. 2)then
        IF(wedge.eq. 1)then
            CALL POLIN2(x1a,x2a1,ya40,6,4,SSD,FS,DCF,dDCF)
        else if (wedge .eq. 2) then
            CALL POLIN2(x1a,x2a2,ya41,6,4,SSD,FS,DCF ,dDCF)
        else if (wedge .eq. 4) then
            CALL POLIN2(x1a,x2a2,ya42,6,4,SSD,FS,DCF ,dDCF)
        else if (wedge .eq. 6) then
            CALL POLIN2(x1a,x2a3,ya43,6,3,SSD,FS,DCF ,dDCF)
        else if (wedge .eq. 8) then
            CALL POLIN2(x1a,x2a4,ya44,6,3,SSD,FS,DCF ,dDCF)
        else
            write(*,*)'Wedge was wrong!'
        END IF
    ELSE IF (Energy .eq. 5)then
        IF(wedge.eq. 1)then
            CALL POLIN2(x1a,x2a1,ya45,6,4,SSD,FS,DCF,dDCF)
        else if (wedge .eq. 2) then
            CALL POLIN2(x1a,x2a2,ya46,6,4,SSD,FS,DCF ,dDCF)
        else if (wedge .eq. 4) then
            CALL POLIN2(x1a,x2a2,ya47,6,4,SSD,FS,DCF ,dDCF)
        else if (wedge .eq. 6) then
            CALL POLIN2(x1a,x2a3,ya48,6,3,SSD,FS,DCF ,dDCF)
        else if (wedge .eq. 8) then
            CALL POLIN2(x1a,x2a4,ya49,6,3,SSD,FS,DCF ,dDCF)
        else
            write(*,*)'Wedge was wrong!'
        END IF
    ELSE
        write(*,*)'Energy was wrong!'
    END IF
ELSE IF (Linac .eq. 5) then
    IF (Energy .eq. 2)then
        IF(wedge.eq. 1)then
            CALL POLIN2(x1a,x2a1,ya50,6,4,SSD,FS,DCF,dDCF)
        else if (wedge .eq. 2) then
            CALL POLIN2(x1a,x2a2,ya51,6,4,SSD,FS,DCF ,dDCF)

```

```

        else if (wedge .eq. 4) then
            CALL POLIN2(x1a,x2a2,ya52,6,4,SSD,FS,DCF ,dDCF)
        else if (wedge .eq. 6) then
            CALL POLIN2(x1a,x2a3,ya53,6,3,SSD,FS,DCF ,dDCF)
        else if (wedge .eq. 8) then
            CALL POLIN2(x1a,x2a4,ya54,6,3,SSD,FS,DCF ,dDCF)
        else
            write(*,*)'Wedge was wrong!'
    END IF
ELSE IF (Energy .eq. 4)then
    IF(wedge.eq. 1)then
        CALL POLIN2(x1a,x2a1,ya55,6,4,SSD,FS,DCF,dDCF)
    else if (wedge .eq. 2) then
        CALL POLIN2(x1a,x2a2,ya56,6,4,SSD,FS,DCF ,dDCF)
    else if (wedge .eq. 4) then
        CALL POLIN2(x1a,x2a2,ya57,6,4,SSD,FS,DCF ,dDCF)
    else if (wedge .eq. 6) then
        CALL POLIN2(x1a,x2a3,ya58,6,3,SSD,FS,DCF ,dDCF)
    else if (wedge .eq. 8) then
        CALL POLIN2(x1a,x2a4,ya59,6,3,SSD,FS,DCF ,dDCF)
    else
        write(*,*)'Wedge was wrong!'
    END IF
ELSE
    write(*,*)'Energy was wrong!'
END IF
ELSE
    WRITE(*,*)'Linac input was wrong!'
END IF
WRITE(*,*)'*****'
WRITE(*,*)'*****The Result is as follow*****'
WRITE(*,*)'*****'
IF(Linac .eq. 1)then
    WRITE(*,*)'Linac = 600C(BR)'
ELSE if(Linac .eq. 2)then
    WRITE(*,*)'Linac = 21EX(BR)'
ELSE IF(Linac .eq. 3)then
    WRITE(*,*)'Linac = 21C(BR)'
Else if(Linac .eq. 4)then
    WRITE(*,*)'Linac = 21EX(COV)'
ELSE
    WRITE(*,*)'Linac = 20CR(Ham)'
END IF
IF(Energy .eq. 1)then
    WRITE(*,*)'Energy = 4X'
ELSE IF(Energy .eq. 2)then
    WRITE(*,*)'Energy = 6X'
ELSE IF(Energy .eq. 3)then
    WRITE(*,*)'Energy = 10X'
ELSE IF(Energy .eq. 4)then
    WRITE(*,*)'Energy = 15X'
ELSE
    WRITE(*,*)'Energy = 18X'
END IF
IF(wedge .eq. 1)then
    WRITE(*,*)'Wedge = open(none)'

```

```

ELSE IF(wedge .eq. 2)then
  WRITE(*,*)'Wedge = 15degree (normal/narrow/upper)'
ELSE IF(wedge .eq. 3)then
  WRITE(*,*)'Wedge = 15degree (wide/lower)'
ELSE IF(wedge .eq. 4)then
  WRITE(*,*)'Wedge = 30degree (normal/narrow/upper)'
ELSE IF(wedge .eq. 5)then
  WRITE(*,*)'Wedge = 30degree (wide/lower)'
ELSE IF(wedge .eq. 6)then
  WRITE(*,*)'Wedge = 45degree (normal/upper)'
ELSE IF(wedge .eq. 7)then
  WRITE(*,*)'Wedge = 45degree (lower)'
ELSE IF(wedge .eq. 8)then
  WRITE(*,*)'Wedge = 60degree (normal/upper)'
ELSE
  WRITE(*,*)'Wedge = 60degree (lower)'
END IF
WRITE(*,*)'SSD  =' ,SSD
WRITE(*,*)'Equi FS=' ,FS
WRITE(*,*)'DCF  =' ,DCF
WRITE(*,*)'Want to calculate another field?(1=Yes,2=No)'
READ(*,*)Another
IF(Another .EQ. 1) go to 12
END

```

```

SUBROUTINE polin2(x1a,x2a,ya,m,n,x1,x2,y,dy)
INTEGER m,n,NMAX,MMAX
REAL dy,x1,x2,y,x1a(m),x2a(n),ya(m,n)
PARAMETER (NMAX=20,MMAX=20)
INTEGER j,k
REAL ymtmp(MMAX),yntmp(NMAX)
do 12, j=1,m
  do 11, k=1,n
    yntmp(k)=ya(j,k)
11  continue
    call polint(x2a,yntmp,n,x2,yntmp(j),dy)
12  continue
    call polint(x1a,ymtmp,m,x1,y,dy)
  return
END

```

```

SUBROUTINE polint(xa,ya,n,x,y,dy)
INTEGER n,NMAX
REAL dy,x,y,xa(n),ya(n)
PARAMETER (NMAX=10)
INTEGER i,m,ns
REAL den,dif,dift,ho,hp,w,c(NMAX),d(NMAX)
ns=1
dif=abs(x-xa(1))
do 11, i=1,n
  dift=abs(x-xa(i))
  if (dift.lt.dif) then

```

```

        ns=i
        dif=dift
    endif
    c(i)=ya(i)
    d(i)=ya(i)
11  continue
    y=ya(ns)
    ns=ns-1
    do 13, m=1,n-1
        do 12, i=1,n-m
            ho=xa(i)-x
            hp=xa(i+m)-x
            w=c(i+1)-d(i)
            den=ho-hp
            if(den.eq.0.)pause
            den=w/den
            d(i)=hp*den
            c(i)=ho*den
12      continue
            if (2*ns.lt.n-m)then
                dy=c(ns+1)
            else
                dy=d(ns)
                ns=ns-1
            endif
            y=y+dy
13  continue
    return
end

```

Appendix G

Layout of the Diode Calculation Worksheet [33]

Diode Calculation Worksheet						
Patient						06-Oct-02
	<input type="checkbox"/> use	<input type="checkbox"/> use	<input type="checkbox"/> use	<input type="checkbox"/> use	<input type="checkbox"/> use	<input type="checkbox"/> use
Field	A	B	C	D	E	F
Energy	4 MV ▼	4 MV ▼	4 MV ▼	4 MV ▼	4 MV ▼	4 MV ▼
Dmax	1.2	1.2	1.2	1.2	1.2	1.2
Wedge	None/EDW ▼	None/EDW ▼	None/EDW ▼	None/EDW ▼	None/EDW ▼	None/EDW ▼
Planned						
Blkd Equiv Sqr	10.0	10.0	10.0	10.0	10.0	10.0
SSD (cm)	100.0	100.0	100.0	100.0	100.0	100.0
Depth (cm)	0.0	0.0	0.0	0.0	0.0	0.0
TMR	1.000	1.000	1.000	1.000	1.000	1.000
Normalization	1.00	1.00	1.00	1.00	1.00	1.00
Prescribed Dose (cGy)	0	0	0	0	0	0
Planned mu	0	0	0	0	0	0
Calc pt Dist	100.0	100.0	100.0	100.0	100.0	100.0
Delivered						
Delivered mu	0	0	0	0	0	0
Measured SSD	100.0	100.0	100.0	100.0	100.0	100.0
Reading	0.0	0.0	0.0	0.0	0.0	0.0
Dose at Diode	0.0	0.0	0.0	0.0	0.0	0.0
Dose at dmax	0.0	0.0	0.0	0.0	0.0	0.0
Expected diode reading						
Wf wedge	1.000	1.000	1.000	1.000	1.000	1.000
Fscorr						
lamda						
Correction Factor						
Expected Reading						
% different						
Field Notes						
	Thomas Kirby, PhD ▼			Sheldon A. Johnson, MD ▼		
Notes: 1. Dose at Diode = Prescription / [(TMR)(Normalization)] [(SSD+depth)/(SSD)] ² 2. Expected Reading = [(Dose at Diode) / (correction factor)] [mu delivered / mu calculated] 3. % different = [(Reading - Expected Reading) / Expected Reading] [100]						



Vita

Kai Huang was born in Sichuan, China. He obtained his bachelor's and master's degrees in physics in July 1990 and July 1993, respectively, from the Sichuan University, China. In 1998 he attended the University of Miami, Florida, where he received a master's degree in physics in May 2000. He entered graduate school of Louisiana State University in August of 2000. He is currently a candidate for a master of science degree in medical physics and health physics, and expects to graduate in December 2002.